2023-12-01

Evaluation Of The Efficacy Of Synthetic Glycovaccines Against Both Murine Acute Chagas Disease And Cutaneous Leishmaniasis

Colin D. Knight
University of Texas at El Paso

EVALUATION OF THE EFFICACY OF SYNTHETIC GLYCOVACCINES AGAINST BOTH MURINE ACUTE CHAGAS DISEASE AND CUTANEOUS LEISHMANIASIS

COLIN DANIEL KNIGHT

Doctoral Program in Biosciences

APPROVED:

Igor C. Almeida, D.Sc., Chair

Rosa A. Maldonado, D.Sc. Co-Chair

Charles T. Spencer, Ph.D.

Katja Michael, Ph.D.

Benjamin Flores, Ph.D.

Charlotte M. Vines Ph.D., Advocate

Stephen L. Crites, Jr., Ph.D.
Dean of the Graduate School

Dedication

This work is dedicated to Dr. Dominic “Nic” Lannutti for his unrelenting dedication to his students. This work is also dedicated the unthinkable number of veterans who fought the good fight and have entered the halls of Valhalla. For you I will never stop chasing my dreams. To my daughters never settle for just enough, always ask questions and challenge the norm. I love you both and apologize for the hardships the obtainment of this degree has caused.

EVALUATION OF THE EFFICACY OF SYNTHETIC GLYCOVACCINES AGAINST BOTH MURINE ACUTE CHAGAS DISEASE AND CUTANEOUS LEISHMANIASIS

by

COLIN DANIEL KNIGHT, BS

DISSERTATION

Presented to the Faculty of the Graduate School of

The University of Texas at El Paso

in Partial Fulfillment

of the Requirements

for the Degree of

DOCTOR OF PHILOSOPHY

Department of Biosciences

THE UNIVERSITY OF TEXAS AT EL PASO

December 2023

Acknowledgements

I first want to acknowledge my very patient and loving wife, Claudia. Although, at the time, my endless rantings about science early in the morning while you tried to enjoy your coffee may have seemed an annoyance, they, however, began to help me develop an ability to explain some complex things “relatively” simply. I know it doesn't seem like much but having been complimented on it over the years all roots back to you. You have been such a source of inspiration and motivation to keep pushing myself. I am so glad we are already beginning to see the payoff.

I want to acknowledge my PhD mentor, Dr. Igor Almeida. Dr Almeida, it has been such an interesting adventure under your mentorship that began long before I joined your lab. During my undergraduate immunology class that you instructed and then in the Special Techniques class you presented, you spoke of the work your group has done with Chagas disease. I found your data so interesting, and when I heard of the baboon study, I was blown away. Once I knew I had been accepted into the Doctoral program, I knew I wanted to do my rotation in your lab. Fast forward about a year, forgetting about an off-balanced ultracentrifuge, I came to your lab hoping to learn MS (which I learned so much about) and all the incredible magic involved. However, you put me on the α-Gal allergy project and, later, this current project that means so much to me. Thank you for inspiring me to dive headfirst into a new field at full speed. I was so scared when I first chose to switch fields of study, but looking back, I am happy I did, and I will be forever grateful for the opportunity to do so.

To my co-mentor, Dr. Rosa Maldonado, thank you for the endless support going back to my first year at EPCC when I was accepted into the Bridges of the Baccalaureate. That summer

research and subsequent yearlong support was the single catalysis that led to this manuscript's completion.

To my Ph.D. advocate and mentor, Dr. Charlotte Vines, I want to thank you from the bottom of my heart for taking a chance on this prior service army medic. I know it is cliché, but no words can express my gratitude for all the support you have provided over the last ten years. You do not realize it, but every time you say, "When you have your Ph.D. or your lab," it stuck. It may sound unbelievable, but those were some of the first positive affirmations I had received. Your endless support, both in the lab and professionally, will never be forgotten, and I am sure it will not end here. Thank you, Charlotte, again, for all you have done.

To Dr. Katja Michael, thank you and your lab for all your assistance with the synthesis of our NGPs. Without the NGPs, this work could not have been done. I also want to thank you for the chance to assist with the early work for the cancer project. And I enjoyed our conversations during the early days of the experiment.

To Dr. Charles Spencer, thank you for your valuable insight and questioning over the many years of poster presentations and now as a member of my committee. I don't know how you manage, but you always have a way of making me double-think myself.

To Dr. Benjamin Flores, I owe you and the LSAMP program way more than a thank you. Your support during our unprecedented times was way beyond what was expected. I am here if you ever need anything.

To my ever-growing family and friends, you know that you all mean the world to me. To my parents, thank you for your support as I found my way through life. From giving me my first chemistry set and microscope to my choice to join the Army, you stood beside me. It was challenging to let me make my own mistakes, but sometimes experiments take a while. To my

children, I want to thank you both for your sacrifice during my time in school and during my time in the Army. Just know that I love you. I am the biggest fan you never knew you had.

Abstract

Chagas disease (CD) and cutaneous leishmaniasis (CL) are neglected tropical diseases caused by the protozoan trypanosomatids, *Trypanosoma cruzi* and *Leishmania* spp., respectively. There are approximately 6-8 million people infected with *T. cruzi* worldwide and ~300,000 people in the US. Between 700,000 and 1.2 million new cases of CL occur worldwide yearly. The approved chemotherapies for both diseases are partially effective and may cause serious adverse events, resulting in premature treatment interruption. Moreover, no effective vaccine for either disease is available. Therefore, developing a vaccine that would provide effective cross-protection against both diseases would provide a cost-effective alternative to the existing toxic chemotherapies. Due to the evolutionary loss of the α1,3-galactosyltransferase (α1,3-GalT) gene in humans and Old-World nonhuman primates, α-galactopyranosyl (α-Gal) epitopes highly expressed on both *Trypanosoma cruzi* and *Leishmania* spp. cell surfaces are highly immunogenic. We have previously shown that synthetic α-Gal-based vaccines can effectively protect against either murine acute *T. cruzi* or *L. major* infection. We also explore a β-galactofuranosyl (β-Gal*f*) epitope as potential vaccine candidate against *T. cruzi* and *L. major* co-infection since this sugar is highly abundant in these kinetoplastids, but absent in humans and all other mammals. We, therefore, hypothesize that a synthetic α-Gal- and/or β-Gal*f*-based vaccine could provide effective cross-protection against a co-infection with *T. cruzi* and *L. major* (and other α-Gal- an/or βGal*f*-expressing *Leishmania* species). Here we use an α1,3-GalT- knockout (α1,3-GalT-KO) murine model to evaluate the efficacy of two new synthetic neoglycoproteins (NGPs), NGP28b and NGP29b, containing nonreducing, terminal α-Gal*p* and β-Gal*f* glycotopes, respectively, found in both parasites and absent in the α1,3-GalT-KO mouse, as potential vaccine candidates against CD

and CL. Our data suggests that both vaccine candidates induce a robust cross-protective immune response. This leads to a significant reduction in the parasite burden, enhances animal survival, and triggers a potent Th1 response. Additionally, these vaccines elicit a cytokine profile that promotes class-switching events in this co-infection experimental model.

Table of Contents

Dedication iii

Acknowledgements v

Abstract viii

Table of Contents x

List of Figures xiv

List of Illustrations xvii

Chapter 1: General Introduction 1

Chagas Disease 1

Epidemiology of Chagas disease 1

T. cruzi lifecycle and routes of infection 2

Clinical manifestations of Chagas disease 4

Current treatments of Chagas disease 5

Leishmaniasis 6

Epidemiology of leishmaniasis 6

Clinical manifestations of tegumentary leishmaniasis 7

Current treatments of leishmaniasis 10

Leishmania spp. lifecycle and routes of infection 10

The α-Gal Epitope 12

Loss of α-Gal Expression in Humans and Old-World Non-Human Primates 12

Human Immunogenicity/Antigenicity to the β-Galactofuranosyl (β-Gal*f*) Glycotope 13

Glycobiology of *Trypanosoma cruzi* Leishmania spp. 15

T. cruzi and *Leishmania* glycocalyx 15

Experimental Vaccine Development for Chagas disease and leishmaniasis. 21

Chapter 2: Synthetic glycovaccines elicit cross-protection against Chagas disease and cutaneous leishmaniasis in a murine co-infection model 24

Rationale for vaccine development against both Chagas disease and cutaneous leishmaniasis 24

Hypothesis 25

Specific Aim 25

Methodology 26
Mice 26
Parasites and mammalian cell culture 26
Neoglycoprotein Vaccines 27
Immunization and parasite challenge 27
In vivo whole-body bioluminescence imaging 28
Chemiluminescent enzyme-linked immunosorbent assay 28
T. cruzi CL Brener$_{Luc}$ TCT lysate preparation 29
Immunoblotting of CL-Brener$_{luc}$ TCT lysate with sera from vaccinated mice ...30
Tissue-Specific qPCR 30
Statistical Analysis 31
Results 32
L. major type-II-like GIPL-based NGPs successfully decrease parasite burden in a murine co-infection model 32
Type-2 GIPL-like NGPs Elicit an Effective Adaptive Immunological Response 36
Type-2 GIPL-like NGPs provide tissue-specific protection from parasitemia...41
Discussion 45
Chapter 3: Type-II GIPLs elicit a robust Th1 immunological profile in splenocytes upon ex-vivo stimulation. 47
Rationale 47
Hypothesis 47
Specific Aim 47
Methodology 48
Mice 48
Parasites and mammalian cell culture 48
T. cruzi CL Brener$_{luc}$ TCT lysate preparation 49
Immunoblotting of CL-Brener$_{luc}$ TCT lysate with sera from vaccinated mice ...49
Neoglycoprotein Vaccines 50
Immunization and parasite challenge 50
Ex-vivo stimulation of splenocytes 51
Statistical Analysis 52
Results 53

Determination of the proper concentration and stimulation time using CL-Brenner$_{luc}$ TCT lysate-vaccinated mice using the Codeplex murine adaptive immune Kit 53

Synthetic glycovaccines elicit a predominant CD4^{+}/Th1^{+} T-cell response upon ex-vivo stimulation. 59

Synthetic glycovaccines elicit an adaptive cytokine response upon ex-vivo stimulation 60

Discussion 67

Chapter 4: Ex-vivo evaluation for the efficacy of b-Galf vaccine, potential use as a veterinary vaccine against Chagas disease and cutaneous leishmaniasis in a murine co-infection model 69

Rationale 69

Hypothesis 70

Specific Aim 70

Methodology 71

Mice 71

Neoglycoprotein Vaccines 71

Immunization 71

Chemiluminescent enzyme-linked immunosorbent assay 72

CL Brener$_{luc}$ TCT parasite lysate preparation 73

Immunoblotting of CL Brener$_{luc}$ TCT lysate with sera from vaccinated mice 73

Ex-vivo stimulation of splenocytes 74

Statistical Analysis 75

Results 76

Evaluation of NGP29b as a Veterinary Vaccine Candidate Against T. cruzi Infection 76

Synthetic β-Galf glycovaccine fails to elicit a CD4^{+} T-cell response upon Ex vivostimulation in a murine model 79

Discussion 81

Chapter 5. Overall Discussion 83

REFERENCES 86

APPENDIX 107

List of Abbreviations 107

Curriculum Vita 111

List of Figures

Figure 1.1. Estimated number of individuals infected with *T. cruzi* living in non-endemic countries. Reproduced from (Rassi, Rassi et al. 2010). 2
Figure 1.3. Status of endemicity of leishmaniasis worldwide. (A) Cutaneous leishmaniasis and (B) visceral leishmaniasis worldwide, 2019. Reproduced from (World Health Organization 2020, March 02). 8
Figure 1.4. Clinical manifestation of CL. (A) Ulcer with raised borders and crusts. (B) Atopic stage of Chiclero's ulcer with deforming scaring of the ear. (C) Diffused cutaneous leishmaniasis. Image reproduced and adapted from (Torres-Guerrero, Quintanilla-Cedillo et al. 2017). 9
Figure 1.5. Life cycle of *Leishmania* spp. Reproduced from (Centers for Disease Control 2020) (https://phil.cdc.gov/details.aspx?pid=3400). 12
Figure 1.6. The surface coat of *T. cruzi*. (A-B) T. cruzi host-cell-derived trypomastigote exhibits a complex cell surface, consisting of several glycoconjugates (glycoproteins and glycolipids) inserted into the plasma membrane via a GPI-anchor. These glycoconjugates include the GIPLs and GPI-anchored proteins (GPI-APs) (i.e., tGPI-mucins, TSs, and MASPs). These GPI-APs are multigene families encoded by ~20% of the parasite genome. Several of the gene members are expressed simultaneously in the mammal-dwelling trypomastigote stage, resulting in considerable surface heterogeneity (Buscaglia, Campo et al. 2006, Acosta-Serrano, Hutchinson et al. 2007, Giorgi and de Lederkremer 2011, De Pablos and Osuna 2012, Mucci, Lantos et al. 2017, Fonseca, da Costa et al. 2019). **(C)** tGPI- Mucin contains a polypeptide core heavily glycosylated with *O*-glycans, making up to 60% of the glycoprotein dry weight. The GPI moiety linked to the C-terminus of the protein is indicated. **(D)** The O-glycans are composed mainly of α-Gal*p* and β-Gal*p* residues **(E)**, and α-GlcNAc linked to threonine (Thr) residues. β-Gal*f* residues (not shown) are also present in some strains (e.g., Colombiana), and sialic acid (Neu5Ac) usually caps the terminal nonreducing ends in many of these *O*-glycans. The terminal, nonreducing α-Galp residues serve as major targets for the highly abundant, lytic anti-α-Gal Abs, produced during both the acute and chronic phases of CD, causing string agglutination and death of the parasites **(F)**. A small portion of these *O*-glycans (10%) exist as linear trisaccharide (Galα1,3Galβ1,4GlcNAcα), while the remaining 90% of the structures are branched and (Buscaglia, Campo et al. 2006) are as yet to be structurally characterized. The hypothetical linkages (*) of the branched *O*-glycans are based on partial liquid chromatography-tandem mass spectrometry (LC-MS/MS) data analysis, following beta-elimination and permethylation of tGPI-mucin-derived *O*-glycans (Almeida et al., unpublished data). Figure and text modified and adapted from(Ortega-Rodriguez, Portillo et al. 2019). 18
Figure 1.7. The surface glycocalyx of *L. major*. The main glycoconjugates present on the surface of leishmanial promastigote cells. From left to right: LPG (lipophosphoglycan); GIPL (glycoinositolphospholipids); GPI (glycosylphosphatidylinositol) fPPG (filamentous proteophosphoglycans); sAP (secreted acid phosphatases); mPPG (membrane proteophosphoglycans). Figure and text modified and adapted from (Cabezas, Legentil et al. 2015). 19
Figure 1.8. Type-II GIPL neoglycoprotein vaccines. **(A)** Schematic representation of type-2 GIPL-1, -2, and -3 of *L. major*. The terminal glycan moiety (G29, G30, or G28) targeted for synthesis in each GIPL is indicated. Gal*p*, galactopyranose; Gal*f*, galactofuranose; Man, mannopyranose; GlcN, glucosamine; *myo*-Ins, *myo*-inositol; P, phosphate; PI,

phosphatidylinositol. **(B)** Composition of the synthetic NGP29b, NGP30b, and NGP28b. **(C)** Upper panel, schematic representation of the synthesis of NGP29b containing a type-2 GIPL-1 glycotope. TCEP-HCl, Tris (2-carboxyethyl) phosphine hydrochloride. The same procedure was used to synthesize NGP30b and NGP28b. Lower panel, MALDI-TOF-MS spectrum of NGP29b to confirm the covalent conjugation of the glycan units to the carrier protein. Singly- ($[BSA]^{+}$ and $[NGP29b]^{+}$) and doubly-charged ($[BSA]^{+2}$ and $[NGP29b]^{+2}$) ions of BSA and NGP29b are indicated. The number of glycan units covalently attached to the BSA moiety is indicated. *m/z*, mass to charge ratio. 20
Figure 2.4: Type-II GIPL-like NGPs elicit an effective adaptive Immunological response. IgG subclass production against either NGP28b (Left), or NGP29b (Right). IgG1 **(A)**, IgG2b **(B)**, IgG2c **(C)**, IgG3 **(D)**, when assessed by CL-ELISA. 41
Figure 2.5: Type-II GIPL-like NGPs provide tissue-specific protection from parasitemia in major tissues. Quantitative PCR was conducted on harvested tissues and normalized using endogenous GAPDH (**A-D**). Compared to the Placebo (co-infection → PBS) group there is a significant decrease in tissue parasite burden. Statistical analysis: Unpaired *t*-test. ****, p<0.0001; ***, p<0.001; **, p<0.01; *, p<0.05 43
Figure 2.6: Type-II GIPL-like NGPs provide tissue-specific protection from parasite burden in the footpad. Images using IVIS were captured on days 32 and 34 following the infection of mice with *L. major*$_{luc}$. The footpad IVIS images were processed by ImageJ, and the mean fluorescence intensity (MFI) was plotted for each group. Statistical analysis: unpaired *t*-test. ****, p<0.0001; ***, p<0.001; **, p<0.01; *, p<0.05 44
Figure 3.2. Secreted cytokine profiles at 16 h. Cell supernatant was collected from *ex-vivo* stimulated $CD4^{+}$ T-cells from mice vaccinated with CL Brener$_{luc}$ TCT lysate at 16 h either in untreated wells (top graphs) or anti-murine CD3e immobilized wells (bottom graphs). Cells were left unstimulated **(A)** or stimulated with either 0.5 mg **(B)** or 1 mg **(C)** of TCT lysate. 55
Figure 3.3. Secreted cytokine profiles at 24hr. Cell supernatant collected from *ex-vivo* stimulated $CD4^{+}$ T-cells from mice vaccinated with *T. cruzi* CL Brener$_{luc}$ TCT lysate at 24 h either in untreated wells (TOP) or anti-murine CD3e immobilized wells (BOTTOM). Cells were left unstimulated (A) or stimulated with either 0.5 mg **(B)** or 1 mg **(C)** of TCT lysate. 57
Figure 3.4. Secreted cytokine profile comparison at 16 and 24hrs when plated in CD3e immobilized wells. Cell supernatant collected from *ex-vivo*-stimulated $CD4^{+}$ T-cells from mice vaccinated with CL Brener$_{luc}$ TCT lysate either stimulated for 16h (top graphs) or 24 h (bottom graphs). Cells were left unstimulated **(A)** or stimulated with either 0.5 mg **(B)** or 1 mg **(C)** of TCT lysate 58
Figure 3.5. Synthetic glycovaccines elicit a predominant $Th1^{+}/CD4^{+}$ T-cell response upon *ex-vivo* stimulation. $CD4^{+}$ T-cells counts for all groups **(A)**, $Th1^{+}/CD4^{+}$ T-cells **(B)**, $Th2^{+}/CD4^{+}$ T-cells **(C)**, and $Th17^{+}/CD4^{+}$ T-cells **(D)**. Statistical analysis: Two-way ANOVA. **** = p<0.0001, ***=p<0.001, **=p<0.01, *p<0.05 59
Figure 3.6: Synthetic glycovaccines elicit robust and coordinated immune responses upon *ex-vivo* stimulation. Proinflammatory secreted cytokines responsible for macrophage and other monocyte recruitment and differentiation at the affected sited. Statistical analysis: One-way ordinary ANOVA. ****, p<0.0001; ***, p<0.001; **, p<0.01; *, p<0.05 61
Figure 3.7. Synthetic glycovaccines activate T-cells upon *ex-vivo* stimulation. Statistical analysis: One-way ordinary ANOVA**.** ****, p<0.0001; ***=p<0.001; **, p<0.01; *, p<0.05 ... 63

Figure 3.8. Synthetic glycovaccines elicit Th1-like cytokine profile in response to *ex-vivo* stimulation. One-way ordinary ANOVA**.** **** = p<0.0001, ***=p<0.001, **=p<0.01, *p<0.05 64
Figure 3.9. Synthetic glycovaccines elicit Th2 cytokines in response to *ex-vivo* stimulation leading to the formation of antibody-secreting B cells. One-way ordinary ANOVA. ****, p<0.0001; ***, p<0.001,; **=p<0.01,;*p<0.05 66
Figure 3.10. Synthetic glycovaccines do not elicit Th17 cytokines in response to *ex-vivo* stimulation..... 67
Figure 4.1. Type-II GIPL-like NGP29b elicits an effective adaptive immunological response upon vaccination in C57BL/6 mice. Total IgG was produced against either NGP29b (left), or 2ME-BSA (right), when assessed by CL-ELISA. Sera collected from mice vaccinated with 20 mg SQ three times at 7-day intervals, and then collected 7 days after the end of vaccination. Statistical analysis: Unpaired *t*-test . ****, p<0.0001; **, p<0.001; *, p<0.01; *, p<0.05. 77
Figure 4.2. Type-II GIPL-like NGP29b elicits an effective adaptive immunological response upon vaccination in C57BL/6 mice. IgM was produced against either NGP29b (left), or 2ME-BSA (right), when assessed by CL-ELISA. Sera collected from mice vaccinated with 20 mg SQ three times at 7-day intervals, and then collected 7 days after the end of vaccination. Unpaired *t*-test. ****, p<0.0001; ***, p<0.001; **, p<0.01; *, p<0.05..... 78
Figure 4.3. Type-II GIPL-like NGP29b Elicit an Effective Adaptive Immunological Response against *T. cruzi* upon vaccination in C57BL/6 mice. Sera collected from vaccinated mice, naïve, and a CD mouse serum pool, probed against 20 μg CL Brener$_{luc}$ TCT lysate..... 79
Figure 4.4. Synthetic β-Galf glycovaccine fails to elicit a CD4^{+} T-cell response upon *ex-vivo* stimulation in a murine model. Statistical analysis: Two-way ANOVA. ****, p<0.0001; ***, p<0.001, **, p<0.01; *, p<0.05..... 80

List of Illustrations

Figure 3.1. Graphical schematic of optimization experiment. 53

Chapter 1: General Introduction

CHAGAS DISEASE

Epidemiology of Chagas disease

Chagas disease (CD)[1], also known as American trypanosomiasis, is caused by the protozoan parasite *Trypanosoma cruzi* (*T. cruzi*). Chagas disease affects approximately 6-8 million people worldwide and an estimated 300,000 people in the United States (Bern 2015, Manne-Goehler, Umeh et al. 2016). Chagas disease is recognized by the WHO as one of the world's 20 most neglected tropical diseases (NTDs). Included in this list are the topmost common debilitating conditions among the world's poorest people (Hotez, Molyneux et al. 2007, Alvar, Vélez et al. 2012). Chagas disease was first identified over 100 years ago by the Brazilian physician Carlos Chagas, who reported on the acute clinical manifestations and the cycle of transmission (Chagas 1909).

Since their discovery, there have been six distinct typing units (DTUs) or genotypes (TcI-VI) of *T. cruzi* characterized that cause disease in humans, and a more recent DTU isolated from bats (Tcbat) (Zingales, Miles et al. 2012, Zingales 2018). However, considered endemic to Latin America, CD has spread worldwide as a result of global migratory flows in recent years (**Figure 1.1**) (Gascon, Bern et al. 2010, Rassi, Rassi et al. 2010, Bern 2015, Manne-Goehler, Umeh et al. 2016). Other countries such as Australia, Canada, and Japan have also lately seen a significant increase in the number of CD cases (Gascon, Bern et al. 2010, Rassi, Rassi et al. 2010, Bern 2015, Manne-Goehler, Umeh et al. 2016).

---

[1] The List of Abbreviations can be found in the Appendix, pages 109-112.

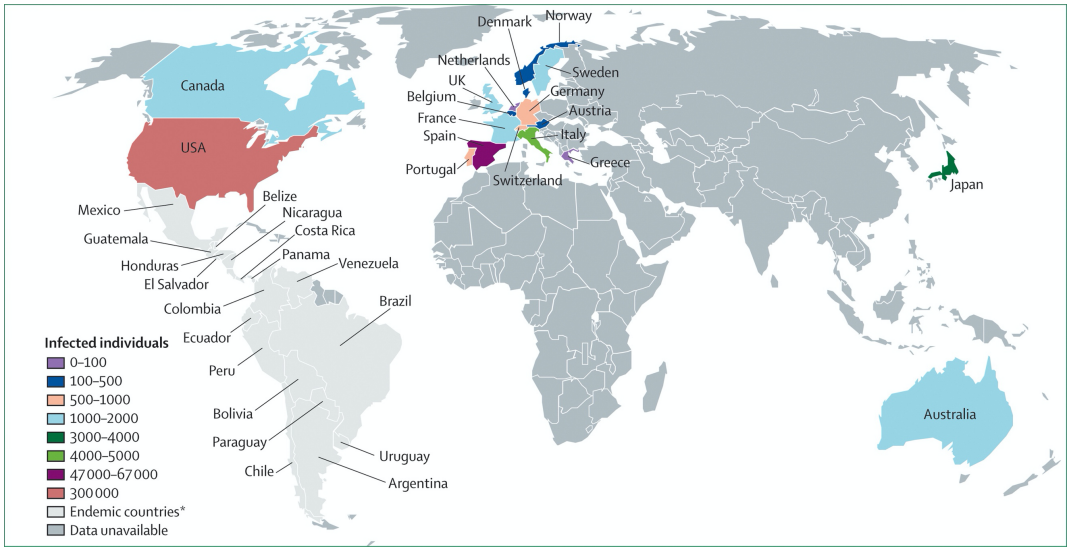

Figure 1.1. Estimated number of individuals infected with *T. cruzi* living in non-endemic countries. Reproduced from (Rassi, Rassi et al. 2010).

T. cruzi lifecycle and routes of infection

T. cruzi infection in humans naturally occurs through vector-borne transmission, the infection cycle begins when a person is bitten by a *T. cruzi*-infected triatomine (Reduviidae) bug, also popularly known as the *kissing bug*. After taking a blood meal, the bug defecates, and *T. cruzi*-containing feces are excreted near the bite wound, exposed eye or oral mucosa, through which the parasite can enter the host's body (**Figure 1.2**) (Rassi, Rassi et al. 2010). This route of infection, however, is not the only way for the parasite to enter and infect humans, as there have been increasing cases of infection through routes such as blood transfusion, organ transplantation, tainted juices, and congenital transmission from mother-to-newborn child. The triatomine bug is infected when it takes a blood meal from an infected mammalian host containing the bloodstream trypomastigote form of the parasite (**Figure 1.2**) (Rassi, Rassi et al. 2010). Once inside the midgut

of the triatomine vector, the parasite then transforms into the replicative epimastigote, where it multiplies by binary fission. Once the bloodmeal is fully digested, the epimastigotes detach from the midgut epithelium and travel to the hindgut, transforming into the infective metacyclic trypomastigote form. This form of the parasite can then be passed in the feces onto the host's skin or exposed eye or oral mucosa after the triatomine has taken a blood meal. Once inside the body, the metacyclic trypomastigote can then enter a multitude of host cells. The metacyclic trypomastigote invades a host cell and transforms into the noninfective intracellular amastigote form, which multiplies by binary fission. After several division cycles that take 2-4 days, the intracellular amastigotes multiply and transform into trypomastigotes, which then burst out of the cell to infect nearby cells or to enter the bloodstream to reach distant organs and tissues. These host-cell-derived trypomastigotes can either infect new cells or be taken up in a blood meal by a triatomine bug, thus completing the natural life cycle of *T. cruzi*.

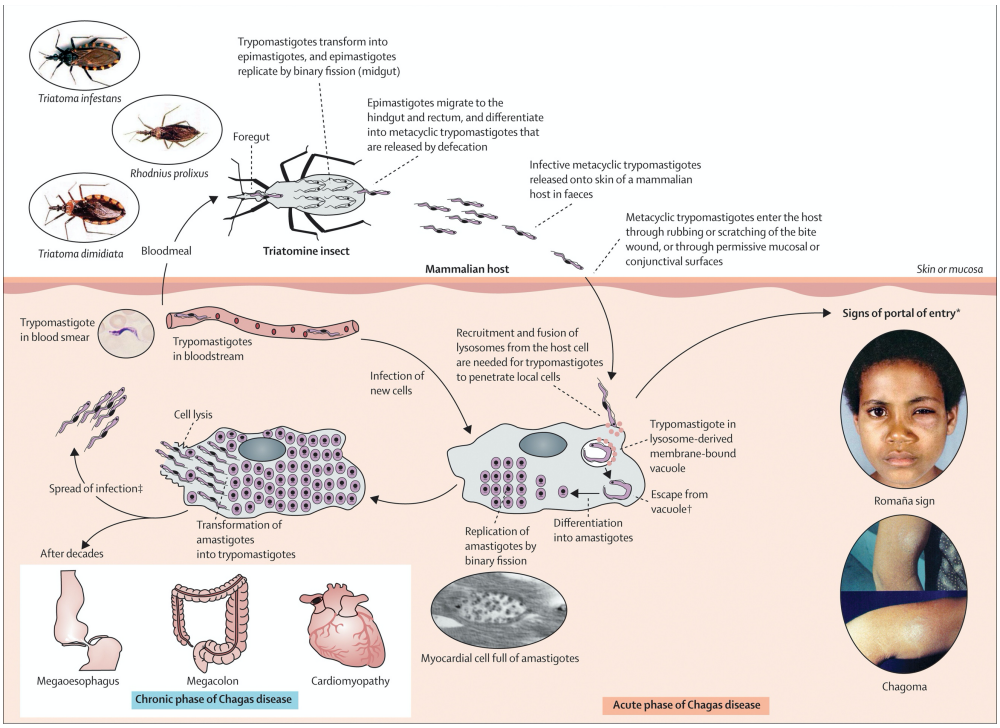

Figure 1.2. Natural life cycle of *Trypanosoma cruzi*. Figure reproduced from (Rassi, Rassi et al. 2010).

Clinical manifestations of Chagas disease

One challenge in preventing the spread of CD from endemic countries is that during the acute phase, patients typically are asymptomatic. Due to very low parasite load, in cases of vector-borne transmission, patients may only present with Romaña sign, which is an acute edema of the eyelid or chagoma (**Figure 1.1**) at the location of the insect bite (Rassi, Rassi et al. 2010).

Even if symptoms occur, they can include prolonged fever, malaise, and swollen organs (liver, spleen, and lymph nodes) that can easily be mistaken for other ailments (Rassi, Rassi et al. 2010, Bern, Martin et al. 2011, Bern 2015). Due to this lack of symptoms, patients are rarely diagnosed during the acute phase when treatment is most effective. During chronic infection, most patients will remain asymptomatic for life due to the ability of the patient's immune system to suppress parasite levels (Dutra, Menezes et al. 2014). However, due to chronic tissue

inflammation, it is estimated that approximately 30% of chronic CD (CCD) patients will develop potentially fatal complications such as cardiomyopathy. This condition often leads to cardiac dysrhythmias, aneurysms, and failure. These patients can also develop digestive mega syndromes resulting in dilatation of the esophagus or colon causing difficulties with eating or passing stool in the presence or absence of cardiac conditions (Tarleton 2001, Rocha, Teixeira et al. 2007, Machado, Dutra et al. 2012).

Current treatments of Chagas disease

Currently, only two therapeutic choices offer remarkable success rates (over 90% cure rate) in treating the acute phase of infection. These same treatments are also employed for chronic infection, though their efficacy decreases to 60-80% (Urbina 2015). These two approved treatment options for acute CD are the chemotherapeutic agents benznidazole (BZN) and nifurtimox (NFX).

Until recently, BZN was the only US Food and Drug Administration (FDA) approved treatment in the United States, and its use is only approved for children 2-12 years of age (U.S Food and Drug Administration 2018, March 27). However, at the discretion of the treating doctor, BZN can treat patients outside the FDA's recommended age group. In August 2020, NFX was also approved by the FDA for use in the treatment of CD in patients under 18 years old (U.S Food and Drug Administration 2021, January 08) Although both these drugs can be very effective in the acute phase of infection, an estimated 20-30% of patients have treatment interruption due to serious side effects or adverse events. Benznidazole may cause allergic dermatitis (itching, rash), bone marrow suppression (anemia, leukopenia, and thrombocytopenia), peripheral neuropathy (pain, weakness, or numbness, particularly in the hands and feet), gastrointestinal symptoms (nausea, vomiting, and abdominal pain), insomnia and dizziness. On the other hand, nifurtimox may cause gastrointestinal disturbances and peripheral neuropathy (similar to benznidazole), psychiatric

symptoms (mood changes, agitation, and sleep disturbances), weight loss, headaches, and dizziness. For this and other reasons (e.g., lack of biomarkers of early assessment of chemotherapy outcomes) only ~1% of CCD patients receive treatment (Manne-Goehler, Reich et al. 2015, U.S Food and Drug Administration 2018, March 27, U.S Food and Drug Administration 2021, January 08).

LEISHMANIASIS

Epidemiology of leishmaniasis

Leishmaniasis, like Chagas disease, is recognized by the WHO as one of the top 13 neglected tropical diseases (Hotez, Molyneux et al. 2007, WHO 2011). It is a worldwide vector-borne disease transmitted through the bite of an infected female *Phlebotomus* (Old World) or *Lutzomyia* (New World) sandflies (Torres-Guerrero, Quintanilla-Cedillo et al. 2017). Broadly, there are three clinical forms of leishmaniasis: cutaneous leishmaniasis [CL]), mucocutaneous (MCL), and visceral (VL), which are caused by over 20 different species of *Leishmania* (Schroeder and Aebischer 2011, World Health Organization 2020, March 02). It is estimated that leishmaniasis threatens 350 million people worldwide and accounts for between 700,000 and one million new cases of CL (**Figure 1.3A**), and 50,000 to 90,000 cases of VL (**Figure 1.3B**) a year (Alvar, Vélez et al. 2012, World Health Organization 2020, March 02). A study in 2012 led by the WHO to examine the distribution and burden of CL and VL. Ninety percent of the global cases of VL occurred in Bangladesh, Brazil, Ethiopia, India, South Sudan, and Sudan (Torres-Guerrero, Quintanilla-Cedillo et al. 2017). In this study they also found that approximately 70% of CL cases were in Afghanistan, Algeria, Brazil, Colombia, Costa Rica, Ethiopia, Iran, Sudan, and the Syrian Arab Republic (Torres-Guerrero, Quintanilla-Cedillo et al. 2017).

Clinical manifestations of tegumentary leishmaniasis

Tegumentary leishmaniasis, the most common form of the infection, typically results in self-healing or chronic cutaneous lesions that are often not life-threatening. Notwithstanding that, these lesions can lead to permanent and disfiguring scarring in patients, typically on the exposed parts of the body such as the arms and face, including the nose and ears (**Figure 1.4**) (Reithinger, Dujardin et al. 2007, Torres-Guerrero, Quintanilla-Cedillo et al. 2017, World Health Organization 2020, March 02). TL has four clinical presentations: (1) cutaneous leishmaniasis (CL), which is characterized by localized or multiple ulcerative skin lesions; (2) disseminated leishmaniasis (DL), which presents multiple non-ulcerative nodules; (3) mucosal or mucocutaneous leishmaniasis (ML), which is characterized by destruction of the nasopharyngeal mucosa that occurs 1-5 years after CL lesions have healed (1-10% of patients); and (4) subclinical form (SC), characterized by absence of any typical clinical symptoms (cutaneous or mucosal lesions), but presence of a strong delayed-type hypersensitivity as detected by Montenegro (or leishmanin) skin test (Marsden 1986, Davies, Reithinger et al. 2000, Scorza, Carvalho et al. 2017). Out of the over 20 different species of leishmania, some of the causal agents for TL are: *L. tropica* (CL), *L. mexicana* (CL, DL), *L. major* (CL), *L. braziliensis* (CL, ML, DL, and SC) (Reithinger, Dujardin et al. 2007, Scorza, Carvalho et al. 2017).

A

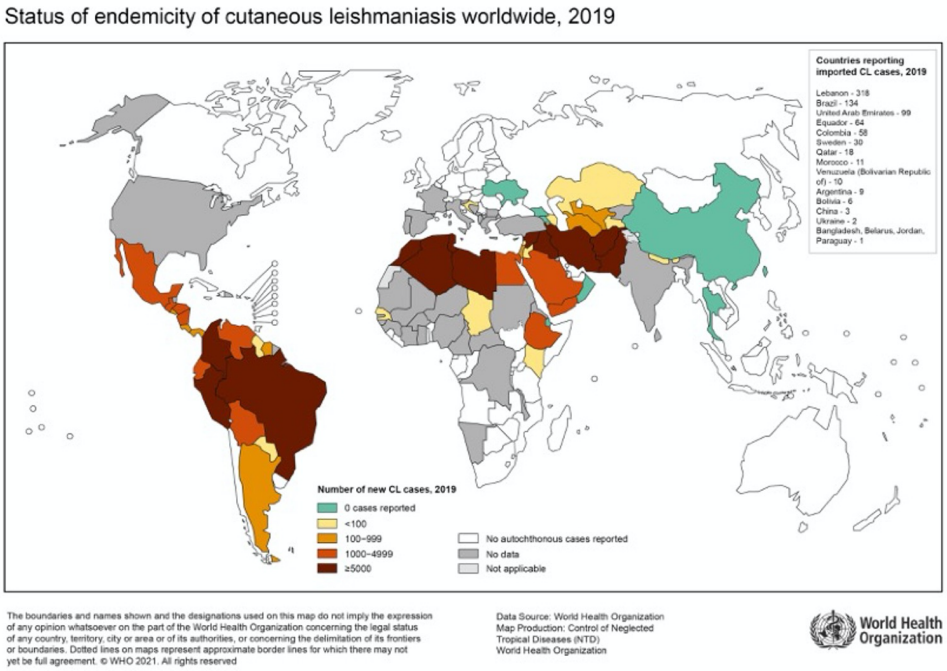

B

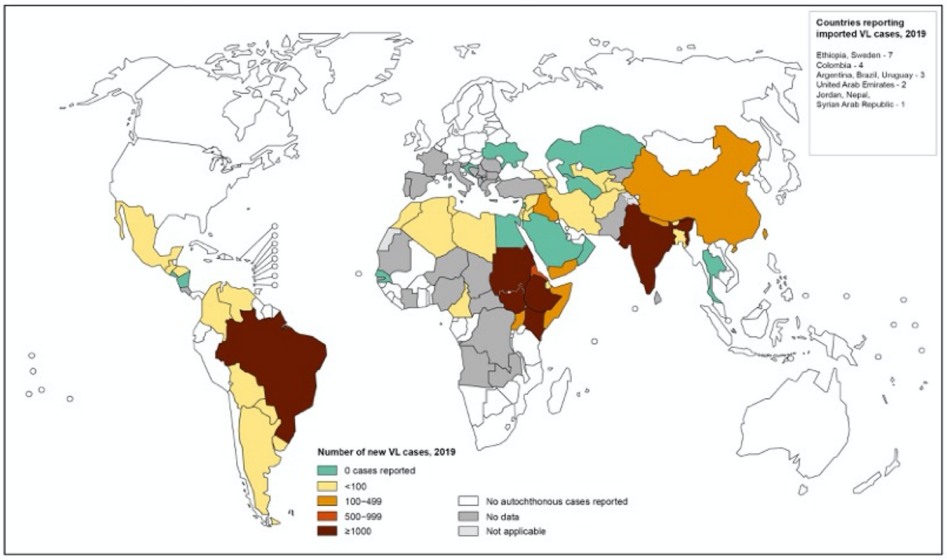

Figure 1.3. Status of endemicity of leishmaniasis worldwide. (A) Cutaneous leishmaniasis and (B) visceral leishmaniasis worldwide, 2019. Reproduced from (World Health Organization 2020, March 02).

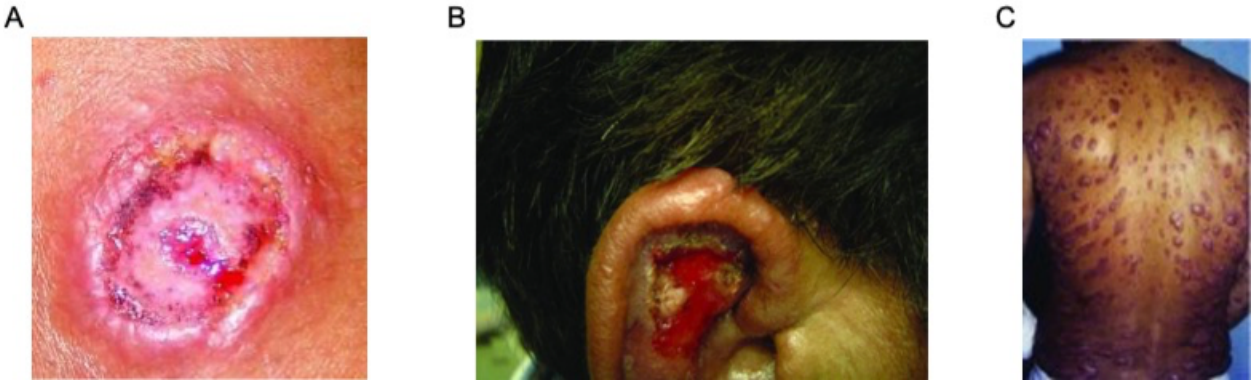

Figure 1.4. Clinical manifestation of CL. (A) Ulcer with raised borders and crusts. (B) Atopic stage of Chiclero's ulcer with deforming scaring of the ear. (C) Diffused cutaneous leishmaniasis. Image reproduced and adapted from (Torres-Guerrero, Quintanilla-Cedillo et al. 2017).

Visceral leishmaniasis, also known as *kala-azar* (black fever), is often fatal if left untreated, and it affects several organs, including the spleen, liver, and bone marrow (Schroeder and Aebischer 2011). VL cases can be found worldwide and typically include at-risk populations like children and immunocompromised and malnourished individuals (Torres-Guerrero, Quintanilla-Cedillo et al. 2017). VL is caused by several *Leishmania* species, including *L. donovani*, *L. infantum*, *L. chagasi*, *L. amazonensis*, and *L. tropica*. The incubation period for the disease ranges from 3 to 8 months before the onset of symptoms (Guerin, Olliaro et al. 2002, Desjeux 2004, Torres-Guerrero, Quintanilla-Cedillo et al. 2017). VL can manifest in a diverse set of symptoms, from fever and night sweats to lymphadenopathy, hepatomegaly, and splenomegaly (Torres-Guerrero, Quintanilla-Cedillo et al. 2017). Patients also experience other symptoms such as anorexia, weakness, and weight loss (Torres-Guerrero, Quintanilla-Cedillo et al. 2017).

Current treatments of leishmaniasis

Unlike CD, there are many treatment options for CL with varied effects depending on the causative species of infection; however, even with antileishmanial treatment, the parasite remains in the human body and can relapse if there is immunosuppression (World Health Organization 2020, March 02). Pentavalent antimonial (Sbv) compounds have been the standard treatment since the 1940s for the treatment of VL; however, these compounds cause very severe cardiac adverse events (Sundar and Chakravarty 2010). Approved by the FDA in 2014, Impavido (miltefosine, hexadecyl 2-(trimethylazaniumyl)ethylphosphate, or 2-[[(hexadecyloxy)hydroxyphosphenyl]oxy]-*N*,*N*,*N*-trimethylethylammonium iner salt) (Dorlo, Balasegaram et al. 2012) can be used in adults and adolescents over 12 years old and weighing greater than 30 kg for the treatment of VL due to *L. donovani,* and for TL/CL caused by *L. braziliensis* (also approved for MCL infection)*, L. guyanensis,* and *L. panamensis* (Food and Drug Administration 2014). Of the liposomal amphotericin B (LAMB) compounds, AmBisome® is also FDA-approved for the treatment of VL and, in some regions, has shown success in treating CL and MCL (Balasegaram, Ritmeijer et al. 2012).

Leishmania spp. lifecycle and routes of infection

Leishmaniasis infection occurs when the parasite is transmitted through the bite of a female sandfly (blood-sucking dipteran from the genus *Phlebotomus* or *Lutzomyia*) during a blood meal of a mammalian host. During the blood meal, the flagellated, motile metacyclic promastigote form of the *Leishmania* spp. parasite is injected into the skin of the mammalian host from the proboscis of the sandfly. Once the metacyclic promastigotes have entered the bite wound, they are then phagocytized by macrophages and other mononuclear phagocytic cells. After phagocytosis, the

metacyclic promastigotes transform into the non-motile replicative amastigote form and proliferate by simple division. The amastigotes will continue to divide within the cell until the cell bursts, releasing the amastigotes into the extracellular environment where they are again phagocytosed and infect other cells. When a sandfly bites an infected mammalian host, it ingests macrophages containing amastigotes as part of the blood meal. The natural transmission cycle reaches completion when, within the sandfly's gut, the amastigotes transform into metacyclic promastigotes. These promastigotes are then capable of migrating to the sandfly's proboscis, from where they can infect a new host (Kaye and Scott 2011, Centers for Disease Control 2020) (**Figure 1.5**).

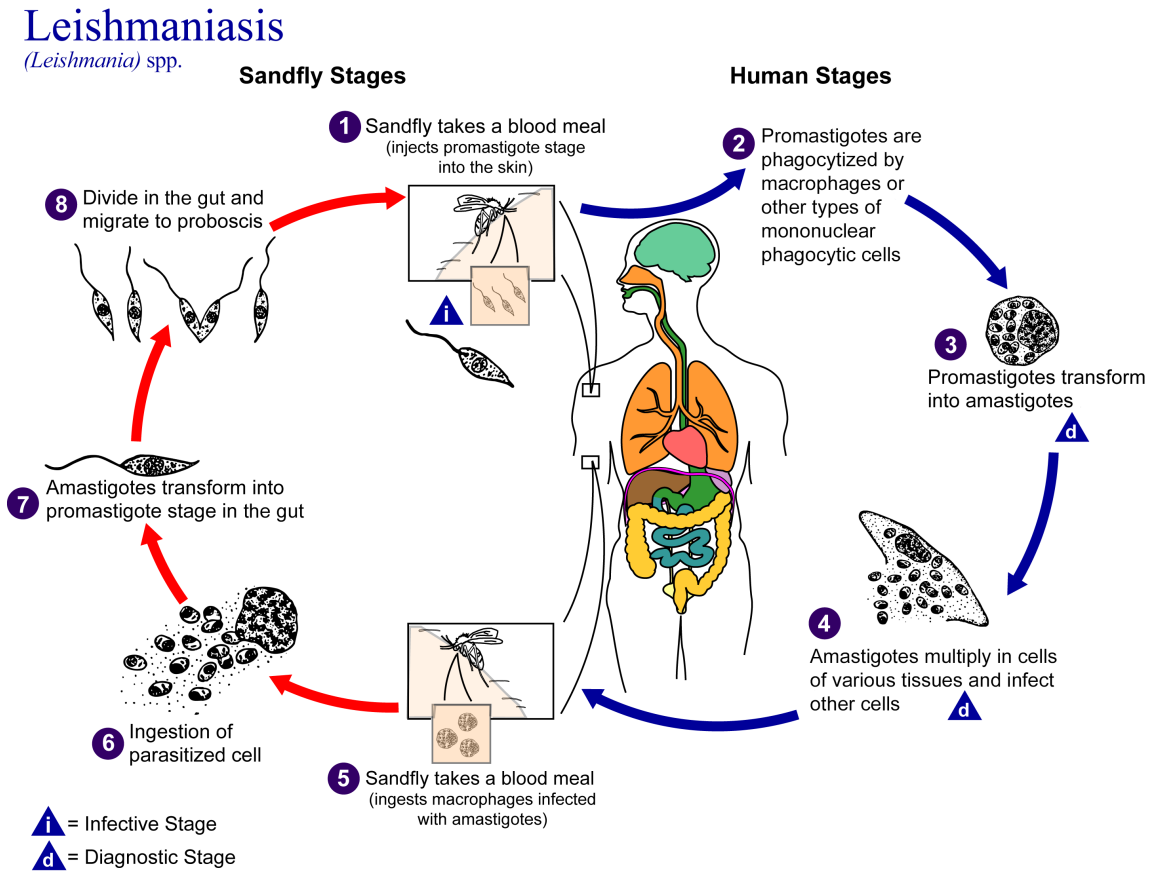

Figure 1.5. Life cycle of *Leishmania* spp. Reproduced from (Centers for Disease Control 2020) (https://phil.cdc.gov/details.aspx?pid=3400).

THE α-GAL EPITOPE

LOSS OF α-GAL EXPRESSION IN HUMANS AND OLD-WORLD NON-HUMAN PRIMATES

Due to an evolutionary loss of functional mutation that is believed to have occurred 28 million years ago, humans and Old-World nonhuman primates (OWNHPs) lack the ability to catalyze the generation of the glycan Galα1-3Galβ1-4GlcNAc (Galili's trisaccharide or epitope, or the α-Gal epitope) (Landsteiner and Miller 1925, Galili, Clark et al. 1987, Macher and Galili 2008, Galili 2016, Singh, Thompson et al. 2021). The α-Gal epitope (or glycotope) is generated by the enzyme UDP-galactose:beta-D-galactosyl-1,4-N-acetyl-D-glucosaminide alpha-1,3-galactosyltransferase, or α1,3-galactosyltransferase (α1,3GalT) enzyme (encoded by the GGTA1 gene; https://www.uniprot.org/uniprot/P50127), which transfers α-galactopyranose (α-Gal*p*) from uridyl-diphosphate-Gal (UDP-Gal) onto the nonreducing terminal end of N-acetyllactosamine (Galβ1,4GlcNAc) of glycoproteins and glycolipids (Galili, Clark et al. 1987, Galili and Swanson 1991, Macher and Galili 2008) (https://enzyme.expasy.org/EC/2.4.1.87) . The loss of function in humans and OWNHPs resulted in a GGTA1 pseudogene that lacks the ability of the α1,3-GalT enzyme (Galili, Clark et al. 1987, Galili and Swanson 1991, Macher and Galili 2008). It is believed that this evolutionary loss of function was driven by the significant selective pressures of pathogenic bacteria during primate evolution (Singh, Thompson et al. 2021). Due to the absence of α-Gal expression in humans and OWNHPs, this epitope elicits a strong immune response. The ongoing stimulation of the immune system by glycans on the O-antigen side chains of lipopolysaccharides (LPS) from Gram-negative enterobacteria (e.g., *E. coli, Klebsiella, Serratia,*

and Salmonella) which express α-Gal, leads humans to produce natural α-Gal antibodies. These antibodies comprise 1-5% of the total IgM and IgG circulating in a healthy adult's bloodstream (Macher and Galili 2008, Galili 2018).

HUMAN IMMUNOGENICITY/ANTIGENICITY TO THE β-GALACTOFURANOSYL (β-GAL*F*) GLYCOTOPE

Another very promising epitope that has been identified as highly immunogenic to humans is the beta-galactofuranosyl (β-Gal*f*) glycotope, synthesized by the enzyme beta-galactofuranosyltransferase (β-Gal*f*T*)*, which catalyzes the transfer of a galactofuranosyl (Gal*f*) moiety from UDP-α-D-Gal*f* to specific acceptors(Richards and Lowary 2009, Chlubnova, Legentil et al. 2012). First identified in 1937 in *Penicillium charlesii* (Haworth, Raistrick et al. 1937), the β-Gal*f* glycotope has since been identified in many pathogenic organisms such as bacteria, fungi, and protozoa to include trypanosomatids (Seničar, Lafite et al. 2020). In *Leishmania major*, the β-Gal*f* epitope, found in lipophosphoglycan (LPG) and type-2 glycoinositolphospholipids (GIPLs) (McConville and Ferguson 1993), is synthesized by the beta- Gal*f*T, also known as LPG1 (Ati, Colas et al. 2018). Terminal nonreducing β-Gal*f* residues are also components of the major GIPL (formerly, lipopeptidoglycan, LPPG) species from *T. cruzi* of all strains thus far studied (de Lederkremer and Colli 1995, Previato, Wait et al. 2004, de Lederkremer and Agusti 2009). Since the β-Gal*f* glycotope is entirely absent in humans, a very strong humoral immune response has been observed in CD patients (Schnaidman, Yoshida et al. 1986, de ARRUDA, COLLI et al. 1989, Golgher, Colli et al. 1993, Travassos and Almeida 1993, Montoya, Gil et al. 2022). Furthermore, unlike anti-α-Gal Abs, normal human serum (NHS) does not normally contain significant amounts of anti-β-Gal*f* Abs unless an individual has been recently infected with a microorganism that expresses β-Gal*f*, *e.g.*, certain *Leishmania* species, bacteria (McNeil, Wallner et al. 1987, Mamat,

Seydel et al. 1999), or fungi (Marino, Rinflerch et al. 2017). Structural analysis of the major GIPLs species of *T. cruzi* epimastigote forms has shown that the conserved oligosaccharide core, Manα1,2Manα1,6Manα1,4GlcN (Man, mannose; GlcN, glucosamine), may be extended with another Man residue, and with one or two β-Gal*f* residues (Previato, Gorin et al. 1990, de Lederkremer, Lima et al. 1991). In fact, the most abundant *T. cruzi* GIPL thus far reported has the glycan core composed of Gal*f*β1,3Manα1,2[Gal*f*β1,3]Manα1,2Manα1,6Manα1,4[AEP6]GlcN (AEP, aminoethylphosphonate; GlcN, glucosamine) (Previato, Gorin et al. 1990, de Lederkremer, Lima et al. 1991). Moreover, some *T. cruzi* strains (Colombiana and Tulahuén) and clone (Dm28c), express mucin *O*-glycans with terminal nonreducing β-Gal*f* residues(Mendonça-Previato, Penha et al. 2013). Studies on the glycosylphosphatidylinositol (GPI) anchors of the mammalian tissue-culture trypomastigote (TCT)-derived mucins (tGPI-mucins, or tGPI-MUCs) of the Y strain have shown that they consist of 4-8 hexoses with a Man/Gal ratio of 4:2.5 (Almeida, Camargo et al. 2000). Previous studies have shown that the sera of chronic CD (CCD) patients contain not only anti-α-Gal Abs, but also anti-β-Gal*f* Abs(Schnaidman, Yoshida et al. 1986, Milani and Travassos 1988, Golgher, Colli et al. 1993, Travassos and Almeida 1993). The major molecular targets of anti-β-Gal*f* Abs in CD are most likely protein-free GIPLs and β-Gal*f*-containing *O*-glycans on GPI-anchored glycoproteins (e.g., GPI-MUCs) of the infective insect-vector-derived metacyclic trypomastigote (Meta) and mammal-dwelling TCT forms (Almeida, Krautz et al. 1993, Golgher, Colli et al. 1993, de Lederkremer and Colli 1995, Serrano, Schenkman et al. 1995, de Lederkremer and Agusti 2009, Giorgi and Lederkremer 2020) Recently, using the reversed immunoglycomics approach, our laboratory and collaborators have reported the synthesis of *T. cruzi* GIPL-derived Gal*f*β1,3Manpα-$(CH_2)_3$SH (glycan G29SH) and Gal*f*β1,3Man*p*α1,2- [Gal*f*β1,3]Man*p*α-$(CH_2)_3$SH (glycan G32SH), and preparation of neoglycoproteins (NGPs) NGP29b and NGP32b (Montoya,

Gil et al. 2022). These novel NGPs were evaluated in a chemiluminescent enzyme-linked immunosorbent assay (CL-ELISA) with sera from CCD and healthy individuals. Receiver-operating characteristic (ROC) analysis revealed that NGP32b can distinguish CCD sera from sera of healthy individuals with 85.3% sensitivity and 100% specificity. This suggests that Gal*f*β1,3Man*p*α1,2-[Gal*f*β1,3]Man*p*α is an immunodominant glycotope in *T. cruzi* and that NGP32b could potentially be employed as a novel biomarker (BMK) for CCD.

GLYCOBIOLOGY OF *TRYPANOSOMA CRUZI* LEISHMANIA SPP.

T. CRUZI AND *LEISHMANIA* GLYCOCALYX

T. cruzi has very complex surface coats that consist of glycoproteins containing highly immunogenic *O*-linked oligosaccharides that are typically anchored to the extracellular surface of the plasma membrane by a GPI anchor (Buscaglia, Campo et al. 2006). The major parasite GPI-anchored proteins are the mucins, *trans*-sialidases (TSs), and mucin-associated surface proteins (MASPs), and the main glycolipids are the glycoinositolphospholipids (GIPLs), as shown in **Figures 1.6 and 1.7**. Throughout the life cycles of both parasites, the differential expression of these GPI-anchored proteins can be observed and has been proposed to be a means of immune evasion. The type-2 GIPLs are the most abundantly expressed surface molecule in the epimastigote and metacyclic forms of *T. cruzi*. The ceramide motif of these GIPLs has been shown to down-regulate murine T-cell activation, while antibody production through B-cell activation still occurs from the glycan chain, demonstrating a mechanism of both immune activation and suppression(Bento, Melo et al. 1996, Gazzinelli, Camargo et al. 1997).

One of the first studies to identify the anti-α-Gal antibodies (Abs) found that patients with Chagas' disease had high levels of antibodies to mouse laminin, which contains the trisaccharide Galα1,3Galβ1,4GlcNAcβ (Galili epitope) on its N-glycans (Szarfman, Terranova et al. 1982). These findings increased interest in the potential of the autoimmune characteristics of the antibodies found in CD cardiomyopathy. This increased interest paved the road for multiple studies where it was determined that mouse and bovine laminins contain large amounts of α-Gal glycotopes (Rao, Goldstein et al. 1983, Arumugham, Hsieh et al. 1986). Furthermore, in a study on the antibodies found in the blood of rhesus monkeys infected with *T. cruzi* and in the blood of patients with American cutaneous leishmaniasis, much higher antibody titers against α-Gal epitopes were observed than the naturally occurring anti-α-Gal antibodies found in healthy human sera (Towbin, Rosenfelder et al. 1987).

In *T. cruzi,* this epitope was discovered when *T. cruzi* trypomastigotes were sequentially extracted with organic solvents and three fractions were obtained. The first fraction, F1, had a strong reaction with patient serum but not with purified Ch anti-α-Gal Abs. The fractions F2 and F3 maintained the reactivity with purified Ch anti-α-Gal Abs (Almeida, Krautz et al. 1993, Almeida, Ferguson et al. 1994). Multiple studies of the glycolipids in multiple *Leishmania* spp. found that some of the GIPLs contain the terminal epitopes Galα1,3Gal, Galα1,6Gal, and Galα1,3Man (McConville, Collidge et al. 1993, McConville and Ferguson 1993, Schneider, Rosat et al. 1993). The protective activity of the anti-α-Gal Abs has been rather well studied in the context of Chagas disease when compared to that of *leishmaniasis*, where the literature is rather sparse. *In vitro* studies where *T. cruzi* trypomastigotes were incubated with purified Ch anti-α-Gal antibodies and complement resulted in classical complement-mediated cytolysis of the parasites (Milani and Travassos 1988, Almeida, Milani et al. 1991). However, this is not the only mechanism

by which anti-α-Gal Abs can effectively kill *T. cruzi*. It has been shown that in the absence of complement the Ch anti-α-Gal Abs primarily of the IgA and IgM isotypes form clusters with the glycoconjugates causing perturbation and destruction of the membrane of the parasite leading to direct cytolysis (Gazzinelli, Pereira et al. 1991, Travassos and Almeida 1993, Pereira-Chioccola, Acosta-Serrano et al. 2000). These mechanisms of parasite lysis do not come without a potential escape mechanism by the parasite, *T. cruzi* is able to sequester sialic acid from the host by the TS enzyme and cap its surface glycoconjugates (especially, tGPI-MUC), thus protecting the parasite against the lysis by Ch anti-α-Gal Abs (Schenkman, Jiang et al. 1991, Pereira-Chioccola, Acosta-Serrano et al. 2000). Previous findings indicate that the negative charge and steric hindrance caused by the sialic acid cap provides a shield to the parasite against the powerful agglutinating and lytic activity of Ch anti-α-Gal Abs (Pereira-Chioccola, Acosta-Serrano et al. 2000). Moreover, we hypothesize that the negative charge giving by the sialyation of the Fc portion (Anthony, Kobayashi et al. 2011) of the NHS anti-α-Gal Abs, which have much lower binding to *T. cruzi* surface than the Ch anti-α-Gal Abs (Almeida, Ferguson et al. 1994, Souto-Padron, Almeida et al. 1994), could also provide a protection to the parasite.

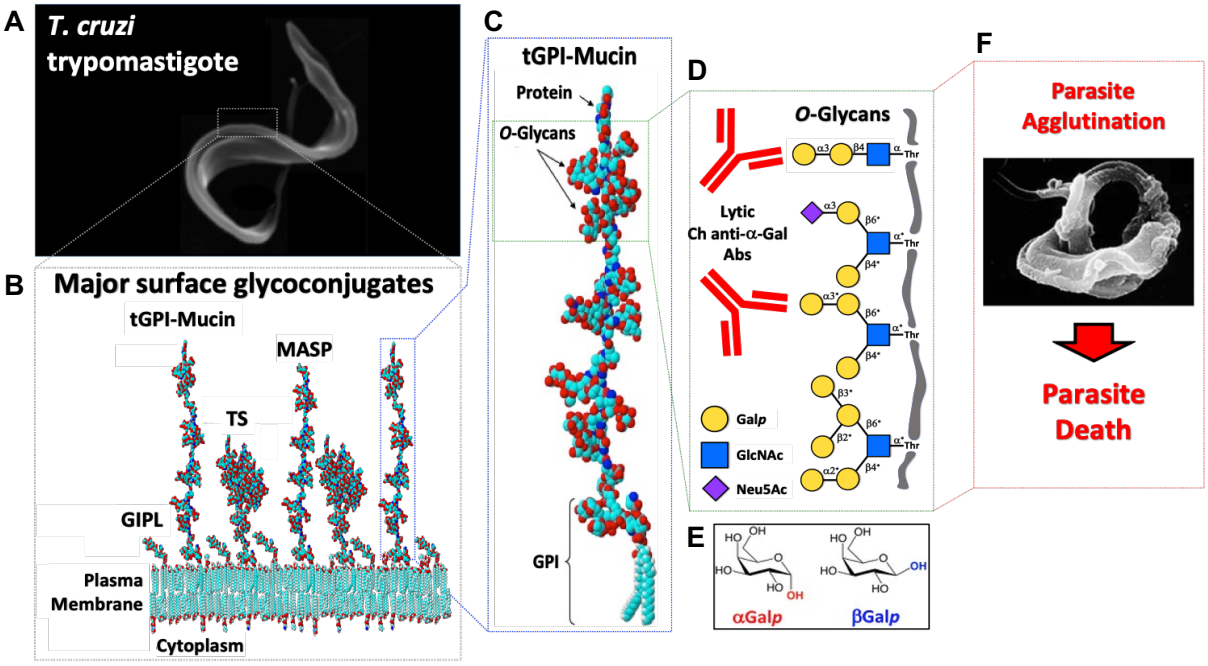

Figure 1.6. The surface coat of *T. cruzi*. (A-B) T. cruzi host-cell-derived trypomastigote exhibits a complex cell surface, consisting of several glycoconjugates (glycoproteins and glycolipids) inserted into the plasma membrane via a GPI-anchor. These glycoconjugates include the GIPLs and GPI-anchored proteins (GPI-APs) (i.e., tGPI-mucins, TSs, and MASPs). These GPI-APs are multigene families encoded by ~20% of the parasite genome. Several of the gene members are expressed simultaneously in the mammal-dwelling trypomastigote stage, resulting in considerable surface heterogeneity (Buscaglia, Campo et al. 2006, Acosta-Serrano, Hutchinson et al. 2007, Giorgi and de Lederkremer 2011, De Pablos and Osuna 2012, Mucci, Lantos et al. 2017, Fonseca, da Costa et al. 2019). **(C)** tGPI- Mucin contains a polypeptide core heavily glycosylated with *O*-glycans, making up to 60% of the glycoprotein dry weight. The GPI moiety linked to the C-terminus of the protein is indicated. **(D)** The O-glycans are composed mainly of α-Gal*p* and β-Gal*p* residues **(E)**, and α-GlcNAc linked to threonine (Thr) residues. β-Gal*f* residues (not shown) are also present in some strains (e.g., Colombiana), and sialic acid (Neu5Ac) usually caps the terminal nonreducing ends in many of these *O*-glycans. The terminal, nonreducing α-Galp residues serve as major targets for the highly abundant, lytic anti-α-Gal Abs, produced during both the acute and chronic phases of CD, causing string agglutination and death of the parasites **(F)**. A small portion of these *O*-glycans (10%) exist as linear trisaccharide (Galα1,3Galβ1,4GlcNAcα), while the remaining 90% of the structures are branched and (Buscaglia, Campo et al. 2006) are as yet to be structurally characterized. The hypothetical linkages (*) of the branched *O*-glycans are based on partial liquid chromatography-tandem mass spectrometry (LC-MS/MS) data analysis, following beta-elimination and permethylation of tGPI-mucin-derived *O*-glycans (Almeida et al., unpublished data). Figure and text modified and adapted from(Ortega-Rodriguez, Portillo et al. 2019).

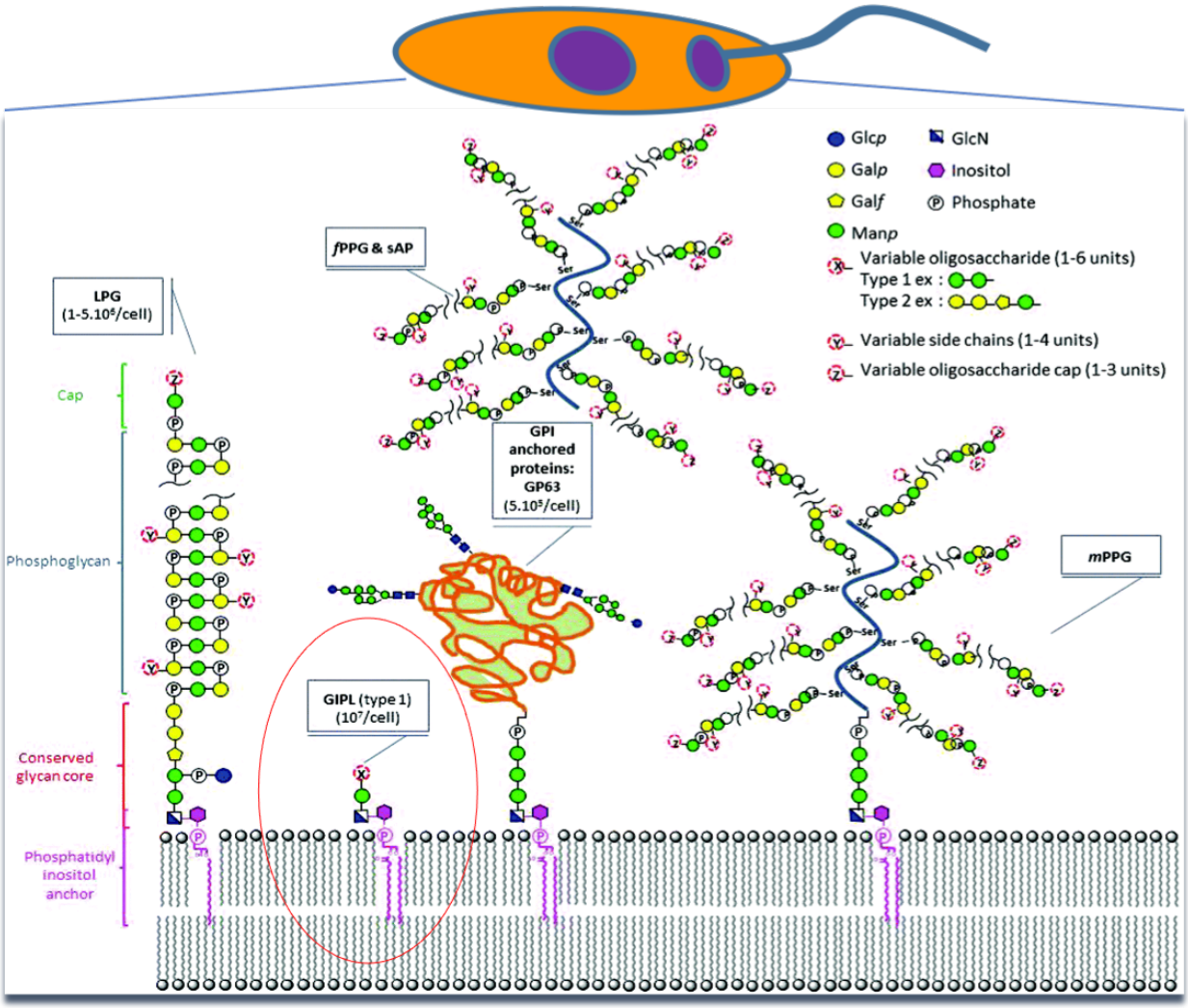

Figure 1.7. The surface glycocalyx of *L. major*. The main glycoconjugates present on the surface of leishmanial promastigote cells. From left to right: LPG (lipophosphoglycan); GIPL (glycoinositolphospholipids); GPI (glycosylphosphatidylinositol) fPPG (filamentous proteophosphoglycans); sAP (secreted acid phosphatases); mPPG (membrane proteophosphoglycans). Figure and text modified and adapted from (Cabezas, Legentil et al. 2015).

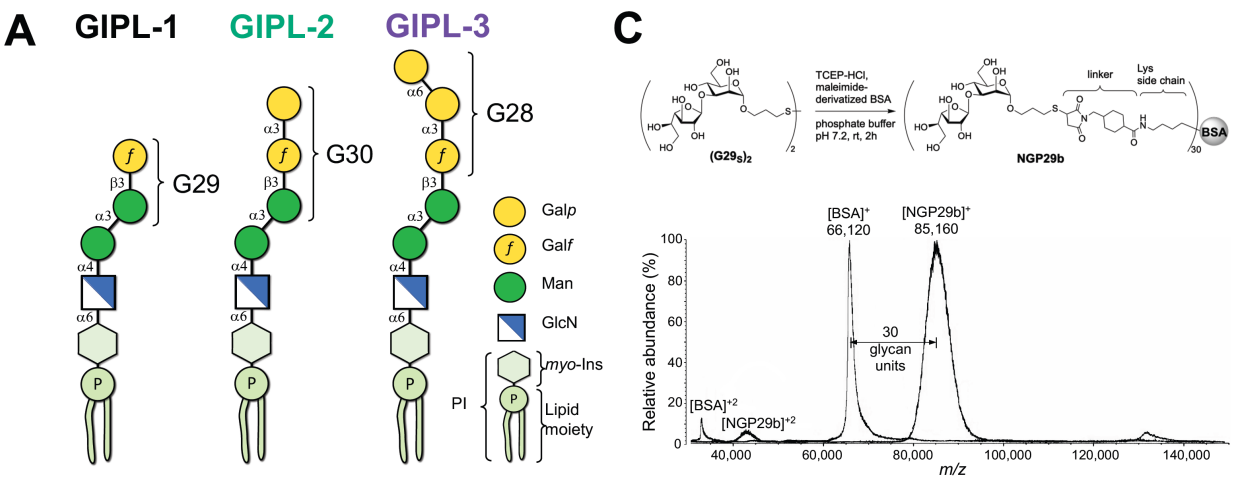

B

NGP	Derived from	Composition
NGP29b	GIPL-1	Gal*f*β1,3Manα−BSA
NGP30b	GIPL-2	Galα(1,3)Gal*f*β1,3Manα−BSA
NGP28b	GIPL-3	Galα(1,6)Galα(1,3)Gal*f*β−BSA

Figure 1.8. Type-II GIPL neoglycoprotein vaccines. **(A)** Schematic representation of type-2 GIPL-1, -2, and -3 of *L. major*. The terminal glycan moiety (G29, G30, or G28) targeted for synthesis in each GIPL is indicated. Gal*p*, galactopyranose; Gal*f*, galactofuranose; Man, mannopyranose; GlcN, glucosamine; *myo*-Ins, *myo*-inositol; P, phosphate; PI, phosphatidylinositol. **(B)** Composition of the synthetic NGP29b, NGP30b, and NGP28b. **(C)** Upper panel, schematic representation of the synthesis of NGP29b containing a type-2 GIPL-1 glycotope. TCEP-HCl, Tris (2-carboxyethyl) phosphine hydrochloride. The same procedure was used to synthesize NGP30b and NGP28b. Lower panel, MALDI-TOF-MS spectrum of NGP29b to confirm the covalent conjugation of the glycan units to the carrier protein. Singly- ($[BSA]^{+}$ and $[NGP29b]^{+}$) and doubly-charged ($[BSA]^{+2}$ and $[NGP29b]^{+2}$) ions of BSA and NGP29b are indicated. The number of glycan units covalently attached to the BSA moiety is indicated. *m/z*, mass to charge ratio.

There have been no vaccines approved for either prophylactic protection or CD treatment. Although there have not been any approved vaccines, research for potential candidates extends back almost 100 years (Rodríguez-Morales, Monteón-Padilla et al. 2015). During this time, many different approaches have been utilized to provide prophylactic protection and therapeutic treatment against CD, including live or attenuated organisms and subunit vaccines (Rios, Vázquez-Chagoyán et al. 2019). Although studies using live or attenuated vaccines in animal models have displayed mixed results dating back to the 1950s, no vaccines using *T. cruzi* parasites have been effective (Rodríguez-Morales, Monteón-Padilla et al. 2015). In a study published in 1991, serum from a human volunteer immunized with heat-killed *S. marcescens* displayed a 3-fold increase in the lysis of metacyclic trypomastigotes due to the production of protective anti-α-Gal Abs against a shared epitope with *T. cruzi* (Almeida, Milani et al. 1991). More recently, with the development of clustered regularly interspaced short palindromic repeats (CRISPR) technology (Doudna and Charpentier 2014), several groups have targeted different genes controlling the virulence of the parasite. However, it has been met with much scrutiny from the community as there is the concern of potential infection of immunocompromised patients (Sánchez-Valdéz, Pérez Brandán et al. 2015). The most promising research in developing a vaccine for CD has been aimed at targeting various subunits of the parasite either in the form of a protein or cDNA vaccine. These vaccines provide the ability to tune the immune response using an adjuvant or, in the case of the cDNA vaccines, even provide additional cytokine production. In a study conducted by Garg and Tarleton, they found that using *T. cruzi* TS genes *ASP-1*, *ASP-2*, and *TSA-1* in conjunction with IL-12 and GM-CSF encoding plasmids resulted in 60-80% survival in mice when challenged with a lethal challenge of *T. cruzi* when compared to 30-60% survival of mice vaccinated with just the antigen-

encoding plasmids (Garg and Tarleton 2002). Even more recently, Portillo et al. showed that the use of an α-Gal-containing vaccine, Galα1,3Galβ1,4GlcNAc bound to human serum albumin (HSA), was able to protect against a lethal challenge of *T. cruzi* and substantially decrease tissue parasitemia and cardiac tissue damage in α1,3GalT-knockout (KO) mice (Portillo, Zepeda et al. 2019).

Unlike CD, there has been a form of vaccination for CL that dates back many decades and relies on the self-healing nature of CL and the subsequent lifelong protection from future infections termed leishmanization, where a small amount of exudate from an active CL lesion was collected from a lesion and inoculated into a CL naïve individual much like the smallpox vaccine (Mohebali, Nadim et al. 2019, Pacheco-Fernandez, Volpedo et al. 2021). As with CD, many different approaches have been employed to develop a vaccine for the prophylactic protection of VL. Early research utilized crude heat-killed parasite preparations that ultimately proved ineffective in clinical trials (Schroeder and Aebischer 2011). Much like CD, more recent research for potential vaccine candidates against leishmaniasis has focused on using cDNA or protein/peptide constructs with and without adjuvants that have provided mixed results in different animal models. One particular surface glycoprotein, Mr 63,000 membrane polypeptide (gp63), has been the focus of many studies (Handman, Button et al. 1990, Abdelhak, Louzir et al. 1995, Badiee, Jaafari et al. 2009, Mazumder, Maji et al. 2011). One early study found that the gp63 fusion protein was insufficient to protect mice from the challenge of *L. major* (Handman, Button et al. 1990). However, when used in conjunction with the Toll-like receptor (TLR-9) ligand agonist CpG ODN it could induce a protective Th1 response (Badiee, Jaafari et al. 2009). Work done using the kinetoplastid membrane protein-11 (KMP-11) has shown that vaccinated hamsters were able to produce a mixed Th1 and Th-2 response against *L. donovani* challenge without the use of an

adjuvant (Basu, Bhaumik et al. 2005). In a similar study using BALB/c mice, exogenous IL-12 was required to protect from *L. major* challenge; however, under the same conditions, there was an increase in parasite burden with *L. donovani* challenge (Bhaumik, Basu et al. 2009). These mixed results provide evidence of the struggles researchers face in developing a vaccine that can provide protection across all strains of *Leishmania*. More recently, it has been shown that an α-Gal-based glycovaccine was able to effectively protect mice against a lethal *L. major* challenge (Iniguez, Schocker et al. 2017). In this study, it was found that mice vaccinated with NGP5b (Galα(1,6)Galβ-BSA) had significantly decreased footpad lesions and parasite load. The group found that the NGP could elicit a strong pro-inflammatory Th1 response, high levels of anti-α-Gal antibodies, and the activation of both memory and effector CD4+ and CD8+ T cells.

Chapter 2: Synthetic glycovaccines elicit cross-protection against Chagas disease and cutaneous leishmaniasis in a murine co-infection model

Rationale for vaccine development against both Chagas disease and cutaneous leishmaniasis

Due to an evolutionary loss of the α1,3-GalT gene in humans, apes, and Old-World monkeys, the α-Gal epitope can produce a robust immunological response. Both *T. cruzi* and *Leishmania* spp. have highly enriched terminal non-reducing α-galactopyranosyl residues on cell surface glycoconjugates. High levels of anti-α-Gal antibodies have been found in patients with CD and CL, demonstrating a robust humoral immune response to this epitope in both parasites (Avila, Rojas et al. 1989). Anti-α-Gal antibodies have been shown to kill *T. cruzi* in a complement-independent pathway due to agglutination of the parasites (Almeida, Milani et al. 1991, Pereira-Chioccola, Acosta-Serrano et al. 2000, Portillo, Zepeda et al. 2019). Previous studies with α-Gal-based NGP vaccines have shown that antibodies targeting the α-Gal epitopes can protect mice against either *T. cruzi* or *L. major* challenge (Iniguez, Schocker et al. 2017, Portillo, Zepeda et al. 2019). Given that *T. cruzi* and New-World (NW, or American) *Leishmania* species are co-endemic, and considering the high cost and severe side effects associated with their treatments, developing a vaccine effective against both parasites could be highly beneficial. Such a vaccine would not only have the potential to prevent fatal infections but also play a crucial role in curbing the global spread of these infections, which were once geographically contained.

Hypothesis

Building on previous work has shown that synthetic glycan-based glycovaccines can effectively protect against either murine acute CD or CL.

We <u>hypothesize</u> that we can develop an NGP vaccine that will effectively protect against both murine acute Chagas disease and New-World cutaneous/tegumentary leishmaniasis simultaneously.

This vaccine will provide a strong and robust immune response and sufficient memory for future recall and protection.

Specific Aim

Evaluation of efficacy of synthetic α-Gal-based glycovaccines for prophylactic protection against both murine acute Chagas disease and New-World cutaneous leishmaniasis.

In this aim, we will monitor survival and physical parasite burden by *in vivo* imaging and weight change. Anti-α-Gal and anti-β-Gal*f* antibody titers will be determined by CL-ELISA for IgG and subtypes IgG1, IgG2b, IgG2c, and IgG3 along with IgM, IgA and IgE. Tissue specific parasite load will be evaluated by real-time qPCR.

Methodology

Mice

C57BL/6 a1,3galactosyltransferase-knockout (a1,3GalT-KO) mice (Tearle, Tange et al. 1996, Thall, Murphy et al. 1996) were generously donated by Dr. Uri Galili, Rush University Medical Center, Chicago, IL. Mice were bred and maintained under biosafety level 2 (BSL-2), pathogen-free conditions at the Laboratory Animal Resources Center at The University of Texas at El Paso (UTEO). All animal procedures and studies were performed according to National Institutes of Health guidelines and approved protocols by the Institutional Animal Care and Use Committee at The University of Texas at El Paso. Female α1,3GalT-KO mice six to ten weeks old were used for all experiments.

Parasites and mammalian cell culture

Transgenic *L. major* promastigotes expressing firefly luciferase (*L. major*$_{Luc}$) (Lmj-FV1- LUC-TK *L. major* Friedlin strain, clone V1) (Roy, Dumas et al. 2000, Thalhofer, Graff et al. 2010) were grown in M199 medium supplemented with 10% heat-inactivated fetal bovine serum (FBS) and 1% penicillin-streptomycin at 28°C. Metacyclic promastigotes were isolated from cell culture by Ficoll gradient during the stationary phase as previously described (Späth and Beverley 2001). Red-shifted firefly luciferase-expressing *T. cruzi* CL Brener clone (CL Brener$_{Luc}$) (Zingales, Pereira et al. 1997) was generously donated by Dr. John Kelly (London School of Tropical Medicine and Hygiene, London, UK). Rhesus monkey kidney epithelial (LLC-MK2) cells (ATCC) were cultured in Dulbecco's modified eagle medium supplemented with 10% FBS and 1% penicillin-streptomycin at 37°C with 5% CO2. To obtain mammalian tissue-culture-derived *T.*

cruzi trypomastigotes (TCT), LLC-MK2 cells were infected with either culture metacyclic trypomastigotes or mouse- derived bloodstream trypomastigotes at a multiplicity of infection (m.o.i.) of 10 for approximately 5-7 days until parasites appeared free swimming in the medium. Medium containing TCTs was collected from cell culture flask and centrifuged for 10 min at 1,500x*g* at 4°C and incubated for 2 h to allow trypomastigotes to swim up away from cell debris pellet. TCTs were collected and washed with sterile PBS by centrifugation at 1,000x*g*, 4°C, and prepared for mouse infections.

Neoglycoprotein Vaccines

The type-II GIPL-like neoglycoprotein (NGP) vaccines Galα*p*1,6Galα*p*1,3Gal*f*β-BSA (KM28b), and Galβ*f*1,3Manα-BSA (KM29b) (**Figure 2.1.G**) were prepared in collaboration with Dr. Katja Michael's Laboratory, at the Dept. of Chemistry and Biochemistry, the University of Texas at El Paso, as previously described (Viana, Montoya et al. 2022). Briefly, mercaptopropyl glycan derivatives were synthesized and covalently coupled to commercially available maleimide-activated bovine serum albumin (BSA) (Pierce, Thermo Fisher Scientific) to generate their respective NGPs. Control NGP was obtained by blocking maleimide sites with 2-mercaptoethanol (2ME-BSA).

Immunization and parasite challenge

Groups of 6–10-week-old female C57BL/6 α1,3GalT-KO mice (n=5 per group) were immunized by subcutaneous injection on their flank with 20 mg/dose/mouse with a series of 3 vaccinations, one prime (P), and two boosts (B1, B2) 7 days apart. Controls groups including 2ME- BSA (placebo/carrier control), PBS, and a naïve group were also included and handled like experimental

groups. Blood was collected by mandibular bleed three days before prime vaccination and every seven days until experiment termination. Twenty-one days after B2 vaccination, mice were challenged in the left footpad with $1x10^5$ *L. major Friedlin*$_{luc}$ (or *L. major*$_{luc}$) metacyclic trypomastigotes. Three weeks after the *L. major* infection, mice were challenged with $1x10^4$ *T. cruzi* CL Brener$_{luc}$ (or *T. cruzi*$_{luc}$) TCTs by intraperitoneal (i.p.) injection. After 120 days post-*L. major* infection, all animals were humanely euthanized in accordance with approved protocols. All mice were monitored for weight loss, toxicity, and abnormal behavior during all stages of experimentation. The footpads were observed for swelling, and an increase of more than 6 mm was considered a criterion for terminating the experiment according to the vertebrate animal protocol. Weight loss of greater than 20% was also grounds for humane treatment termination.

In vivo whole-body bioluminescence imaging

Whole-body parasite burden was assessed in all mice using IVIS Lumina III *In Vivo* Imaging System (PerkinElmer), as previously described (Lewis, Fortes Francisco et al. 2014, Portillo, Zepeda et al. 2019). Mice were injected i.p. with 150 mg/kg D-luciferin, potassium salt (Gold Biotechnology), in 100 µL PBS, and anesthetized under 2% isoflurane gas with oxygen,10 min after D-luciferin injection. Live animal images were acquired using automatic exposure.

Chemiluminescent enzyme-linked immunosorbent assay

Anti-α-Gal antibody titers in the sera of immunized mice were determined by chemiluminescent enzyme-linked immunosorbent assay (CL-ELISA). A total of 50 µL per well- containing 125 ng of either NGP28 or NGP29 diluted in carbonate-bicarbonate buffer (CBB, pH 9.6) was immobilized on 96-well MaxiSorp microplates (NUNC, Thermo Fisher Scientific) and incubated

overnight at 4°C. Free binding sites were blocked using 200 µL per well of 1% BSA in phosphate-buffered saline pH 7.2, containing 0.05% Tween 20 (PBST, pH 7.2) for 1 h at 37°C. Mouse sera were diluted at 1:100 in PBST, and 50 µL was loaded into each well in triplicate and incubated for 1 h at 37°C. Then, 50 µL donkey anti-mouse IgG-biotin (Jackson ImmunoResearch Laboratories, Inc., West Grove, PA), or Ig isotype directly conjugated to HRP (goat anti-mouse IgG1, goat anti-mouse IgG2b, goat anti-mouse IgG2c, goat anti-mouse IgG3, goat anti-mouse IgM, goat anti-mouse IgA, or rat anti-mouse IgE (Abcam, Cambridge, MA), diluted 1:5000 in 1% BSA in PBST was added and the microplates incubated for 1 h at 37°C. Fifty microliters Pierce High Sensitivity NeutrAvidin-Horseradish Peroxidase (HRP) (Thermo Fisher Scientific), at 1:5,000 dilution in 1% BSA PBST, was loaded into each well and incubated for 1 h at 37°C. Between each incubation step above, plates were washed three times with 200 µL PBST. Finally, 50 µL SuperSignal ELISA Pico Chemiluminescent Substrate (Thermo Fisher Scientific) diluted in 0.1% BSA in CBB at 1:1:8 (substrate:enhancer:CBB, v/v/v) was loaded into each well. Relative luminescent units (RLU) were obtained by reading plate with Cytation 5 imaging reader (BioTek, Agilent Technologies).

T. cruzi CL Brener$_{Luc}$ TCT lysate preparation

Mammalian tissue-culture-derived *T. cruzi* trypomastigotes (TCT) were obtained as described above. Briefly, LLC-MK2 cells were infected with either culture metacyclic trypomastigotes or mouse-derived bloodstream trypomastigotes at a m.o.i. of 10 for approximately 5-7 days until parasites appeared freely swimming in the medium. Medium containing TCTs was collected from a HYPERFlask (Corning, Thermo Fisher Scientific) and centrifuged for 10 min at 1,500x*g* at 4°C, and incubated for 2h to allow trypomastigotes to swim up away from cell debris pellet. TCTs were collected and washed with sterile PBS by centrifugation at 1,000x*g*, 4°C, and the resuspended in 100 µL PBS containing 1% HaltTM Protease Inhibitor Cocktail (Thermo Fisher Scientific), plus 50 µg Nα-tosyl-lysine chloromethyl ketone hydrochloride (TLCK, Millipore, Sigma-Aldrich, St.

Louis, MO) (HaltT+TLCK) and subjected to 5 cycles of freezing/thawing in a dry ice/ethanol bath and a hot water bath. Samples were then brought to 1 mL with the addition of 900 µL PBS containing HaltT+TLCK. Protein concentration was then determined using the Pierce™ BCA Protein Assay Kit (Thermo Scientific), following the manufacturer's protocol, and stored at -80°C until used.

Immunoblotting of CL-Brener$_{luc}$ TCT lysate with sera from vaccinated mice

Samples containing 20 µg TCT lysate were prepared in a loading buffer in each lane of 12% Mini-PROTEAN TGX™ Precast Protein Gels (Bio-Rad) and allowed to resolve. The proteins were transferred to a PVDF membrane using the GenScript eBlot L1 protein transfer system. After transfer, the polyvinyl fluoride (PVDF) membrane was carefully wrapped in cellophane, and wells were individually cut using a sterile scalpel. The membrane was then blocked in 5% milk/TBST for 1 h, at room temperature (RT). Membranes were then individually incubated with respective sera at 1:100 dilution in 5% milk/TBST overnight (ON), by rocking at 4°C. Membranes were then probed using R&D anti-mouse IgG-HRP at 1:5,000 dilution in 5% milk/TBST at RT for 2 h. Between each incubation step, the membranes were washed 3X 5 min each in TBST by rocking at RT. Finally, the membrane was then briefly incubated (1 min) to CL reagent (Pierce™ ECL Western Blotting Chemiluminescent Substrate (Thermo Fisher Scientific; reagents A:B (1:1, v/v)), and exposed to a CL-XPosure™ Film (Thermo Fisher Scientific) **for 15-120 sec** and manually developed.

Tissue-Specific qPCR

At the experimental endpoint, mice were euthanized per the approved protocol, and tissues were collected in RNA later and stored at -80°C until further processed. At this time, the individual

tissues were weighed, and ice-cold tissue lysis buffer (Roche Diagnostics, Indianapolis, IN) was added at a ratio of 1 µL per 250 mg of tissue and then dissociated using gentlemax™M tubes on the gentleMACS™ Tissue Dissociator (Miltenyi Biotec, Auburn, CA). DNA was then extracted using the KingFisher Duo Prime- MagMax DNA multi-sample ultra 2.0 kit (Thermo Fisher Scientific). Following extraction, all DNA samples were diluted 1:100 in TE before 5 µL of diluted DNA was added to the 15 µL master mix and used for real-time quantitative PCR (qPCR). T. cruzi satellite DNA was done by using specific primers. Cruzi 1 (5′ ASTCGGCTGATCGTTTTCGA–3′) and Cruzi 2 (5′–AATTCCTCCAAGCAGCGGATA–3′), both at 750 nM and the TaqMan probe Cruzi 3 (6FAM–CACACACTGGACACCAA–MGB–NFQ) at 50 nM. The TaqMan assay GAPDH VIC NFQ-MGB was assessed using the following primers for tissue normalization and as an internal control. Standard curves were done with a spiked pool of naive tissue lysate (heart, colon, stomach, small intestine, and fat tissue) with 1×10^5 parasites/µL and diluting 1/10 in naive mouse DNA. PCR conditions were as detailed above and consisted of 50 °C for 2 min, 95 °C for 10 min, followed by 40 cycles at 95 °C and 58 °C for 1 min; fluorescence was collected after each cycle.

Statistical Analysis

All data points are represented as the average of triplicate values with their corresponding standard error of the means (S.E.M.). Kaplan-Meyer survival rate curves, unpaired *t*-test, One-way ANOVA, or Two-way ANOVA were utilized in the statistical analysis, as indicated in the figure legends. Graphs and statistical analysis were achieved using GraphPad Prism 10 Software, (GraphPad Software, Inc., La Jolla, CA).

Results

L. major type-II-like GIPL-based NGPs successfully decrease parasite burden in a murine co-infection model

In this study, two type-II GIPL-like synthetic NGP vaccines were evaluated for their potential ability to prophylactically protect against a co-infection of both *L. major* and *T. cruzi* in a C57BL/6 α1,3galactosyltransferase-knockout (α1,3GalT-KO) mouse model. To determine the effectiveness of the vaccines, female α1,3GalT-KO mice aged 6-10 weeks old (n=5 per group) were primed with 20 mg of either NGP28b or NGP29b (**Figure 2.1G**) by subcutaneous injection on the left abdominal flank and then boosted subcutaneously in the exact general location at days 7 and 14 again with 20mg of respective NGP. Blood was collected and pooled three days before prime vaccination and then collected every seven days after that to follow antibody response until experiment termination. Twenty-one days after the second vaccine boost, mice were infected with $1x10^5$ luciferase-expressing *L. major* (*L. major*$_{Luc}$) parasites by intradermal injection of the left footpad. Measurements of the footpad were taken weekly, and daily monitoring for signs of infection and edema; greater than 6mm of edema was the reason to remove the animal from the study. Twenty-one days after *L. major* infection, mice were infected with $1x10^4$ firefly luciferase-expressing *T. cruzi* CL Brener clone (CL Brener$_{luc}$) by i.p. injection. mice were infected with a 10-fold lower number of parasites than had been used in previous studies (Iniguez, Schocker et al. 2017, Portillo, Zepeda et al. 2019) to mitigate compounding issues from both parasites.

The survival of mice was tracked throughout the experiment (**Figure 2.1B**). By day 60 post-*L. major* infection, all infected mice co-infected with both parasites, but not the vaccinated ones succumbed to infection. The group vaccinated with only the carrier protein, BSA, with the

maleimide sites blocked with 2-mercaptoethanol (2-ME-BSA), only had a 20% survival showing that the carrier protein was insufficient to elicit a protective immune response against the parasites. NGP5, a type-II GIPL-3-like vaccine, had shown promise in previous studies against L. major infection alone (Iniguez, Schocker et al. 2017) only provided 40% protection (data not shown) in our current co-infection study. NGP28b, a more extended Type-1 GIPL-like vaccine, provided the best overall survival at 80% compared to 60% of the type-2 GIPL-3-like vaccine of NGP29b.

The weights of the mice were monitored weekly and normalized based on their beginning weight, and the groups' average was plotted based on grams gained or lost (**Figure 2.1B**). Records of all mice weights were maintained, and any mouse that lost more than 20% of its starting weight was removed from the study for humane reasons, as determined by the IACUC protocol. All mice lost weight after the *T. cruzi* infection. However, began to regain weight just after day 100 of the experiment. NGP29b group had the least amount of physical burden due to the infections seen by the least amount of weight loss, whereas the other treatment groups appear to have had more physical burden than even the non-vaccinated infected group.

The *In Vivo* Imaging System (IVIS, PerkinElmer) further assessed the physical burden. All groups were imaged weekly while under Isoflurane sedation with oxygen, and parasite burden was determined based on total flux [p/s]. *L. major*$_{luc}$ infection of the left footpad was suppressed in most groups up to the time of *T. cruzi* CL Brener$_{luc}$ infection. In contrast, the Placebo (co-infection followed by PBS) group showed high levels of *L. major*$_{Luc}$ infection (**Figure 2.1C**). In the IVIS imaging of the abdomen for *T. cruzi*$_{luc}$, we observed that NGP28b and NGP29b effectively prevented substantial parasite invasion compared to all other groups (**Figure 2.1D**). Over the course of the study, IVIS images were collected to visually assess the overall parasite burden (**Figure 2.1E**). As we can see by day 30 all mice had developed some degree of parasite burden.

Both NGP28b- and NGP29b-vaccinated mice had low levels of parasite invasion by this time point; however, by day 90, there was a complete loss of luminescence in the abdomen of the vaccinated mice. In the groups receiving the carrier protein (2ME-BSA) and the Placebo (co-infection followed by PBS), all mice succumbed to the disease, except for two in the 2ME-BSA carrier protein group. These two mice seemed to have a low-level infection from the outset of the experiment.

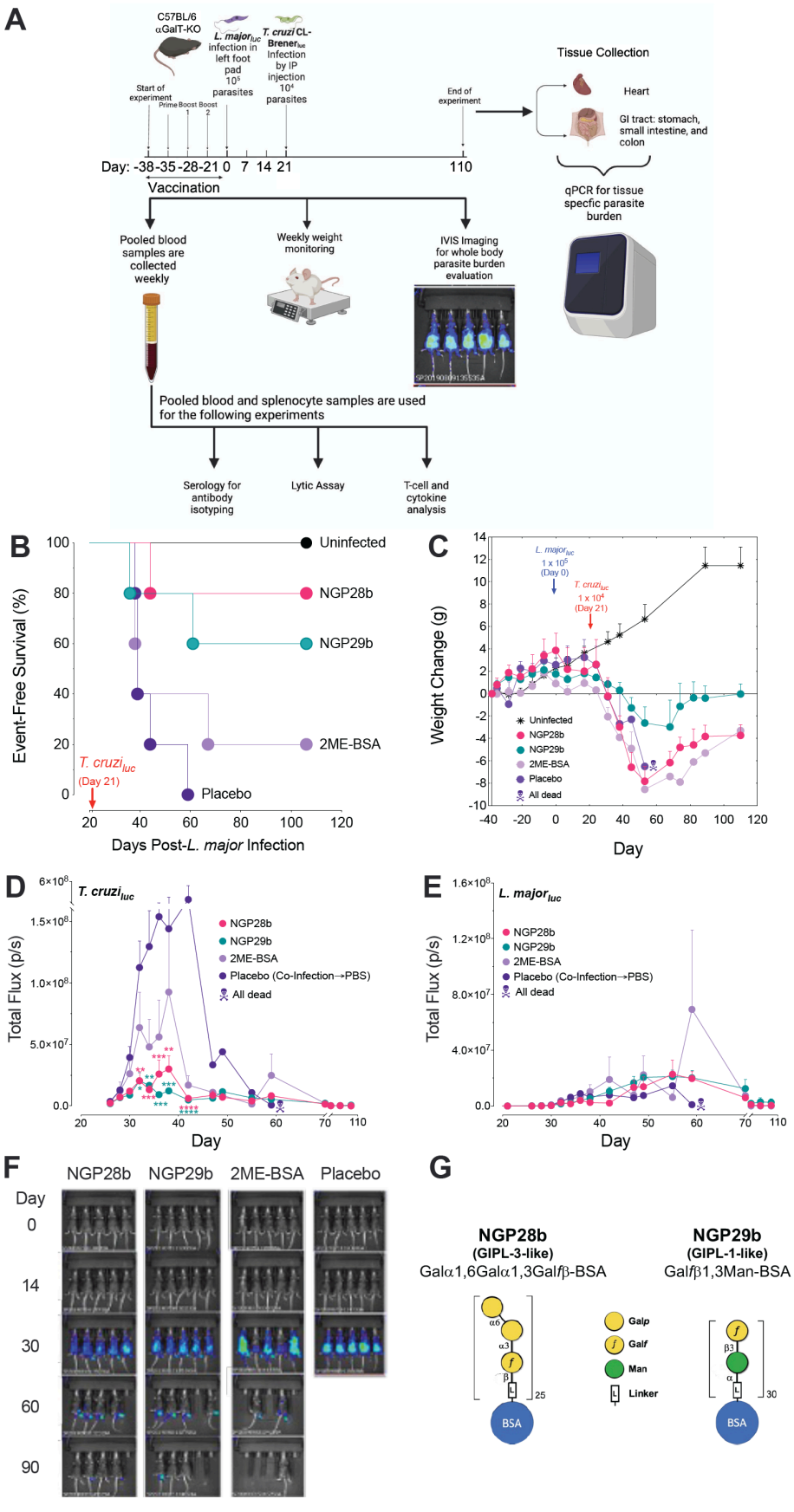
A
C57BL/6 αGalT-KO
L. major luc infection in left foot pad 10^5 parasites
T. cruzi CL-Brener luc Infection by IP injection 10^4 parasites
Start of experiment
Prime Boost Boost
1 2
Day: -38 -35 -28 -21 0 7 14 21
Vaccination
End of experiment
110
Tissue Collection
Heart
GI tract: stomach, small intestine, and colon
qPCR for tissue specfic parasite burden
Pooled blood samples are collected weekly
Weekly weight monitoring
IVIS Imaging for whole body parasite burden evaluation
Pooled blood and splenocyte samples are used for the following experiments
Serology for antibody isotyping
Lytic Assay
T-cell and cytokine analysis
B
Event-Free Survival (%)
Uninfected
NGP28b
NGP29b
2ME-BSA
Placebo
T. cruzi luc (Day 21)
Days Post-L. major Infection
C
Weight Change (g)
L. major luc 1 x 10^5 (Day 0)
T. cruzi luc 1 x 10^4 (Day 21)
Uninfected
NGP28b
NGP29b
2ME-BSA
Placebo
All dead
Day
D
T. cruzi luc
Total Flux (p/s)
NGP28b
NGP29b
2ME-BSA
Placebo (Co-Infection→PBS)
All dead
Day
E
L. major luc
Total Flux (p/s)
NGP28b
NGP29b
2ME-BSA
Placebo (Co-Infection→PBS)
All dead
Day
F
NGP28b
NGP29b
2ME-BSA
Placebo
Day
0
14
30
60
90
G
NGP28b
(GIPL-3-like)
Galα1,6Galα1,3Galfβ-BSA
NGP29b
(GIPL-1-like)
Galfβ1,3Man-BSA
Galp
Galf
Man
Linker
BSA
BSA

Figure 2.1. *L. major* type-2-like GIPL-based NGPs successfully decrease parasite burden in a murine co-infection model. **(A)** Immunization protocol. **(B)** Kaplan-Meyer graph for mouse survival was tracked for the entire experiment and graphed starting after the infection of *T. cruzi*. When compared with our infected-only group, all groups survived longer overall. NGP28b showed an 80% survival rate, whereas NGP29b had a 70% survival rate. **(C)** Mouse weight was monitored for the entire experiment to determine the toxic effect of the infection. All infected mice lost weight after infection of *L. major*, except for the naïve uninfected group. All other treatment groups regained weight with NGP29b mice returning to their starting weight. IVIS imaging was completed weekly (**D**)Total parasite burden of *L. major*$_{luc}$ in the left footpad measured in total flux [p/s] by IVIS. **(E)** Total parasite burden of CL-Brener *T. cruzi*$_{luc}$ of whole-body abdomen measured in total flux [p/s] by IVIS. **(F)** IVIS images taken over the course of the study show the progression of the disease. (**G**) The two neoglycoprotein vaccines used in these studies. For all groups, n=5. Statistical analysis: Unpaired *t*-test. *, $p<0.05$; **, $p<0.01$; ***, $p<0.001$; ****, $p<0.0001$.

Type-2 GIPL-like NGPs Elicit an Effective Adaptive Immunological Response

Sera collected from each mouse was pooled together by the treatment group every seven days, starting three days before the first prime vaccination. Pooled sera were analyzed by CL-ELISA for antibody production to determine adaptive immunological response. Sera was tested against both NGP28b and NGP29b as the antigen for the CL-ELISA and analyzed for RLU on the Cytation 7 imaging reader (BioTek). All vaccinated groups produced exceptional secondary immune responses within twenty-one days of the second vaccine boost and very nice memory recall after infection with CL Brener$_{luc}$ *T. cruzi* (**Figure 2.2A,B**). Of the two vaccinated groups, NGP29b displayed higher total IgG reactivity to both NGP28b and NGP29b antigens (**Figure 2.2A,B**). When sera from mice vaccinated with either NGP28b or NGP29b was used as the primary antibody against CL Brener$_{luc}$ TCT lysate, we observed a very strong reactivity to products in the range of tGPI-mucins (tGPI-MUCs) (at 70-250 kDa relative molecular mass) (Almeida, Ferguson et al. 1994) and to tGIPLs (<10 kDa relative molecular mass) (**Figure 2.2C**).

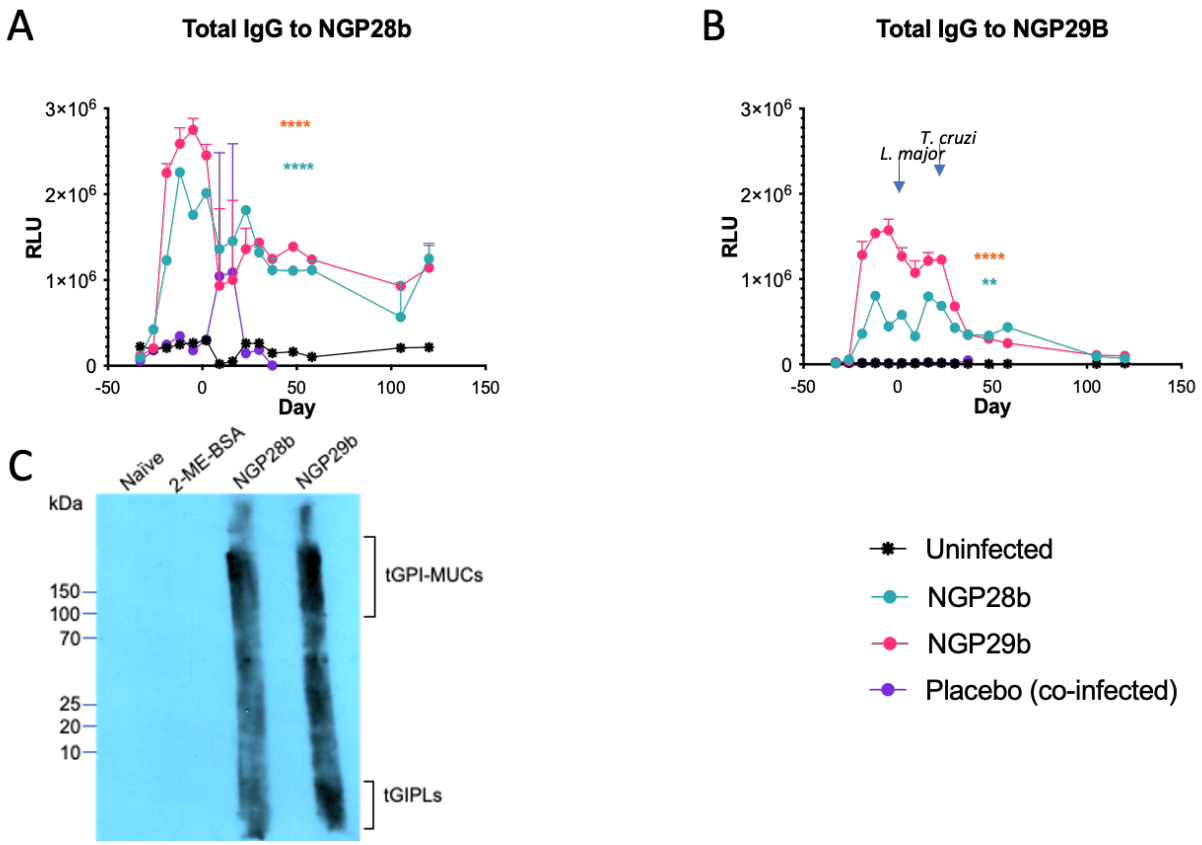

Figure 2.2. Type-II GIPL-like NGPs elicit an effective adaptive immunological response. Total IgG was produced against either NGP28b **(A)** or NGP29b **(B)**, when assessed by CL-ELISA. Sera collected from vaccinated mice just before *L. major Friedlin*$_{luc}$ infection probed against *T. cruzi* CL Brener$_{luc}$ TCT lysate (C). One-way ordinary ANOVA. **** = p<0.0001, ***=p<0.001, **=p<0.01, *p<0.05

There are four subclasses of IgG isotypes present in the C57BL/6 α1,3GalT-KO mouse model, consisting of IgG1, IgG2b, IgG2c, and IgG3. In our study, we observed that a robust IgG1 response was elicited by vaccination with our NGPs and that there was a memory recall following the parasite challenge (**Figure 2.3A**). NGP29b activated the expression of IgG2b against both antigens (**Figure 2.3B**). For the IgG2c isotype, we see a similar trend with NGP29b (**Figure 2.3C**). However, only after infection with *T. cruzi* do we see the expression of antibodies against either antigen in the NGP28b groups. This observation could be a class-switching event elicited by the parasite itself. This is interesting since IgG2 tends to target carbohydrates associated with LPS (Ferrante, Beard et al. 1990), and this activation was due to the dependency of potential epitopes

found on the surface of the parasite that is cross-reacting with the NGPs. IgG3 has been found to assist in effector cell function (Ferrante, Beard et al. 1990), so we can see that before infection, all vaccines produced IgG3 antibodies that recognized the NGP28b antigen and, after infection, produced a very elaborate memory response (**Figure 2.3**). However, when NGP29b was used as the antigen, we only saw an initial response caused by the vaccination of only NGP29b and no memory response activated by any groups.

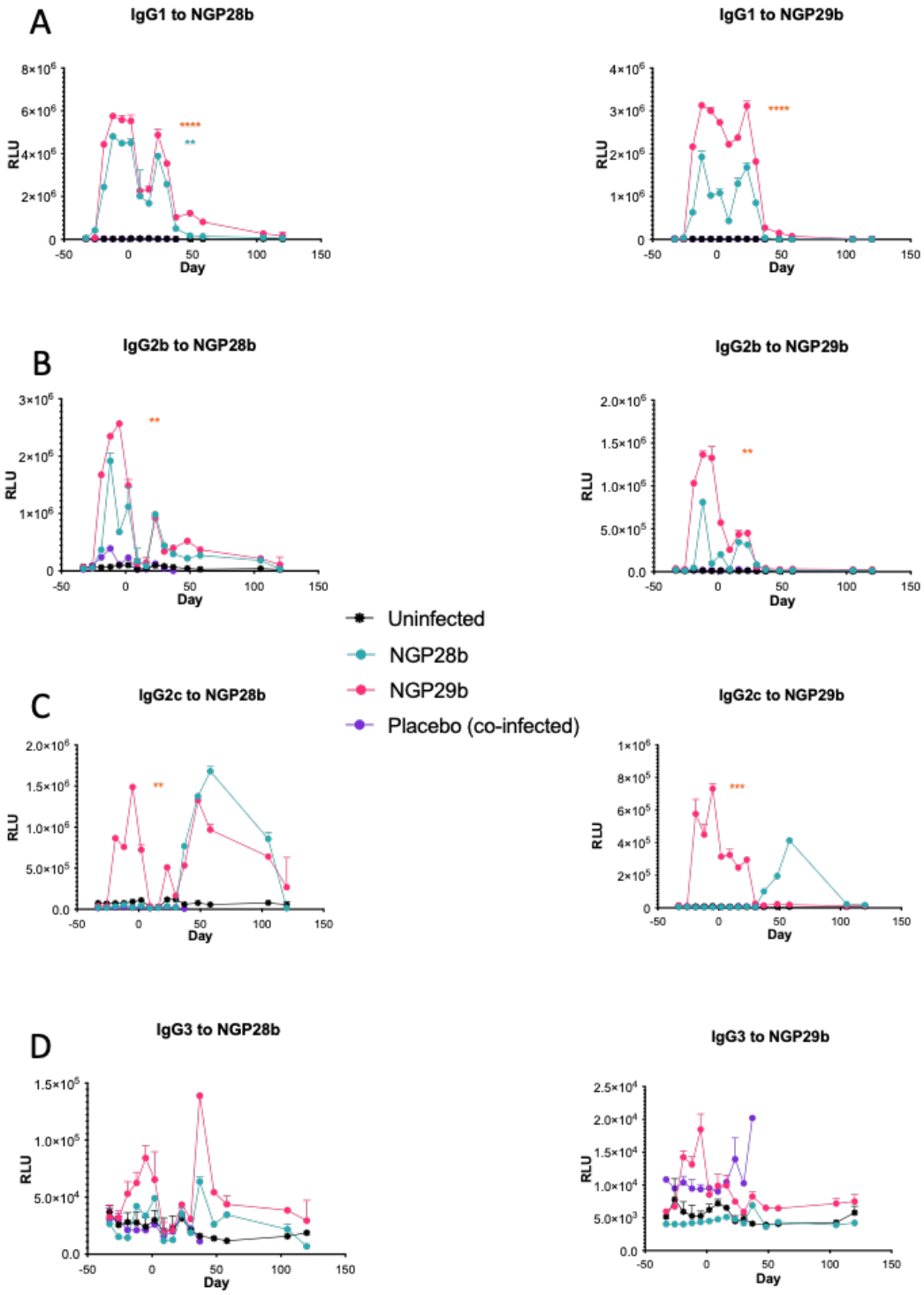

Figure 2.3. Type-II GIPL-like NGPs elicit an effective adaptive immunological response. IgG subclass production against either NGP28b (Left), or NGP29b (Right). IgG1 **(A)**, IgG2b **(B)**, IgG2c (C), IgG3 (D). When assessed by CL-ELISA. One-way ordinary ANOVA. **** = $p<0.0001$, ***=$p<0.001$, **=$p<0.01$, *$p<0.05$

To determine if there was further class switching we analyzed for the presence of IgM, IgA, and IgE. Our data suggest that there is a class-switching event happening just after infection with *T. cruzi* resulting in an elevation of free IgM in the sera that quickly subsides with parasite clearance (**Figure 2.4A**). We were unable to detect any difference in the level of IgA and IgE compared to the naïve mice. This finding leads us to determine that our vaccines are not eliciting any allergic response (**Figure 2.4B,C**).

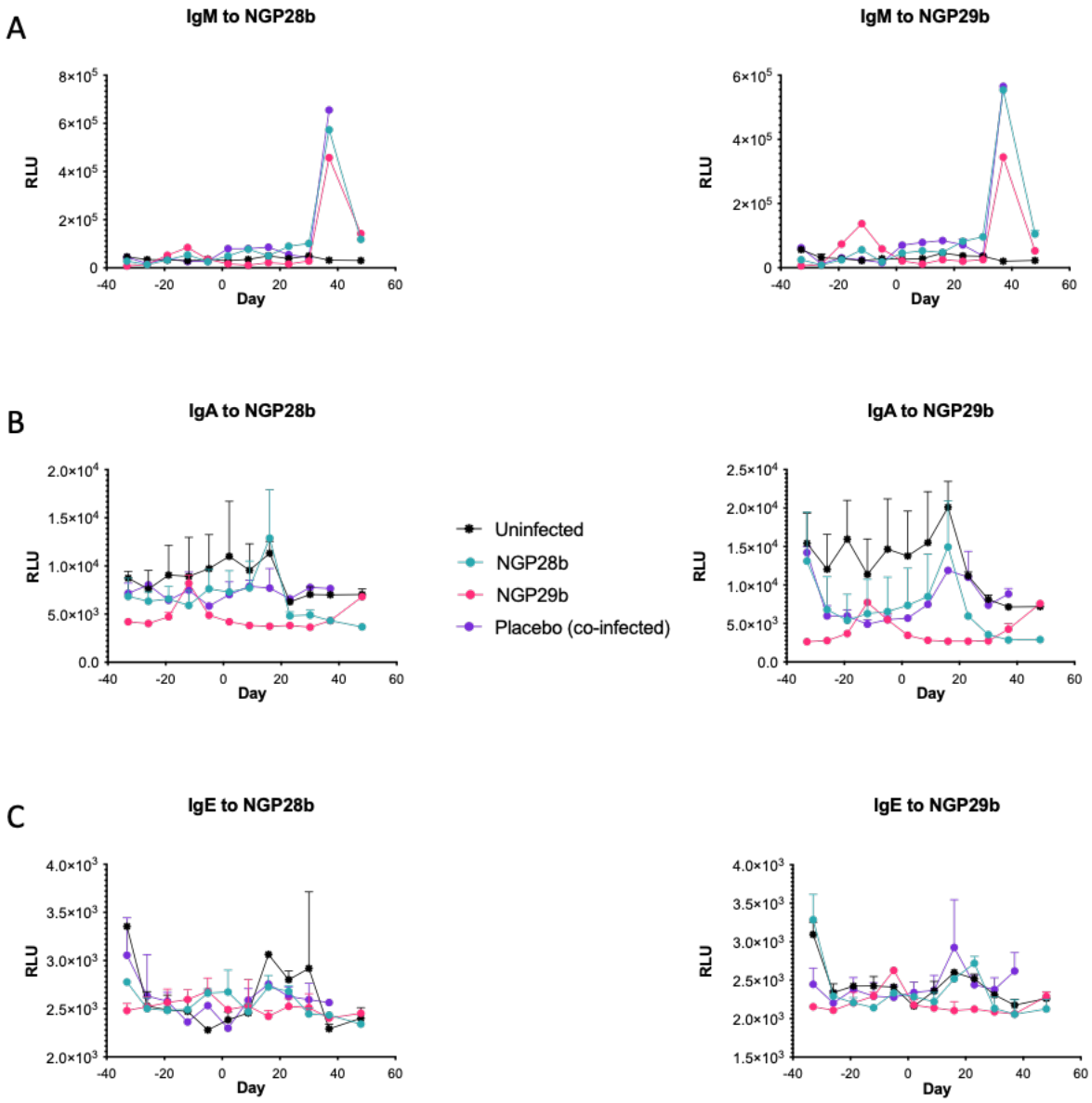

Figure 2.4: Type-II GIPL-like NGPs elicit an effective adaptive Immunological response. IgG subclass production against either NGP28b (Left), or NGP29b (Right). IgG1 **(A)**, IgG2b **(B)**, IgG2c **(C)**, IgG3 **(D)**, when assessed by CL-ELISA.

Type-2 GIPL-like NGPs provide tissue-specific protection from parasitemia.

To determine tissue-specific parasite burden, the real-time quantitative polymerase chain reaction (qPCR) assay was employed, and parasite levels were normalized using Glyceraldehyde 3-phosphate dehydrogenase (GAPDH) as an internal control and are presented in parasite equivalent

per milligram of tissue (par. eq./mg tissue). When the stomach was assessed, we saw a significant decrease in the parasite load in both vaccination groups compared to the co-infected and placebo-treated groups (**Figure 2.5**). The small intestine and heart revealed a significant decrease in parasitemia levels for both vaccine groups. However, there also was a significant decrease in the placebo group (**Figure 2.5**). The footpad was isolated using ImageJ from the IVIS images from days 32 and 34 post-*L. major* infection and the mean fluorescent intensity (MFI) was obtained for the left footpad. We can observe a significant decrease in MFI in the 2-ME-BSA- and NGP29b-vaccinated groups but not in the NGP28b-vaccinated group, compared to the co-infected Placebo group (**Figure 2.6**). However, the NGP29b vaccine was the only group with a more significantly reduced MFI compared to the Placebo group.

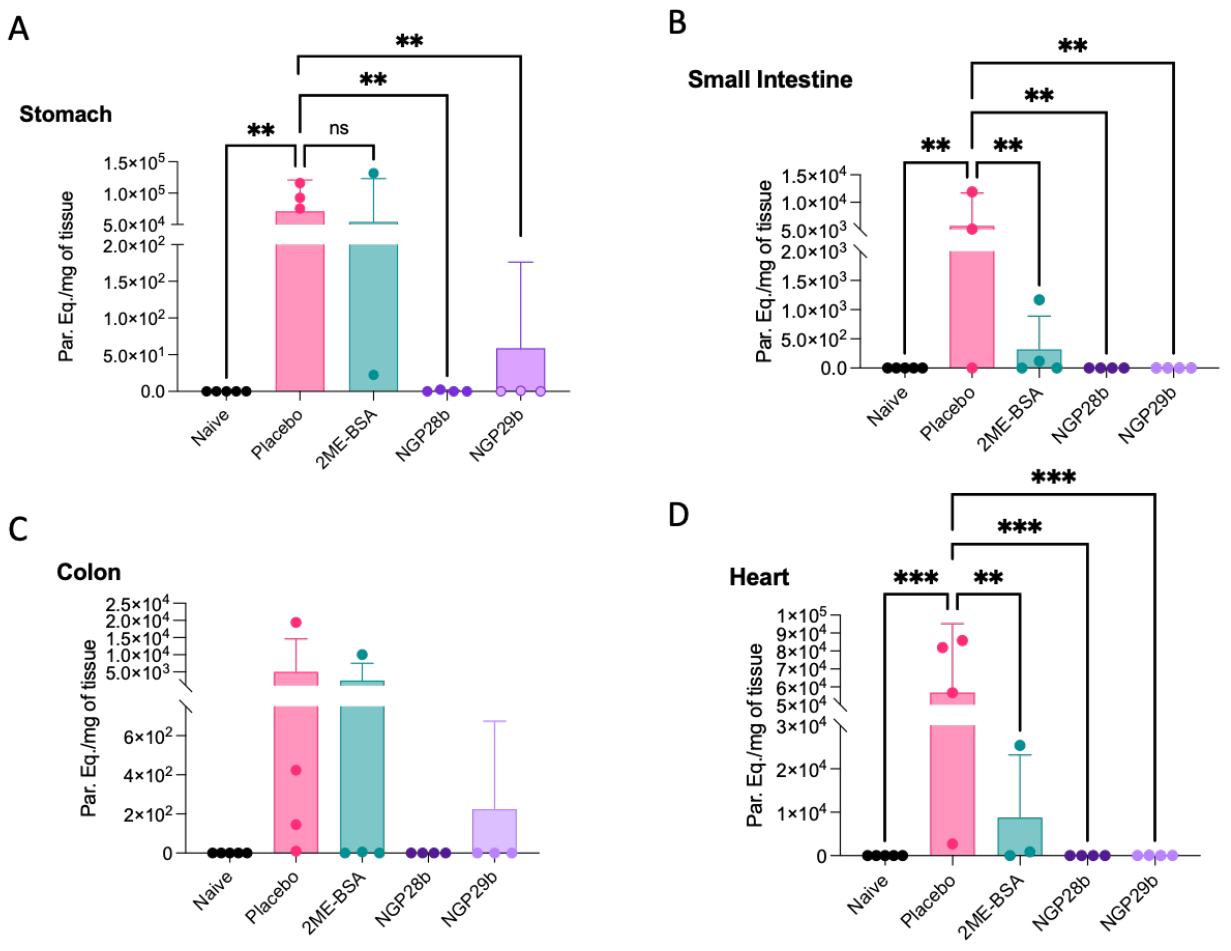

Figure 2.5: Type-II GIPL-like NGPs provide tissue-specific protection from parasitemia in major tissues. Quantitative PCR was conducted on harvested tissues and normalized using endogenous GAPDH (**A-D**). Compared to the Placebo (co-infection → PBS) group there is a significant decrease in tissue parasite burden. Statistical analysis: Unpaired *t*-test. ****, p<0.0001; ***, p<0.001; **, p<0.01; *, p<0.05

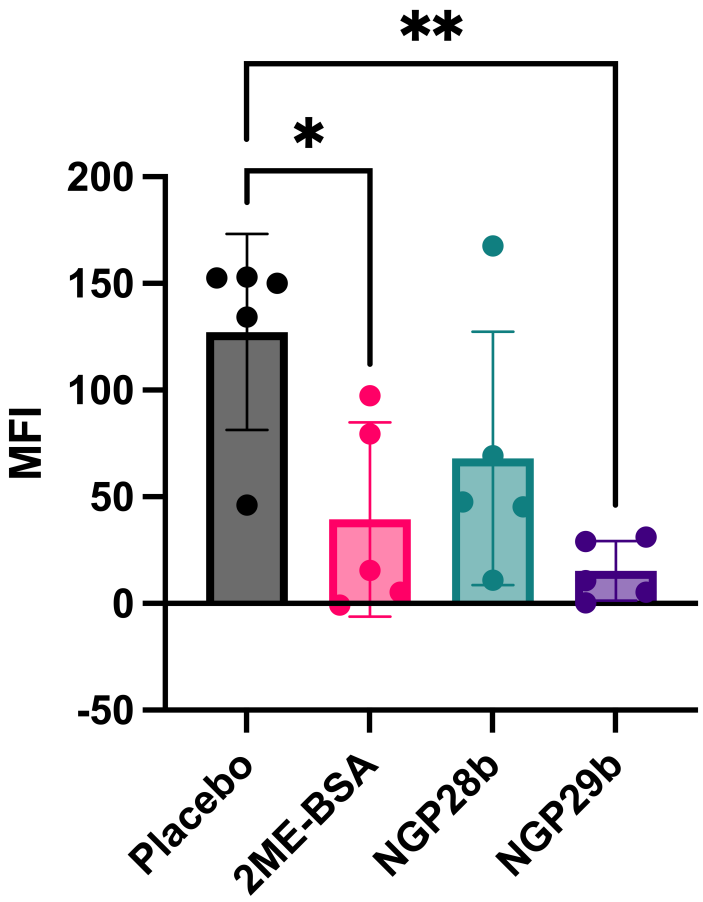

Figure 2.6: Type-II GIPL-like NGPs provide tissue-specific protection from parasite burden in the footpad. Images using IVIS were captured on days 32 and 34 following the infection of mice with *L. major*$_{luc}$. The footpad IVIS images were processed by ImageJ, and the mean fluorescence intensity (MFI) was plotted for each group. Statistical analysis: unpaired *t*-test. ****, p<0.0001; ***, p<0.001; **, p<0.01; *, p<0.05

Discussion

Our study highlights the promising potential of NGP28b and NGP29b as immunogens against co-infections of *L. major* and *T. cruzi* in mice. Both NGP28b and NGP29b elicited strong immune responses, indicating their potential as effective vaccines against these parasites. A key finding is the higher survival rates with NGP28b (80%) and NGP29b (60%) compared to other NGPs, demonstrating a superior protective effect. This increased survival correlates with the immune response, suggesting that NGP28b and NGP29b offer better defense against co-infection.

The ability of NGP28b and NGP29b to elicit specific antibodies against tGPI-MUCs and tGIPLs before parasite exposure is crucial. This pre-existing antibody response may aid early detection and neutralization of the targeted antigens, enhancing defense mechanisms. The reduction in overall parasite burden in both NGP28b and NGP29b groups, confirmed by IVIS and qPCR analyses, further underscores the effectiveness of these vaccines. The lower parasite load in vaccinated groups indicates successful control of parasitic replication and spread, likely contributing to higher survival rates.

Interestingly, NGP28b shows a more notable protective effect with an 80% survival rate, compared to 60% of NGP29b. This difference in effectiveness might be due to variations in immune responses or vaccine-specific factors. Further research into these distinct mechanisms could inform better vaccine design and strategies. Understanding the lasting impact of the immune response is essential for assessing NGP28b and NGP29b as durable vaccines against co-infections with *L. major* and *T. cruzi*.

In summary, this study strongly supports the immunogenicity and effectiveness of NGP28b and NGP29b in generating a robust immune response against L. major and T. cruzi co-infection.

These results highlight the potential of these vaccines in fighting parasitic co-infections and emphasize the need for further research to optimize their efficiency and longevity.

Chapter 3: Type-II GIPLs elicit a robust Th1 immunological profile in splenocytes upon ex-vivo stimulation.

Rationale

T-cells play a pivotal role in the adaptive immune response. Characterizing T-cell populations in response to an α-Gal vaccines are essential for elucidating the specific mechanisms through which these vaccines work. This knowledge can help optimize vaccine design and administration. Cytokines are key signaling molecules that orchestrate immune responses. The analysis of cytokine expression can provide insights into the overall immune response triggered by α-Gal vaccines. This can shed light on the type of immune response (e.g., Th1, Th2, or Th17) elicited by the vaccine, which is important for tailoring treatment strategies.

Hypothesis

We **hypothesize** that the NGP28b and NGP29b vaccines will elicit a robust immunological response in murine splenocytes when stimulated *ex vivo,* resulting in a $Th1^{+}/CD4^{+}$ response characterized by a Th1 proinflammatory cytokine expression profile.

Specific Aim

Immunological characterization of T-cell and Cytokine response to α-Gal vaccines. In this aim, murine Spleenocytes were collected and evaluated by In vitro stimulation to determine T-cell populations by Flow cytometry. Cell supernatant was also collected and analyzed for cytokine expression using the ISOPLEXIS Codeplex assay.

Methodology

Mice

C57BL/6 α1,3galactosyltransferase-knockout (α1,3GalT-KO) mice (Tearle, Tange et al. 1996, Thall, Murphy et al. 1996) were generously donated by Dr. Uri Galili, Rush University Medical Center, Chicago, IL. Mice were bred and maintained under biosafety level-2 (BSL-2), pathogen-free conditions at the Laboratory Animal Resources Center at The University of Texas at El Paso. All animal procedures and studies were performed according to National Institutes of Health guidelines and approved protocols by the Institutional Animal Care and Use Committee at The University of Texas at El Paso. Female α1,3GalT-KO mice six to ten weeks old were used for all experiments.

Parasites and mammalian cell culture

Transgenic *L. major* promastigotes expressing firefly luciferase (*L. majorLuc*) (Lmj-FV1- LUC-TK *L. major* strain Friedlin, clone V1) (Roy, Dumas et al. 2000, Thalhofer, Graff et al. 2010) were grown in M199 medium supplemented with 10% heat-inactivated fetal bovine serum (FBS) and 1% penicillin-streptomycin at 28°C. Metacyclic promastigotes were isolated from cell culture by Ficoll gradient during the stationary phase as previously described (Späth and Beverley 2001). Red-shifted firefly luciferase-expressing *T. cruzi* CL Brener clone (CL Brener*luc*) (Zingales, Pereira et al. 1997, Zingales, Miles et al. 2012, Zingales 2018) was generously donated by Dr. John Kelly (London School of Tropical Medicine and Hygiene, UK). Rhesus monkey kidney epithelial (LLC-MK2) cells (ATCC) were cultured in Dulbecco's modified eagle medium supplemented with 10% FBS and 1% penicillin-streptomycin at 37°C with 5% CO_2. Mammalian

tissue-culture-derived *T. cruzi* trypomastigotes (TCT) were obtained following the previously explained protocol.

T. cruzi CL Brener$_{luc}$ TCT lysate preparation

Mammalian tissue-culture-derived *T. cruzi* trypomastigotes (TCTs) were obtained as previously outlined. In brief, LLC-MK2 cells were infected with either culture metacyclic trypomastigotes or mouse-derived bloodstream trypomastigotes at a multiplicity of infection (m.o.i) of 10. This process lasted approximately 5-7 days, until parasites were observed freely swimming in the medium. The TCT medium was then collected from a HYPER Flask and centrifuged for 10 min at 1,500x*g* at 4°C. It was incubated for 2 h to allow trypomastigotes to separate from the cell debris pellet. The TCTs were then collected and washed with sterile PBS by centrifugation at 1,000x*g*, 4°C, followed by resuspension in 100 µL PBS with 1% Halt™ Protease Inhibitor Cocktail (Thermo Fisher Scientific), plus 50 µg Nα-Tosyl-L-lysine chloromethyl ketone hydrochloride (TLCK, Millipore, Sigma-Aldrich) (Halt+TLCK). The samples underwent 5 freezing/thawing cycles in a dry ice/ethanol bath and a hot water bath. Subsequently, they were diluted to 1 mL with 900 µL PBS containing Halt+TLCK protease inhibitors. Protein concentration was determined using the Pierce™ BCA Protein Assay Kit (Thermo Scientific), following the manufacturer's protocol, and then stored at -80°C until use.

Immunoblotting of CL-Brener$_{luc}$ TCT lysate with sera from vaccinated mice

Samples containing 20 µg TCT lysate were prepared in a loading buffer in each lane of 12% Mini-PROTEAN TGX™ Precast Protein Gels (Bio-Rad) and allowed to resolve. The proteins were transferred to a PVDF membrane using the GenScript eBlot L1 protein transfer system. After transfer, the polyvinyl fluoride (PVDF) membrane was carefully wrapped in cellophane, and wells were individually cut using a sterile scalpel. The membrane was then blocked in 5% milk/TBST

for 1 h, at room temperature (RT). Membranes were then individually incubated with respective sera at 1:100 dilution in 5% milk/TBST overnight (ON), by rocking at 4°C. Membranes were then probed using R&D anti-mouse IgG-HRP at 1:5,000 dilution in 5% milk/TBST at RT for 2 h. Between each incubation step, the membranes were washed 3X 5 min each in TBST by rocking at RT. Finally, the membrane was then briefly incubated (1 min) to CL reagent (Pierce™ ECL Western Blotting Chemiluminescent Substrate (Thermo Fisher Scientific; reagents A:B (1:1, v/v)), and exposed to a CL-XPosure™ Film (Thermo Fisher Scientific) **for 15-120 sec** and manually developed.

Neoglycoprotein Vaccines

The type-II GIPL-like neoglycoprotein (NGP) vaccines Galα*p*1,6Galα*p*1,3Gal*f*β-BSA (KM28b), and Galβ*f*1,3Manα-BSA (KM29b) (**Figure 2.1G**) were kindly prepared in collaboration with Dr. Katja Michael's Laboratory, at the Dept. of Chemistry and Biochemistry, the University of Texas at El Paso, as previously described (Viana, Montoya et al. 2022). Briefly, mercaptopropyl glycan derivatives were synthesized and covalently coupled to commercially available maleimide-activated bovine serum albumin (BSA) (Pierce, Thermo Fisher Scientific) to generate their respective NGPs. Control NGP was obtained by blocking maleimide sites with 2-mercaptoethanol (2ME-BSA).

Immunization and parasite challenge

Groups of 6–10-week-old female C57BL/6 α1,3GalT-KO mice (n=5 per group) were immunized by subcutaneous injection on their flank with 20 mg/dose/mouse with a series of 3 vaccinations, one prime (P), and two boosts (B1, B2) 7 days apart. Control groups included 2ME-BSA (carrier

protein control), Placebo (co-infection→PBS), and Uninfected (naïve) groups were also included and handled like experimental groups. Blood was collected by mandibular bleed three days before prime vaccination and every seven days until experiment termination. Twenty-one days after B2 vaccination, mice were challenged in the left footpad with $1x10^5$ *L. major Friedlin*$_{luc}$ metacyclic trypomastigotes. Three weeks after *L. major* infection, mice were challenged with $1x10^4$ *T. cruzi* CL Brener$_{luc}$ TCTs by intraperitoneal (i.p.) injection. After 120 days post-*L. major* infection, all animals were humanely euthanized in accordance with the approved vertebrate animal protocol. All mice were monitored for weight loss, toxicity, and abnormal behavior during all stages of experimentation. Footpad was monitored for edema of the footpad, and more than 6-mm change was a reason for experimental termination. A weight loss exceeding 20% was also considered a criterion for humanely terminating treatment.

Ex-vivo stimulation of splenocytes

At the experimental endpoint, half of each spleen was collected and manually separated through a 70µm nylon cell strainer. Single-cell isolates were collected for *ex-vivo* stimulation in complete RPMI containing 10% heat-inactivated fetal bovine serum, 100 units/µL of penicillin, 100 µg/µL of streptomycin, and 0.25 µg/µL of Gibco Amphotericin B, and 55mM 2-Mercaptoethanol. Cells were plated at $1x10^6$ per well on 96-well Falcon plates immobilized with 10 µg/µL of murine Anti-CD3e. Cells were stimulated with 1ug of either NGP or Lysate per well or eBioscience cell stimulation cocktail for 36 hours at 37°C, 5% CO2. After incubation, cells were treated with 50 µL BD Golgi Stop, following the manufacturer's protocol. Cell cells not blocked received 50 µL fresh complete RPMI medium plus 55 mM 2-mercaptoethanol. Cells were returned to the incubator for additional 4 h to allow the intracellular accumulation of cytokines. Cells and

supernatant were then collected for analysis by ICS Flow cytometry and IsoPlexis murine adaptive cytokine panel.

Cells were collected from the plate, and wells were rinsed two times with complete media and added to the tube containing the respective cells. Cells were pelleted and washed two times with FBS, then counted adjusting volume to $1x10^6$/cells per μL. Cells were fixed using ice-cold BD Cytofix (Cat# 554655) per the manufacturer's protocol. Cells were pelleted and washed two times before being resuspended in 1x BD Perm/Wash™ buffer (Cat# 554723) and incubated for 15 min in the dark at RT. Cells were then centrifuged at 250x*g* for 10 min and supernatant was removed. Cells were then resuspended in 50 μL BD Perm/Wash™ buffer and 20 μL/tube of BD CD4 T-cell phenotyping antibody cocktail or appropriate negative control. Cells were then incubated at RT for 30 min in the dark. Cells should be protected from light throughout the staining procedure. After incubation cells were washed 2x with FBS and then resuspended in 300 μL of FBS and analyzed on the Beckman Coulter Gallios Flow Cytometer for CD4, Th1 (INF-γ), Th2 (IL-4), and Th17 (IL-17α) cell populations. Cell culture supernatant from cells not treated with Golgi stop was collected at the stimulation endpoint and used for secreted cytokine analysis with the IsoPlexis murine adaptive cytokine panel.

Statistical Analysis

All data points are represented as the average of triplicate values with their corresponding standard error of the means (S.E.M.). Kaplan-Meyer survival rate curves, unpaired *t*-test, One-way ANOVA, or Two-way ANOVA were utilized in the statistical analysis, as indicated in the figure legends. Graphs and statistical analysis were achieved using Graph Pad Prism 10 Software (GraphPad Software, Inc., La Jolla, CA).

RESULTS

Determination of the proper concentration and stimulation time using CL- Brenner$_{luc}$ TCT lysate-vaccinated mice using the Codeplex murine adaptive immune Kit

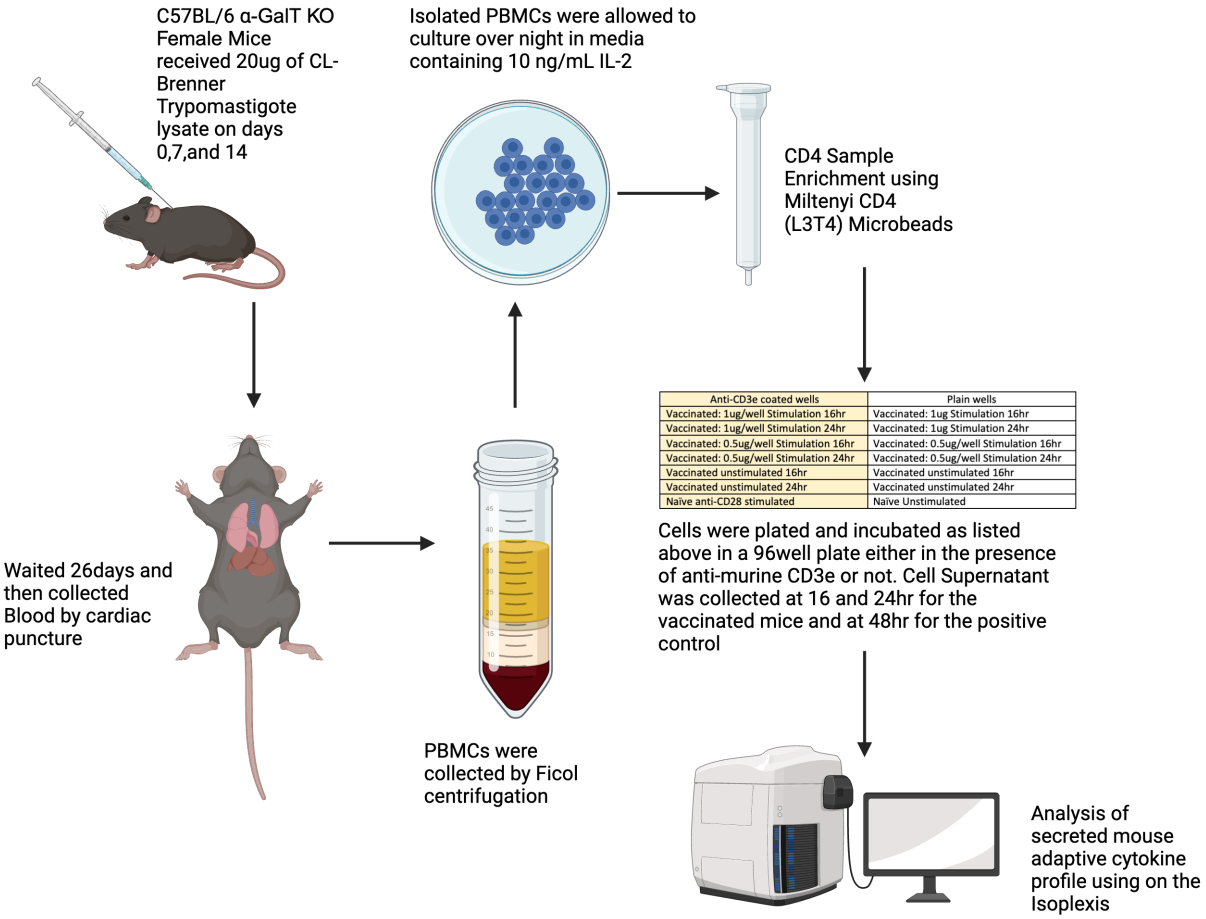

Figure 3.1. Graphical schematic of optimization experiment.

To first determine that proper conditions needed to properly assess cytokine profiles of vaccinated mice, female C57BL/6 α-GalT KO mice were vaccinated with either 20 µg of *T. cruzi* CL Brener$_{luc}$ TCT lysate or PBS at days 0, 7, and 14. On day 40, 26 days after the last boost blood

was collected by cardiac puncture, and PBMCs were isolated by Ficoll gradient. Isolated PBMCs were allowed to recover overnight in a T25 tissue culture flask with IL-2. The following day PBMCs were collected from overnight recovery and enriched for CD4+ T-cells using the Miltenyi CD4 Microbeads. Enriched samples were then plated on 96-well plates either containing immobilized anti-murine CD3e or left untreated at a density of $1x10^5$ per well. CD4+ T-cells were then either stimulated with 0.5 or 1 μg of lysate per well. Naïve cells were stimulated with anti-murine CD28 in the presence of 10 μg/μL anti-murine CD3 as a positive control. At 16 and 24 h, or 48 h for naïve positive control, cell supernatant samples were collected for secreted cytokine analysis using the IsoPlexis Codeplex murine adaptive immune assay.

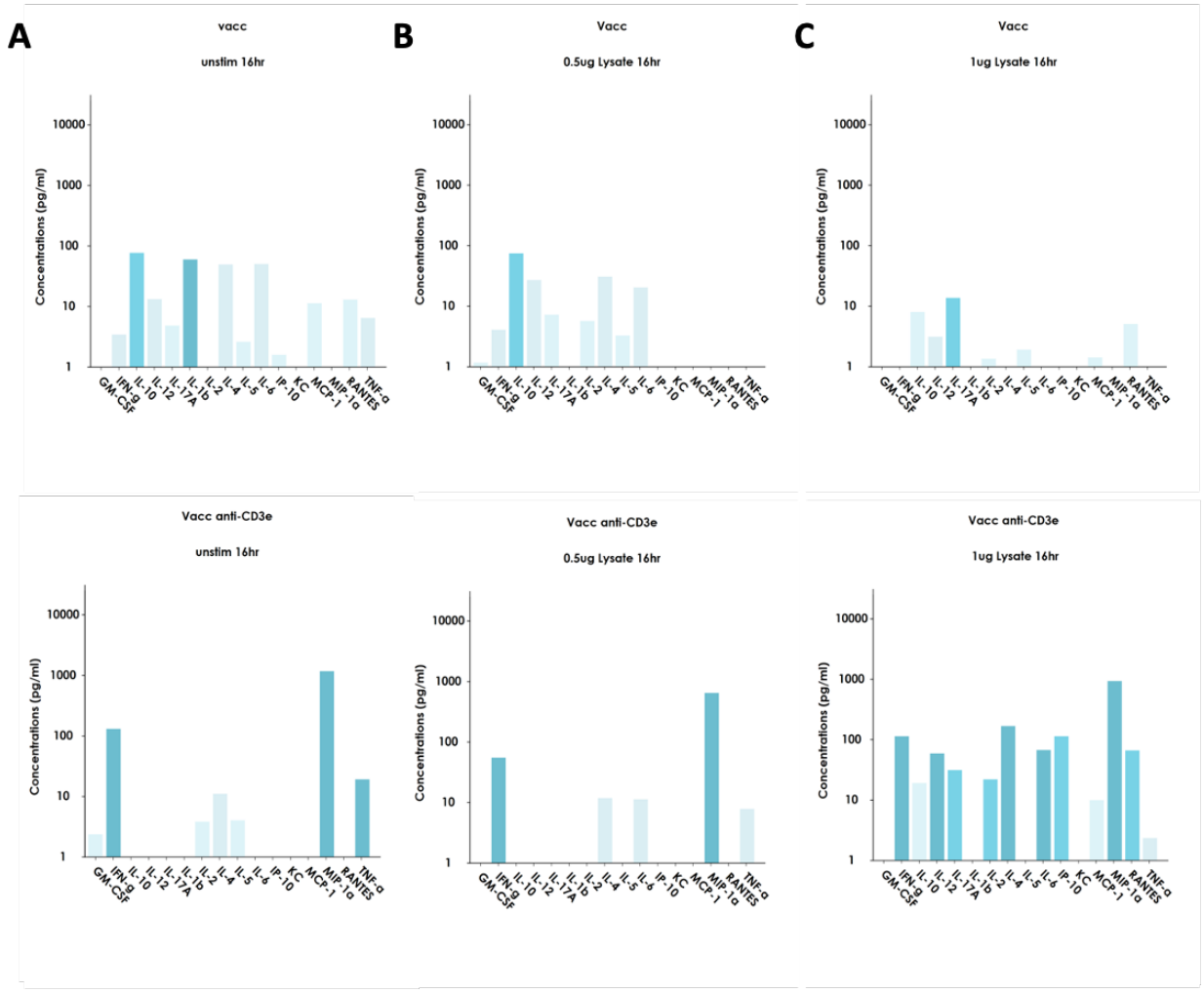

Figure 3.2. Secreted cytokine profiles at 16 h. Cell supernatant was collected from *ex-vivo* stimulated CD4+ T-cells from mice vaccinated with CL Brener$_{luc}$ TCT lysate at 16 h either in untreated wells (top graphs) or anti-murine CD3e immobilized wells (bottom graphs). Cells were left unstimulated **(A)** or stimulated with either 0.5 mg **(B)** or 1 mg **(C)** of TCT lysate.

When we examine the cell supernatant collected at the 16-hour time point, it becomes evident that the majority of the samples exhibited relatively low levels of cytokine expression. However, a notable exception can be observed in the samples plated in wells immobilized with 10 µg/µL anti-murine CD3e and subsequently stimulated with 1 µg of TCT lysate (**Figure 3.2**). These

samples exhibited a significant upregulation of cytokine production, indicating a distinct and potent immune response.

Advancing to the 24-hour mark (**Figure 3.3**), we again noticed a significant difference in the cytokine profiles among the experimental groups. The cells exposed to the presence of 10 µg/µL anti-murine CD3 exhibited higher cytokine profiles than those plated in wells lacking this essential co-stimulatory factor. This compelling observation underscores the pivotal role of CD3e in *ex-vivo* T-cell stimulation, replicating the pivotal process of T-cell activation as it occurs in vivo in response to antigen recognition (Menon, Moreno et al. 2023). These findings underscore the significance of CD3e in facilitating the faithful recapitulation of in vivo T-cell activation processes, shedding light on the mechanisms that underlie this crucial aspect of immune response regulation.

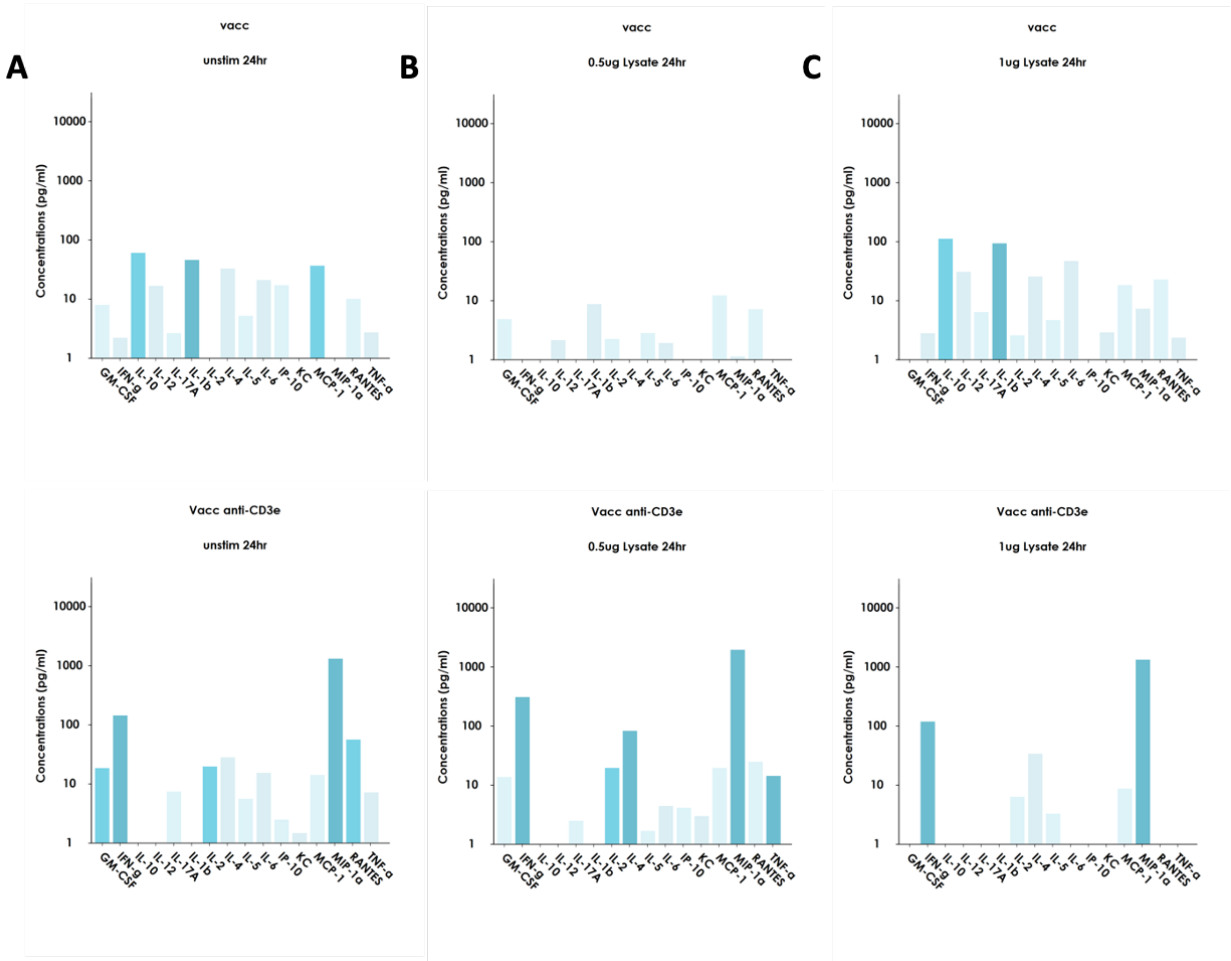

Figure 3.3. Secreted cytokine profiles at 24hr. Cell supernatant collected from *ex-vivo* stimulated CD4+ T-cells from mice vaccinated with *T. cruzi* CL Brener$_{luc}$ TCT lysate at 24 h either in untreated wells (TOP) or anti-murine CD3e immobilized wells (BOTTOM). Cells were left unstimulated (A) or stimulated with either 0.5 mg **(B)** or 1 mg **(C)** of TCT lysate.

When we look at the cell supernatant of cells from naïve and mice vaccinated with TCT lysate at the 16- and 24-h time point, either unstimulated (naïve) or stimulated with 0.5 µg or 1 µg per well of TCT lysate (**Figure 3.4**). Over the course of the 24-hour experiment, we see that the naïve unstimulated maintain a relatively low secreted cytokine profile (**Figure 3.4A**). A very similar cytokine profile can also be observed in both the 16- and 24-h group stimulated with 0.5 µg TCT lysate (**Figure 3.4B**). However, when we look at the cytokine profiles for the 1.0-µg stimulated group (**Figure 3.4C**), there is an obvious increase in secreted cytokines at the 16-h time point compared to all other groups. This observation leads to the conclusion that stimulation with

1.0 µg of CL Brener$_{luc}$ TCT lysate for 16 h was sufficient for *ex-vivo* stimulation of CD4+ T-cells enriched from PBMCs of CL Brener$_{luc}$ TCT lysate-vaccinated mice.

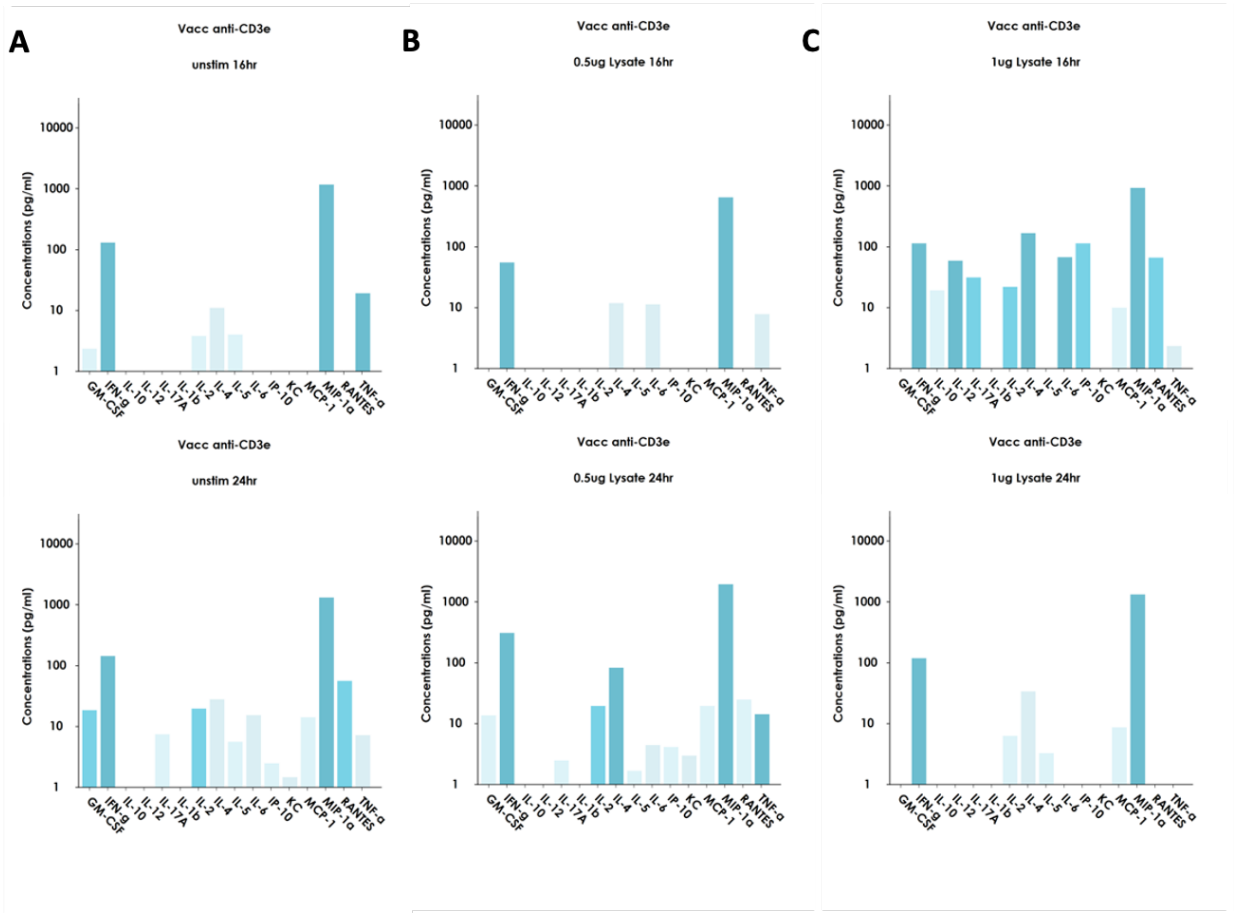

Figure 3.4. Secreted cytokine profile comparison at 16 and 24hrs when plated in CD3e immobilized wells. Cell supernatant collected from *ex-vivo*-stimulated CD4+ T-cells from mice vaccinated with CL Brener$_{luc}$ TCT lysate either stimulated for 16h (top graphs) or 24 h (bottom graphs). Cells were left unstimulated **(A)** or stimulated with either 0.5 mg **(B)** or 1 mg **(C)** of TCT lysate.

Synthetic glycovaccines elicit a predominant CD4⁺/Th1⁺ T-cell response upon ex-vivo stimulation.

To fully understand how our synthetic glycovaccines elicit a protective response we investigated the CD4+ T-helper (Th) cell phenotypes for Th1⁺, Th2⁺, and Th17+ populations. Female C57Bl/6 α1,3GalT-KO mice were vaccinated with 20 µg of either PBS (naïve), NGP28b, or NGP29b and then infected with *L. major*$_{luc}$ and *T. cruzi* CL Brener$_{luc}$ (or *T. cruzi*$_{luc}$), as described in Chapter 2. Briefly mice received three vaccinations of 20 µg each of respective treatment 7 days apart. Twenty days after vaccination, mice were infected in the left footpad with 10^5 *L. major* metacyclic promastigotes, followed by 10^4 CL Brener$_{luc}$ TCTs 21 days later. At the experimental endpoint on day 108, half of each spleen was collected for *ex-vivo* stimulation for the CD4⁺ T-helper cells population and cytokine profiling.

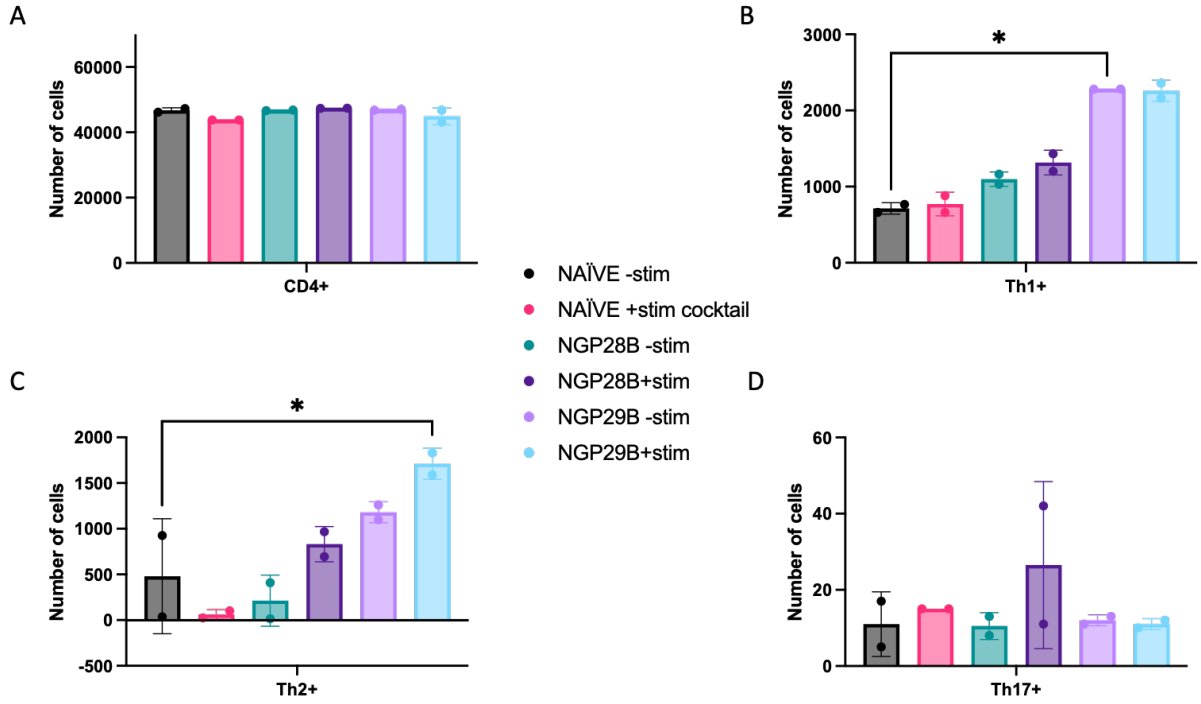

Figure 3.5. Synthetic glycovaccines elicit a predominant Th1⁺/CD4⁺ T-cell response upon *ex- vivo* stimulation. CD4⁺ T-cells counts for all groups **(A)**, Th1⁺/CD4⁺ T-cells **(B)**, Th2⁺/CD4⁺ T-cells **(C)**, and Th17⁺/CD4⁺ T-cells **(D)**. Statistical analysis: Two-way ANOVA. **** = p<0.0001, ***=p<0.001, **=p<0.01, *p<0.05

Single-cell splenocytes were allowed to recover overnight in the presence of 10 ng/μL of IL-2. In the following day, cells were plated in 96-well tissue culture plates immobilized with 10 μg/μL anti-murine CD3e. Cells were probed for CD4, and utilizing intracellular cytokine staining, cells were probed for interferon-gamma (INF-γ) for $Th1^+$, IL-4 for $Th2^+$, and IL17a for $Th17^+$ cells. Greater than 40,000 events were captured in the CD4 gate (**Figure 3.5A**) for each group. Analysis of the $Th1^+/CD4^+$ T-cell populations revealed a significantly higher population in the NGP29b unstimulated group (**Figure 3.5B**). Although insignificant, there is still a higher population of $Th1^+/CD4^+$ cells after stimulation in the NGP29b group (**Figure 3.5B**). When $Th2^+/CD4^+$ cells were evaluated, there was no significance between the unstimulated groups. However, we can see a higher trend in the population of $Th2^+/CD4^+$ cells in both NGP-vaccinated groups compared to the naïve. After stimulation, we observed that the NGP groups have an increase in the $Th2^+/CD4^+$ populations, in particular NGP29b induced a significant increase compared to the naïve populations (**Figure 3.5C**). When the $Th17^+/CD4^+$ cell populations were analyzed, we observed no significant change in the populations amongst all the groups (Figure 3.5D). We can conclude from our flow cytometry data that our NGP vaccines, most notably NGP29b, elicit a predominant $Th1^+/CD4^+$ T-cell phenotype, however it is worthy of noting the $Th2^+/CD4^+$ cell population elicited by these vaccines also.

Synthetic glycovaccines elicit an adaptive cytokine response upon ex-vivo stimulation

To examine the adaptive immune cytokine response to *ex-vivo* stimulation of splenocytes from vaccinated and infected mice, cell culture media was collected just prior to cell harvest and analyzed using the Isoplexis murine adaptive cytokine panel. When we look at those cytokines associated with macrophage and T-cell activation, there is a significant increase in levels of the cytokines, monocyte chemoattractant protein-1 (MCP-1 (CCL2)), and regulated on activation, normal T cell expressed and secreted (RANTES (CCL5)) (Figure 3.6). Both cytokines are known for their role in recruitment of immune cells to the affected tissue. MCP-1 is crucial in the

migration of monocytes (Deshmane, Kremlev et al. 2009, Singh, Anshita et al. 2021), whereas RANTES is known to be a secreted by activated T-cells to recruit monocytes within the tissues (Cavaillon 1994). Although Granulocyte-macrophage colony-stimulating factor (GM-CSF) is not significantly different from the other groups, we can see a higher level than the other groups. GM-CSF is also a known proinflammatory cytokine primarily due to its role as a growth and differentiation factor for macrophages and granulocytes (Cavaillon 1994). These chemokines working together bring together the critical components for eliciting an adaptive immune response.

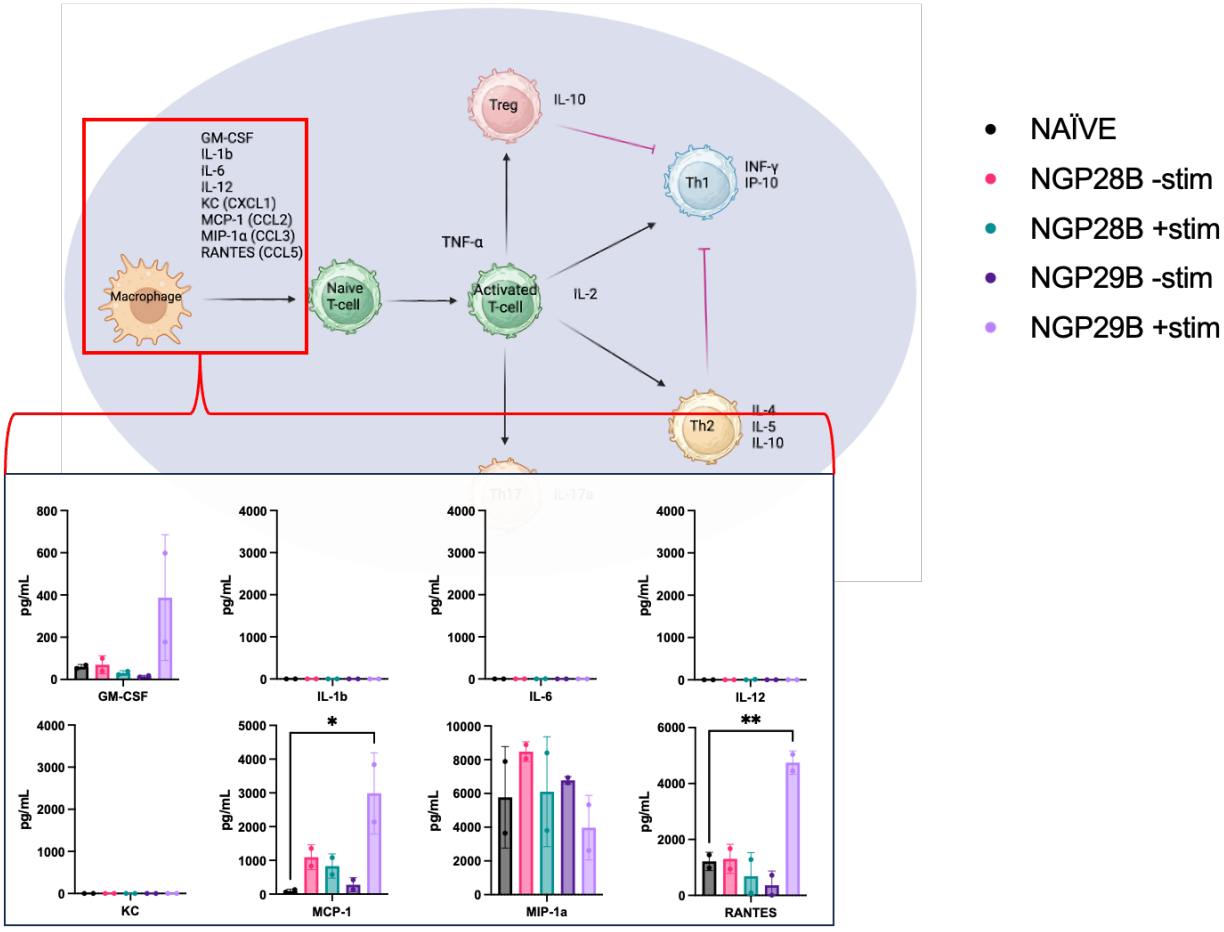

Figure 3.6: Synthetic glycovaccines elicit robust and coordinated immune responses upon *ex-vivo* stimulation. Proinflammatory secreted cytokines responsible for macrophage and other monocyte recruitment and differentiation at the affected sited. Statistical analysis: One-way ordinary ANOVA. ****, p<0.0001; ***, p<0.001; **, p<0.01; *, p<0.05

Next we evaluate those secreted cytokines that are related to the activation of naïve T-cells and their differentiation into terminal effector or memory cells. When looking at the proinflammatory cytokine tumor necrosis factor alpha (TNF-α) that is produced we do not we any significant difference between groups however there again much like GM-CSF we can see a trend to a higher level of production secreted TNF-α (**Figure 3.7**). The regulation of TNF-α plays an essential role in the recruitment of other inflammatory cells to the affected site when secreted by activated macrophages, T-cells and Natural Killer (NK) cells (Atzeni and Sarzi-Puttini 2013). Another cytokine that is secreted by activated T-cells and cytotoxic lymphocytes (CTL) is interlukin-2 (IL-2). IL-2 is known to be responsible for the further growth and differentiation of activated T-cells, proliferation of CTLs, T-helper, and NK cells(Hodi and Soiffer 2002). When we look at our NGP29b stimulated group we see a significant increase in the levels of IL-2 (**Figure 3.7**). Again, this cytokine profile is not only showing homing cytokines critical for leukocytes trafficking to the affected tissue, but also activation of more specific T-cell subsets and further advancing the adaptive immune response.

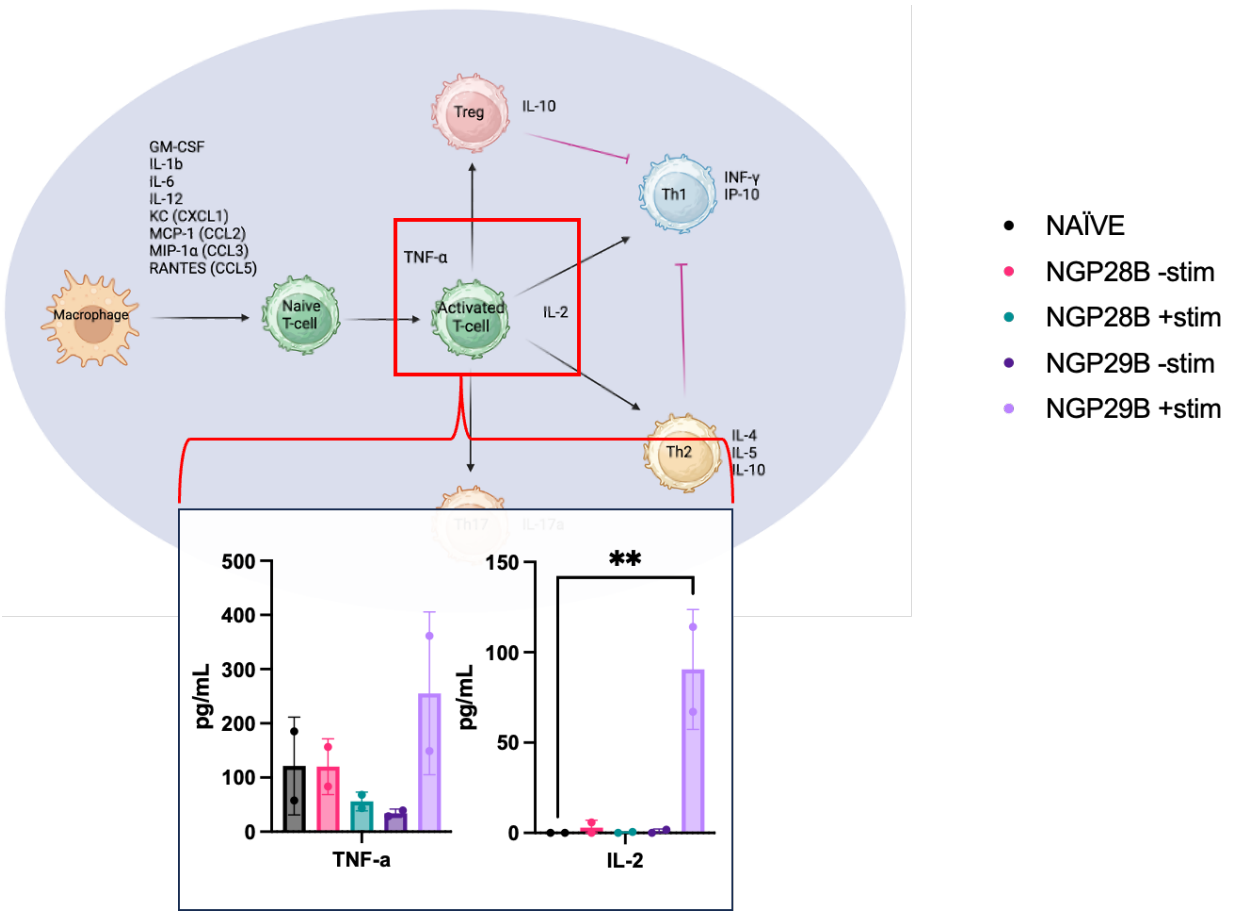

Figure 3.7. Synthetic glycovaccines activate T-cells upon *ex-vivo* stimulation. Statistical analysis: One-way ordinary ANOVA**.** ****, p<0.0001; ***=p<0.001; **, p<0.01; *, p<0.05

To ultimately understand what type of immune response is being elicited and to further support our flow cytometry data we examine the key cytokines associated with Th1 type responses, interferon-gamma (INF-γ) and INF-γ inducible protein-10 (IP-10). INF-γ has long been one of the hallmark cytokines secreted by Th1 cells and has been implicated in cell-mediated immune responses and tissue-specific autoimmunity (Tau and Rothman 1999). In our *ex-vivo* experiment, we found that both our NGPs had an equal or lower level of secreted INF-γ compared to our naïve unstimulated group (**Figure 3.8**). IP-10 is known to be induced by type-I and -II INFs and LPS, and a strong chemoattractant for activated T cells (Dufour, Dziejman et al. 2002) is seen

significantly increased in our NGP29b group compared to all other groups of this study (**Figure 3.8**).

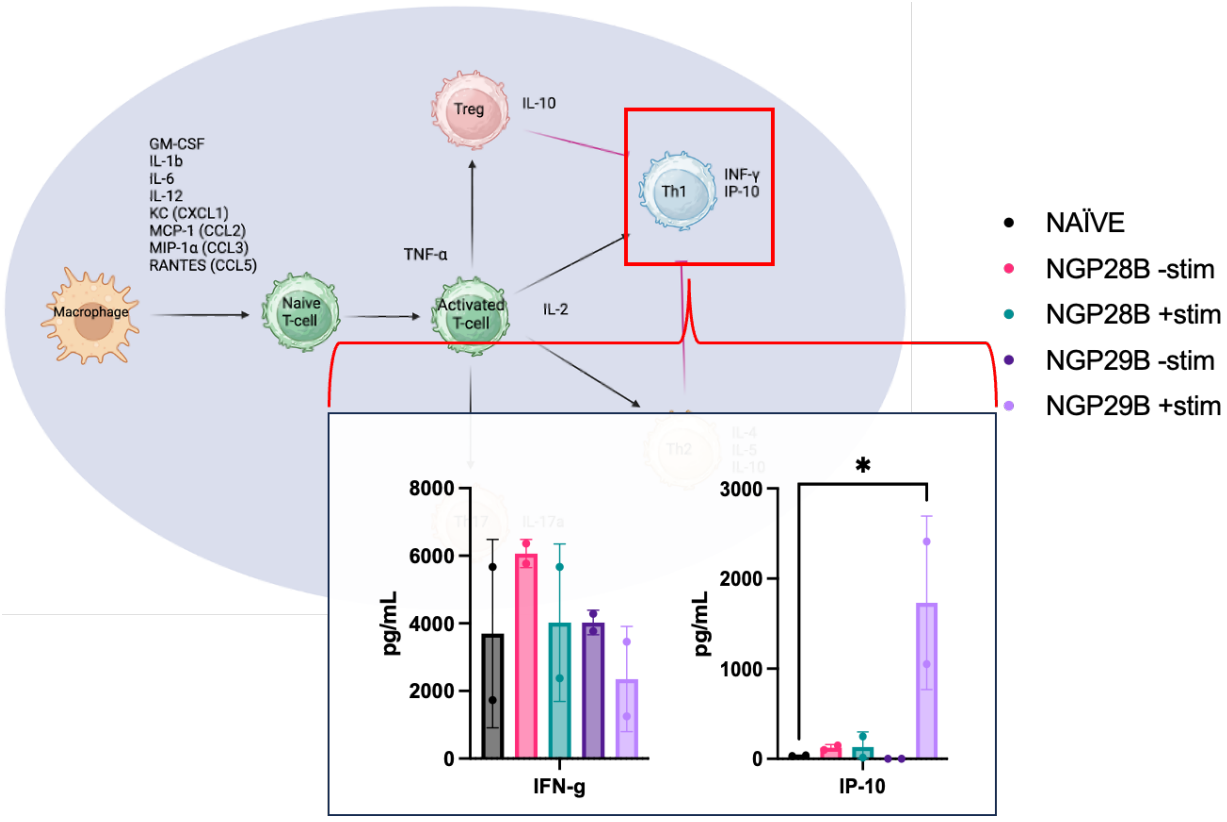

Figure 3.8. Synthetic glycovaccines elicit Th1-like cytokine profile in response to *ex-vivo* stimulation. One-way ordinary ANOVA**.** **** = p<0.0001, ***=p<0.001, **=p<0.01, *p<0.05

When we next look at the cell types that are known to control the immune response, like Th2 and Tregs, we examined three cytokines interleukin-4 (IL-4), interleukin-5 (IL-5), and interleukin-10 (IL-10). IL-4 is a cytokine that has many functions in controlling the immune response, such as its key role in the development of Th2 cells and signaling for a move advanced immune response against extracellular parasites (Kopf, Le Gros et al. 1993, Zhu 2015). IL-4 secretion by Th2 cells also plays a pivotal role in the signaling to B-cells for class switching to IgG1 and IgE (Kopf, Le Gros et al. 1993). Although in our study we do not see a significant increase in the secretion of IL-4, it is interesting to note that in the NGP28b-vaccinated groups, we

had very low levels of expression, whereas, in the NGP29b stimulated group, we have levels comparable to the naïve (**Figure 3.9**). Once B cells become activated, they upregulate the expression of IL-5R and become sensitive to IL-5 secreted by Th2 cells, resulting in the generation of a B cells (ACS) (Emslie, D'Costa et al. 2008). Our data show that there is a significant increase in the secretion of IL-5 in our stimulated NGP29b when compared to the naïve group (Figure 3.9). the NGP29b unstimulated and both stimulated and unstimulated all had low levels of IL-5; however, it is worth noting that when the NGP28b cells were stimulated, we can see a decrease in the level of IL-5 (**Figure 3.9**). IL-10 has a well-known role as an immunosuppressive cytokine secreted by many cell types including Th2, NKT cells, NK cells, and Tregs, to name a few (Moore, de Waal Malefyt et al. 2001, Iyer and Cheng 2012). IL-10 is vital in limiting tissue damage and preventing autoimmune conditions (Iyer and Cheng 2012). Levels of secreted IL-10 again are significantly higher in our stimulated NGP29b when compared to the naïve group (Figure 3.9).

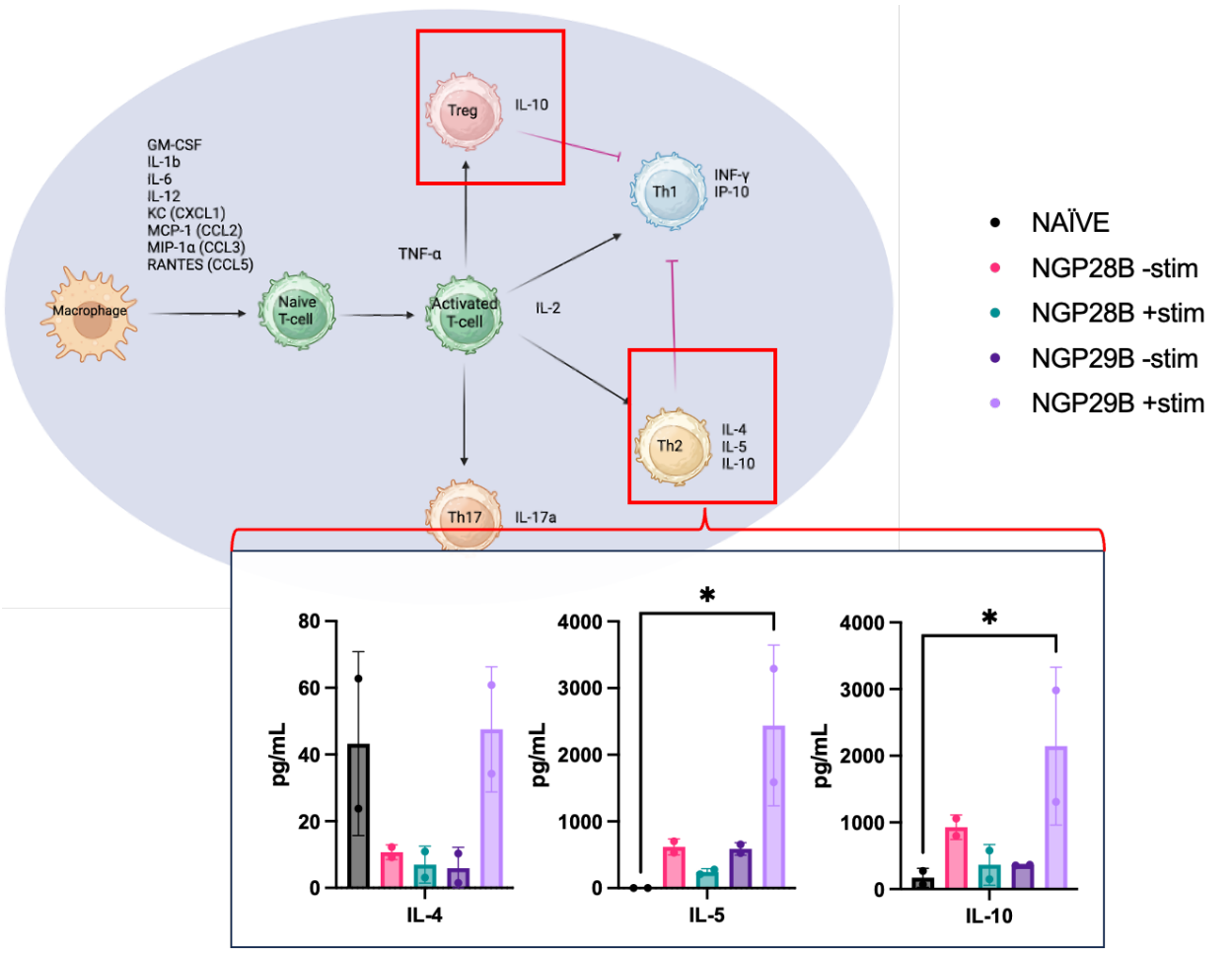

Figure 3.9. Synthetic glycovaccines elicit Th2 cytokines in response to *ex-vivo* stimulation leading to the formation of antibody-secreting B cells. One-way ordinary ANOVA. ****, p<0.0001; ***, p<0.001,; **=p<0.01,;*p<0.05

Finally, we examine the main cytokine associated with the Th17 cellular response interleukin-17A (IL-17A). IL17A was identified as the signature cytokine of a distinct population of CD4+ T-cells (McGeachy, Cua et al. 2019). Although this proinflammatory cytokine has been associated with autoimmune diseases, its primary function is to induce IL-6 and G-CSF to promote innate inflammation (Gaffen, Jain et al. 2014). In our current study we did not see a significant difference in the secreted levels of IL-17A amongst our groups (**Figure 3.10**).

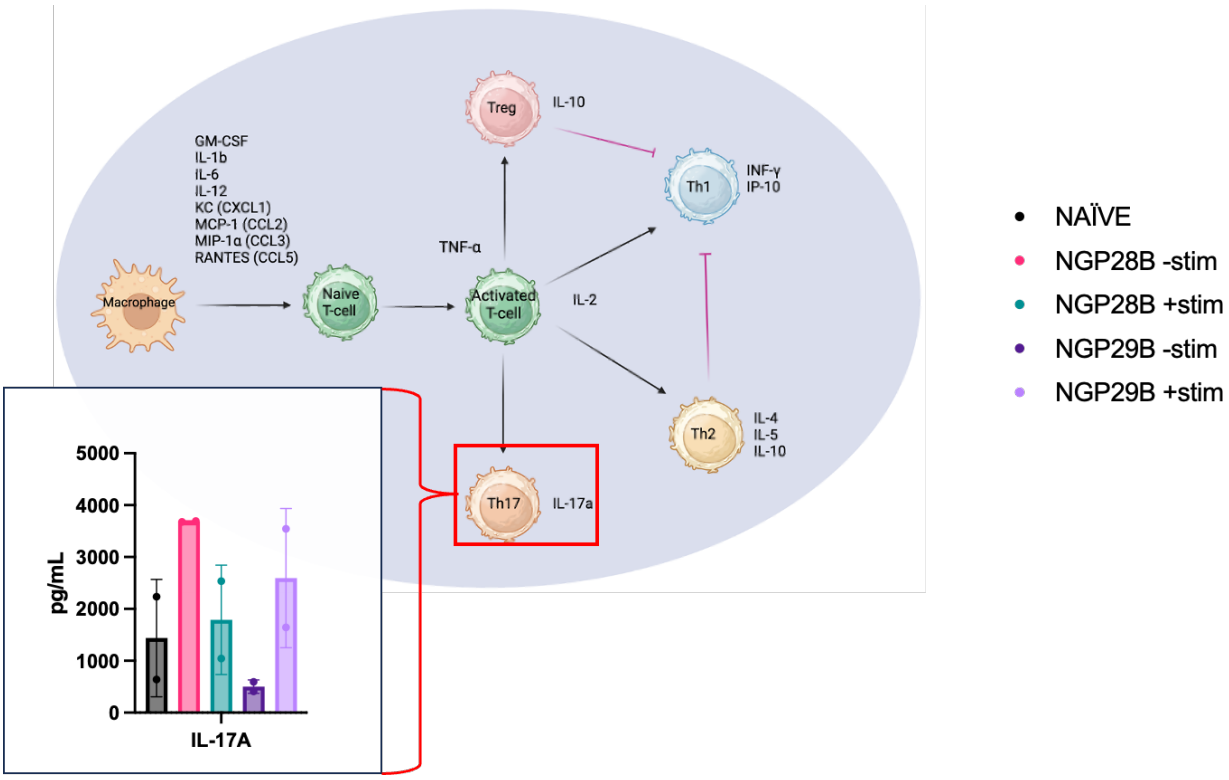

Figure 3.10. Synthetic glycovaccines do not elicit Th17 cytokines in response to *ex-vivo* stimulation.

DISCUSSION

The findings presented in this study provide valuable insights into the immunogenicity of NGP28b and NGP29b vaccines. The *ex-vivo* stimulation protocol established in this chapter revealed a robust CD4+ Th1+ response in splenocytes when restimulated with the respective NGPs, underscoring the efficacy of these vaccines in inducing a cellular immune response.

The results from ICS flow cytometry analysis demonstrated a significant increase in Th1+ T-cells for both NGP28b and NGP29b compared to the naïve group. This observation aligns with the notion that these vaccines can effectively enhance the Th1 arm of the immune system, which is crucial for combating intracellular pathogens and promoting cell-mediated immunity.

Interestingly, per the Th1/Th2 balance hypothesis, the study uncovered a CD4+ Th2+ immune response elicited by both NGPs. However, an intriguing divergence emerged in the case of NGP29b, which exhibited a notable and significant increase in CD4+ Th2+ cells compared to

the naïve group. These data suggest that NGP29b may have a unique immunomodulatory effect, potentially influencing the balance between Th1 and Th2 responses.

The cytokine profile analysis further supports these findings, providing a comprehensive view of the adaptive immune response triggered by NGP28b and NGP29b. The secretion of adaptive cytokines is indicative of the intricate network of immune signals orchestrated by these vaccines, contributing to the overall immune milieu.

While the study sheds light on the immunological profiles of NGP28b and NGP29b, it is essential to acknowledge certain limitations. The ex-vivo stimulation protocol utilized here may not fully recapitulate the complex in vivo immune environment. Additionally, the study primarily focused on CD4+ T-cell responses, and future investigations could delve into the involvement of other immune cell populations to provide a more comprehensive understanding.

In conclusion, the current study underscores the immunogenic potential of NGP28b and NGP29b vaccines, elucidating their capacity to elicit Th1 and Th2 responses. The distinctive Th2-biased response observed with NGP29b warrants further exploration, offering avenues for refining vaccine strategies and advancing our understanding of immune modulation. The findings contribute valuable insights to the ongoing efforts in developing effective vaccines against infectious agents, paving the way for future research and clinical applications.

Chapter 4: Ex-vivo evaluation for the efficacy of b-Galf vaccine, potential use as a veterinary vaccine against Chagas disease and cutaneous leishmaniasis in a murine co-infection model

Rationale

Drawing upon the valuable insights from the previous two chapters of our research and utilizing the fact that all mammals share a common inability to synthesize the β-Gal*f* epitope, the key epitope found within NGP29b. Our study explored the viability of NGP29b as a potential vaccine candidate for domesticated mammals in their defense against *T. cruzi* and *Leishmania* infection. To conduct this investigation, we employed the C57BL/6 wild-type mouse strain, known for its reliability as an experimental model organism.

Our rationale for this research this study lies in the growing concern regarding T. cruzi and Leishmania infections, which affect domesticated mammalian pets and livestock. These parasitic diseases not only pose health risks to animals and humans but also raise the specter of potential food contamination. By assessing NGP29b's potential as a vaccine candidate, our study aims to address these multifaceted challenges. This research seeks to contribute significantly to veterinary medicine by developing preventive measures that not only protect animal and human health in shared environments but also mitigate the risk of food contamination associated with these infections.

Through the comprehensive analysis of NGP29b's immunogenic properties and its ability to trigger protective responses in the immune system of the C57BL/6 wild-type mouse strain, we hope to provide valuable insights that may pave the way for future vaccinations and treatments, safeguarding both our beloved pets and those who care for them.

Hypothesis

We **hypothesize** that an β-Gal*f* vaccine (NGP29b) will elicit a robust immunological response in C57BL/6 wild-type murine splenocytes vaccinated with NGP29b and then stimulated *ex vivo,* resulting in a robust $Th1^{+}/CD4^{+}$ immune response.

Specific Aim

***Ex-vivo* evaluation for the efficacy of β-Gal*f* vaccine, potential use as a veterinary vaccine against Chagas disease and cutaneous leishmaniasis in a murine co-infection model.**

In this aim, we will utilize C57BL/6 wild-type mice vaccinated with NGP29b, a β-Gal*f*-containing NGP. Anti-β-Gal*f* antibody titers will be determined by CL-ELISA for IgG and IgM. $CD4^{+}$ T-cell populations will be evaluated by flow cytometry.

Methodology

Mice

C57BL/6 mice were obtained from Jackson Labs. Mice were bred and maintained under biosafety level 2, pathogen-free conditions at the Laboratory Animal Resources Center at The University of Texas at El Paso. All animal procedures and studies were performed according to National Institutes of Health guidelines and approved protocols by the Institutional Animal Care and Use Committee at The University of Texas at El Paso. Three male and three female C57BL/6 mice six to ten months old were used for all experimental groups.

Neoglycoprotein Vaccines

The type-II GIPL-like neoglycoprotein (NGP) vaccines Galβ*f*1,3Manα-BSA (NGP29b) was prepared in collaboration with Dr. Katja Michael's laboratory, at the Dept. of Chemistry and Biochemistry, the University of Texas at El Paso, as previously described (Viana, Montoya et al. 2022). Briefly, mercaptopropyl glycan derivatives were synthesized and covalently coupled to commercially available maleimide-activated bovine serum albumin (BSA) (Pierce, Thermo Fisher Scientific) to generate their respective NGPs. The hapten carrier molecule was obtained by blocking maleimide sites with 2-mercaptoethanol (2ME-BSA).

Immunization

Groups of 6–10-month-old male and female C57BL/6 mice (n=6 per group 3m, 2f) were immunized by subcutaneous injection on their flank with 20 mg/dose/mouse with a series of 3 vaccinations, one prime (P), and two boosts (B1, B2) 7 days apart. Control groups included 2ME-BSA (carrier protein control), Placebo (co-infection→PBS), and Uninfected (naïve) groups were

also included and handled like experimental groups. Blood was collected by mandibular bleed three days before prime vaccination and every seven days until experiment termination on day 21.

Chemiluminescent enzyme-linked immunosorbent assay

Anti-β-Gal*f* antibody titers in the sera of immunized mice were determined by chemiluminescent enzyme-linked immunosorbent assay (CL-ELISA). A total of 50 µL per well- containing 125 ng of either NGP29b diluted in carbonate-bicarbonate buffer (CB Buffer, pH 9.6) was immobilized on 96-well MaxiSorp microplates (NUNC, Thermo Fisher Scientific) and incubated overnight at 4°C. Free binding sites were blocked using 200 µL per well of 1%BSA in 1x Phosphate Buffer Solution with 0.05% Tween 20 (PBST, pH 7.2) for 1 h at 37°C covered from light. Plates were washed three times with 200 µL PBST. Mouse sera were diluted in PBST at 1:100 and 100 µL was loaded into the top wells in triplicate and then serially diluted to 1:800 and incubated for 1 h at 37°C, covered from light. Plates were washed three times with 200 µL of PBST. Then, 50 µL Donkey anti-mouse IgG-biotin (Jackson ImmunoResearch Laboratories) or the directly conjugated Goat anti-mouse IgM-HRP (Abcam, Cambridge, MA) diluted 1:2000 in 1% BSA in PBST was added and the microplates incubated for 1 h at 37°C, covered from light. Plates were washed three times with 200 µL PBST. 50 µL Pierce High Sensitivity NeutrAvidin-HRP 1:5000, diluted in 1%BSA PBST, was loaded into each well and incubated for 1 h at 37°C covered from light. Plates were washed three times with 200 µL of PBST. 50 µL of SuperSignal ELISA Pico Chemiluminescent Substrate (Thermo Fisher Scientific) diluted in 0.1% BSA in carbonate-bicarbonate buffer at 1:1:8 was loaded into each well. Relative Luminescent Units (RLU) were obtained by reading plate with Cytation 5 imaging reader (BioTek).

CL Brener$_{luc}$ TCT parasite lysate preparation

Mammalian tissue-culture-derived *T. cruzi* trypomastigotes (TCT) were obtained as previously described above. Briefly, LLC-MK2 cells were infected with either culture metacyclic trypomastigotes or mouse- derived bloodstream trypomastigotes at a multiplicity of infection (m.o.i.) of 10 for approximately 5-7 days until parasites appeared free swimming in the medium. Medium containing TCTs was collected from a hyper cell culture flask and centrifuged for 10 min at 1,500xg at 4°C and incubated for 2h to allow trypomastigotes to swim up away from cell debris pellet. TCT's were collected and washed with sterile PBS by centrifugation at 1,000xg, 4°C, and the resuspended in 100ul of PBS containing 1% Halt™ Protease Inhibitor Cocktail (Thermo Fisher Scientific)/ ± 50 μg of Nα-Tosyl-L-lysine chloromethyl ketone hydrochloride (TLCK: Millipore Sigma) and subjected to 5 cycles of freeze/thaw in a dry ice/ETOH bath and a hot water bath. Samples were then brought to 1mL with 900 µL of PBS containing protease inhibitors. Protein concentration was then determined using the Pierce™ BCA Protein Assay Kit (Thermo Scientific) following the manufacturer's protocol and then stored at -80 until used.

Immunoblotting of CL Brener$_{luc}$ TCT lysate with sera from vaccinated mice

Samples containing 20 µg of lysate were prepared in a loading buffer in each lane of 12%% Mini-PROTEAN® TGXTM Precast Protein Gels and allowed to resolve. The proteins were transferred to a PVDF membrane using the GenScript eBlot L1 protein transfer system. After transfer, the PVDF membrane was carefully wrapped in cellophane, and wells were individually cut using a sterile scalpel. The membrane was then blocked in 5% milk/TBST for 1 hour at room temp. Membranes were then individually incubated with respective sera at 1:100 in 5% milk/TBST overnight rocking at 4°c. In the following, the membranes were washed 3x 5 min each in 1XTBST

on the rocker. Membranes were then probed using R&D anti-mouse IgG-HRP at 1:5000 in 5% milk/TBST at RT for 2 hours. After incubation, the membrane was washed 3x 5 min each in 1XTBST on the rocker. The membrane was then briefly exposed to CL reagent (Pierce™ ECL Western Blotting Chemiluminescent Substrate: Thermo Scientific; reagents A:B (1:1, v/v), and then films were manually exposed and developed.

Ex-vivo stimulation of splenocytes

At experimental end point half of each spleen was collected and manually separated through a 70-μm nylon cell strainer. Single cell isolates were collected for *ex-vivo* stimulation in complete RPMI, containing 10% heat inactivated fetal bovine serum, 100 units/μL of penicillin, 100 μg/mL of streptomycin, and 0.25 μg/mL of Gibco Amphotericin B, and 55mM 2-Mercaptoethanol. Cells were plated at $1x10^6$ per well on a 96-well Falcon plates immobilized with 10 μg/mL of murine Anti-CD3e. Cells were stimulated with 1ug of either NGP or Lysate per well or eBioscience cell stimulation cocktail for 36 h at 37°C, under 5% CO_2. After incubation cells were treated with 50 μL BD Golgi Stop, following the manufacture's protocol. Cell cells not being blocked received 50 μL fresh complete RPMI plus 55 mM 2-mercaptoethanol medium. Cells were returned to incubator for additional 4 h to allow the intracellular accumulation of cytokines. Cells and supernatant were then collected for analysis by ICS Flow cytometry and murine adaptive cytokine panel.

Cells were collected from the plate, and wells were rinsed two times with complete media and added to the tube containing the respective cells. Cells were pelleted and washed two times with FBS, then counted adjusting volume to $1x10^6$/cells per μL. Cells were fixed using ice-cold BD Cytofix (Cat# 554655) per manufacturer's protocol. Cells were pelleted and washed 2 times before being resuspended in 1x BD Perm/Wash™ buffer (Cat# 554723) and incubated for 15 min

in the dark at RT. Cells were then centrifuged at 250x*g* for 10 min and supernatant was removed. Cells were then resuspended in 50 μL of BD Perm/Wash™ buffer and 20 μL/tube of BD CD4 T-cell phenotyping antibody cocktail or appropriate negative control. Cells were then incubated at RT for 30 min in the dark. Cells should be protected from light throughout the staining procedure. After incubation cells were washed 2x with FBS and then resuspended in 300 μL FBS and analyzed on the Beckman Coulter Gallios Flow Cytometer for CD4, Th1 (INF-γ), Th2 (IL-4), and Th17 (IL-17α) cell populations.

Statistical Analysis

All data points are represented as the average of triplicate values with their corresponding standard error of the means (S.E.M.). Kaplan-Meyer survival rate curves, unpaired *t*-test, One-way ANOVA, or Two-way ANOVA were utilized in the statistical analysis, as indicated in the figure legends. Graphs and statistical analysis were achieved using Graph Pad Prism 10 Software (GraphPad Software, Inc., La Jolla, CA).

Results

Evaluation of NGP29b as a Veterinary Vaccine Candidate Against T. cruzi Infection

The investigation into NGP29b as a potential vaccine candidate aimed at bolstering defense against *T. cruzi* infection in C57BL/6 mice, deficient in synthesizing the critical β-Gal*f* sugar, revealed intriguing insights into the humoral immune response post-vaccination. Sera collected on day 21 following the start of the vaccination series were subjected to detailed analysis for both IgG and IgM levels, shedding light on the vaccine's immunogenicity and potential efficacy.

Upon examining the titration of sera against NGP29b and the carrier molecule 2ME-BSA, distinct patterns in IgG production were observed (**Figure 4.1**). The 2ME-BSA vaccinated cohort exhibited markedly elevated IgG levels against both antigens. However, this reactivity displayed a diminishing trend with increasing serum dilutions, indicating a concentration-dependent response. Conversely, the NGP29b-vaccinated group displayed comparatively lower IgG production. Nevertheless, a significant elevation was evident, notably surpassing the normal mouse sera pool (NMSP) baseline at a 1:100 sera dilution.

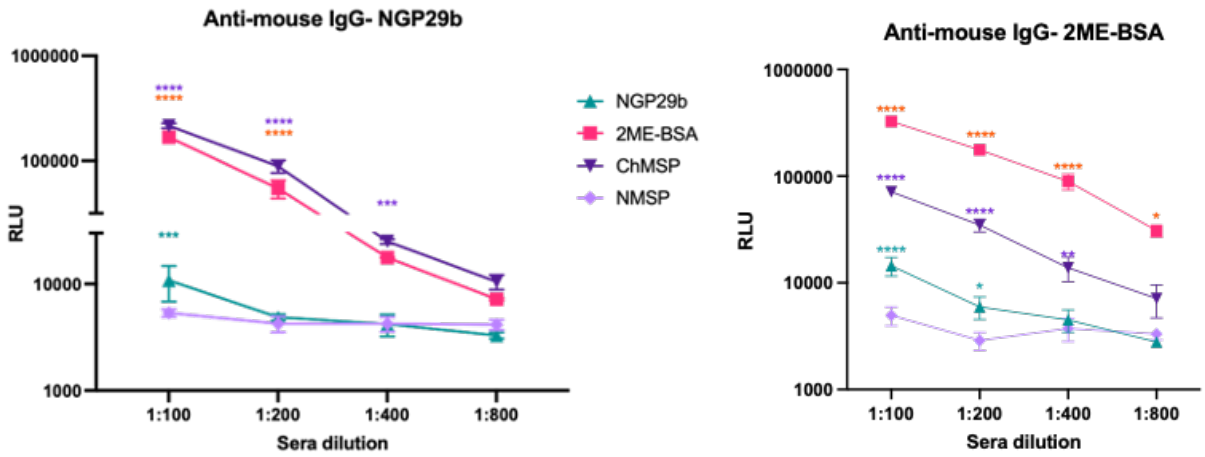

Figure 4.1. Type-II GIPL-like NGP29b elicits an effective adaptive immunological response upon vaccination in C57BL/6 mice. Total IgG was produced against either NGP29b (left), or 2ME-BSA (right), when assessed by CL-ELISA. Sera collected from mice vaccinated with 20 mg SQ three times at 7-day intervals, and then collected 7 days after the end of vaccination. Statistical analysis: Unpaired *t*-test . ****, $p<0.0001$; **, $p<0.001$; *, $p<0.01$; *, $p<0.05$.

Parallel to the IgG findings, evaluating free IgM levels against NGP29b and 2ME-BSA also showcased a robust response post-vaccination (**Figure 4.2**). Both the NGP29b- and 2ME-BSA-vaccinated groups exhibited a substantial increase in IgM levels against their respective antigens compared to the NMSP. This rise in IgM expression, akin to the IgG response, exhibited an anticipated decline in reactivity as serum dilutions increased. Intriguingly, both NGP29b and the hapten 2ME-BSA induced a similar IgM expression profile, contrasting the divergent IgG responses observed between the groups.

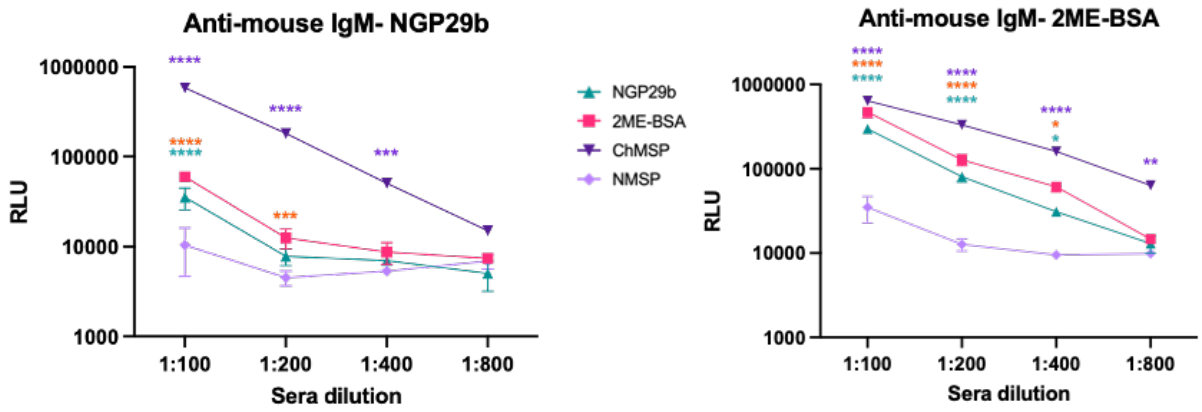

Figure 4.2. Type-II GIPL-like NGP29b elicits an effective adaptive immunological response upon vaccination in C57BL/6 mice. IgM was produced against either NGP29b (left), or 2ME-BSA (right), when assessed by CL-ELISA. Sera collected from mice vaccinated with 20 mg SQ three times at 7-day intervals, and then collected 7 days after the end of vaccination. Unpaired *t*-test. ****, p<0.0001; ***, p<0.001; **, p<0.01; *, p<0.05.

Immunoblotting experiments targeting CL-Brener$_{luc}$ TCT lysate aimed to elucidate whether the IgG generated post-vaccination would exhibit reactivity against specific proteins associated with *T. cruzi* parasites. Employing an acute CD mouse sera pool as a positive control, all vaccinated groups displayed reactivity to proteins glycosylated in known regions, including tGPI-MUCs (relative molecular mass of 70–250 kDa) (Almeida, Ferguson et al. 1994) and tGIPLs (relative molecular mass of <10 kDa) (**Figure 4.3**). This observation suggests a potential cross-reactivity between the induced IgG and distinct parasite antigens, highlighting the immunological potential of the NGP29b vaccine candidate against *T. cruzi* infection.

These findings underscore the nuanced humoral responses elicited by NGP29b vaccination, showcasing its promise as a viable candidate for bolstering defense mechanisms against *T. cruzi* infection in mammals. The observed immunogenicity and cross-reactivity patterns warrant further exploration to harness the full potential of NGP29b in combating *T. cruzi*-related pathogenesis.

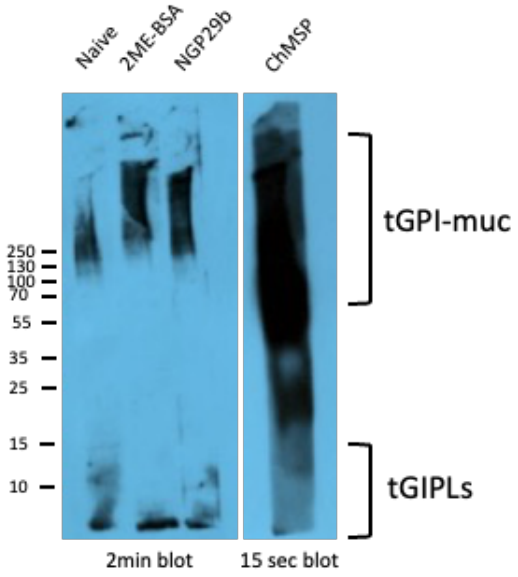

Figure 4.3. Type-II GIPL-like NGP29b Elicit an Effective Adaptive Immunological Response against *T. cruzi* upon vaccination in C57BL/6 mice. Sera collected from vaccinated mice, naïve, and a CD mouse serum pool, probed against 20 µg CL Brener$_{luc}$ TCT lysate.

Synthetic β-Galf glycovaccine fails to elicit a CD4⁺ T-cell response upon Ex vivostimulation in a murine model

In our quest to comprehensively fathom how these synthetic glycovaccines trigger a protective immune response, we embarked on a thorough investigation of the CD4⁺ T-helper (Th) cell phenotypes, meticulously scrutinizing the Th1⁺, Th2⁺, and Th17⁺ populations.

The experimental design involved the vaccination of cohorts, each comprising three female and three male C57Bl/6 mice. These groups were administered 20 µg of either PBS (as a control for naïve response), the hapten 2ME-BSA, or NGP29b. This vaccination regimen entailed three administrations spaced precisely seven days apart. On day 21, 7 days after the third vaccination, the mice were humanely euthanized, and their spleens were meticulously collected to undergo *ex vivo* stimulation to analyze the CD4⁺ T-helper cell population and cytokine profiling.

The isolated splenocytes underwent a recovery phase overnight, complemented by 10 ng/µL of IL-2. Subsequent to this recovery, the cells were carefully plated onto 96-well tissue culture plates coated with 10 µg/µL anti-murine CD3e. These cells were subjected to probing for CD4 expression, followed by intricate intracellular cytokine staining targeting critical molecules like INF-γ for $Th1^+$, IL-4 for $Th2^+$, and IL17a for $Th17^+$ cells.

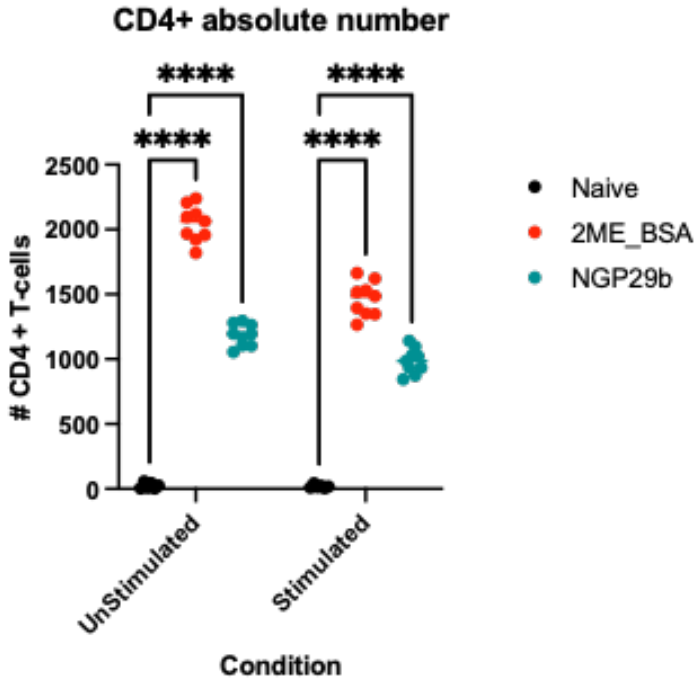

Figure 4.4. Synthetic β-Galf glycovaccine fails to elicit a $CD4^+$ T-cell response upon *ex-vivo* stimulation in a murine model. Statistical analysis: Two-way ANOVA. ****, $p<0.0001$; ***, $p<0.001$, **, $p<0.01$; *, $p<0.05$.

Regrettably, despite these elaborate procedures, our analysis through flow cytometry revealed a perplexing observation. Although there was a significant increase in the population of $CD4^+$ cells, there was notably a very limited number of cells interrogated (**Figure 4.4**). Moreover, the intended intracellular staining designed to detect internalized cytokines yielded no observable results, failing to indicate the presence of the targeted cytokines within the sampled cells.

This unforeseen and puzzling outcome has prompted a reassessment of our methodologies and a deeper exploration into potential factors that might underlie the absence of a discernible $CD4^+$ T-cell response and the failure to detect the anticipated cytokine expression within the studied cell populations.

Discussion

The research on NGP29b as a vaccine candidate against *T. cruzi* and *Leishmania* infection in C57BL/6 mice has shed light on the humoral immune response following vaccination. Our detailed analysis of serum samples after vaccination provided a thorough evaluation of IgG and IgM levels, revealing key aspects of the vaccine's immunogenicity and potential effectiveness. Notably, in the serum titration against NGP29b and the hapten 2ME-BSA, distinct patterns in IgG production were observed. The 2ME-BSA-vaccinated group showed significantly increased IgG levels against both antigens, displaying a concentration-dependent response that decreased with higher serum dilutions. In comparison, the NGP29b-vaccinated group exhibited lower but still significantly increased IgG production.

The analysis of free IgM levels against NGP29b and 2ME-BSA revealed strong responses post-vaccination in both groups. There was a marked increase in IgM levels against their respective antigens compared to the NMSP baseline. Similar to IgG, the IgM response declined with increasing serum dilutions. Interestingly, while IgG responses varied between the NGP29b and 2ME-BSA groups, the patterns of IgM expression were remarkably similar.

Our immunoblotting experiments targeting CL-Brener$_{luc}$ TCT lysate aimed to determine if the IgG generated post-vaccination would react with specific T. cruzi parasite proteins. All vaccinated groups showed reactivity to glycosylated proteins in known regions, such as tGPI-mucins (70–250 kDa) and tGIPLs (<10 kDa), comparable to the acute CD mouse sera pool, serving

as a positive control. This suggests potential cross-reactivity between induced IgG and various parasite antigens, highlighting NGP29b's immunological promise against *T. cruzi* infection. These findings underscore the complex and detailed humoral responses elicited by NGP29b vaccination, supporting its potential as a defense against *T. cruzi* infection in mammals. The observed immunogenicity and cross-reactivity warrant further research to fully utilize NGP29b in addressing *T. cruzi* and other trypanosomatid diseases (e.g., CL).

While focusing on humoral responses, we also examined $CD4^+$ T-helper (Th) cell phenotypes. Despite our comprehensive approach, including various treatments and ex-vivo stimulation, the CD4+ cell response observed through flow cytometry was unexpectedly limited. Additionally, our intracellular staining for cytokine detection within cells showed no results, contrary to the expected expression of $Th1^+$, $Th2^+$, and $Th17^+$ cytokines. This calls for reevaluating our methods and a deeper investigation into factors affecting the lack of a distinct CD4+ T-cell response and cytokine expression. Further research and methodological refinement are crucial to understanding the complex immune responses induced by synthetic glycovaccines.

Chapter 5. Overall Discussion

The initial findings derived from our comprehensive studies significantly contribute to the immunology and vaccine development fields. Specifically, we have embarked on an innovative and pioneering exploration to understand the potential of NGP28b and NGP29b as immunogens within the complex landscape of a murine model co-infected with both *L. major* and *T. cruzi*. It is worth noting that this represents one of the first instances where researchers have sought to evaluate a prophylactic vaccine capable of protecting against the dual threat of Chagas disease and tegumentary leishmaniasis. This unique approach opens up a promising avenue for addressing the formidable challenge posed by these two debilitating diseases.

In the context of this groundbreaking investigation, our experimental data has yielded compelling insights, particularly regarding the comparative effectiveness of NGP28b and NGP29b in conferring immunity against co-infections, as mentioned above. Our results are remarkable, as they indicate that NGP28b exhibits superior protective properties compared to NGP29b. Our analyses of survival rates and in vivo imaging substantiate this superior performance, which reveals that NGP28b affords a significantly heightened overall protection against both the *L. major* and *T. cruzi* infections.

One of the most intriguing aspects of our research lies in exploring IgG antibody titers. We have observed that NGP29b has the remarkable ability to induce a higher production of antibodies. Moreover, these antibodies possess an intriguing quality – they exhibit cross-reactivity not only with NGP29b but also with NGP28b. This remarkable observation underscores the versatility and potential of NGP29b as a vaccine candidate. The fact that NGP29b's smaller molecular structure can elicit a more expansive antibody response with heightened cross-reactivity is a promising avenue for further investigation.

On the other hand, NGP28b, with its larger molecular structure, presents a different facet of immunogenicity. Our research has uncovered that NGP28b generates a broader spectrum of potential epitopes, thus resulting in a more robust, albeit less epitope-specific antibody response.

The distinct nature of this response, as illuminated by our IgG isotype data, presents a rich area for future exploration. The balance between epitope diversity and specificity, as influenced by the vaccine's molecular size, could be a pivotal factor in shaping the efficacy of these vaccine candidates.

In addition to these novel insights, our study delves into the immune responses at the cellular level, revealing that both NGP28b and NGP29b elicit a $Th1^{+}/CD4^{+}$ response in splenocytes, emphasizing their capacity to induce a cellular immune response. The observed CD4+ Th2+ immune response aligns with the Th1/Th2 balance hypothesis, with NGP29b showing a significant increase in CD4+ Th2+ cells compared to the naïve group. These findings are further supported by the adaptive cytokine profile analysis, providing a comprehensive understanding of the multifaceted immune responses triggered by these vaccines.

In parallel, the investigation into NGP29b's humoral immune response showcases its potential against *T. cruzi* and *Leishmania* infection. Our meticulous analysis of IgG and IgM levels post-vaccination unveils distinctive patterns in antibody production between NGP29b and the hapten molecule 2ME-BSA. NGP29b triggers elevated IgG and IgM levels, hinting at its promising role in fortifying defense mechanisms against *T. cruzi* and *Leishmania* infection.

However, despite these strides in understanding humoral responses, our exploration of CD4+ T-cell phenotypes faced unexpected limitations. The observed restricted population of CD4+ cells and the failure to detect targeted cytokine expression demand a reevaluation of methodologies and further investigation into factors influencing the immune response triggered by synthetic glycovaccines.

In summary, these findings highlight the potential of NGP28b and NGP29b in combatting co-infections, showcasing diverse immune responses, and emphasizing the need for continued exploration to optimize vaccine efficacy against complex diseases.

Our study is driven by the mounting concerns surrounding *T. cruzi* and *Leishmania* infections, impacting domesticated mammalian pets, livestock, and even posing risks of food contamination. These parasitic diseases not only endanger animal and human health but also

underscore the necessity for a human vaccine. By investigating NGP29b's potential as a vaccine candidate, our research aims to tackle these multifaceted challenges. Notably, this endeavor in veterinary medicine holds promise not only for developing preventive measures safeguarding animals and humans in shared environments but also for addressing the urgent need for a human vaccine against these infections.

REFERENCES

Abdelhak, S., H. Louzir, J. Timm, L. Blel, Z. Benlasfar, M. Lagranderie, M. Gheorghiu, K. Dellagi and B. Gicquel (1995). "Recombinant BCG expressing the leishmania surface antigen Gp63 induces protective immunity against Leishmania major infection in BALB/c mice." Microbiology (Reading) **141 (Pt 7)**: 1585-1592.

Acosta-Serrano, A., G. R. Hutchinson, D. Pridmore, B. A. Smith, M. Swain, A. V. Jager, A. Osuna, A. Tandya, M. C. Taylor, J. M. Kelly, M. J. Lehane and D. I. Pritchard (2007). "A Trypanosome Suppressing Factor from a Mutant Bacterium of the Rhizobium–Agrobacterium Group." PLoS Pathogens **3**(4): e1000099.

Almeida, I. C., M. M. Camargo, D. O. Procópio, L. S. Silva, A. Mehlert, L. R. Travassos, R. T. Gazzinelli and M. A. Ferguson (2000). "Highly purified glycosylphosphatidylinositols from Trypanosoma cruzi are potent proinflammatory agents." The EMBO Journal **19**(7): 1476-1485.

Almeida, I. C., M. A. Ferguson, S. Schenkman and L. R. Travassos (1994). "Lytic anti-alpha-galactosyl antibodies from patients with chronic Chagas' disease recognize novel O-linked oligosaccharides on mucin-like glycosyl-phosphatidylinositol-anchored glycoproteins of Trypanosoma cruzi." Biochem J **304 (Pt 3)**: 793-802.

Almeida, I. C., M. A. Ferguson, S. Schenkman and L. R. Travassos (1994). "Lytic anti-alpha-galactosyl antibodies from patients with chronic Chagas' disease recognize novel O-linked

oligosaccharides on mucin-like glycosyl-phosphatidylinositol-anchored glycoproteins of *Trypanosoma cruzi*." Biochem J **304 (Pt 3)**: 793-802.

Almeida, I. C., G. M. Krautz, A. U. Krettli and L. R. Travassos (1993). "Glycoconjugates of Trypanosoma cruzi: a 74 kD antigen of trypomastigotes specifically reacts with lytic anti-alpha-galactosyl antibodies from patients with chronic Chagas disease." J Clin Lab Anal **7**(6): 307-316.

Almeida, I. C., S. R. Milani, P. A. Gorin and L. R. Travassos (1991). "Complement-mediated lysis of Trypanosoma cruzi trypomastigotes by human anti-alpha-galactosyl antibodies." J Immunol **146**(7): 2394-2400.

Alvar, J., I. D. Vélez, C. Bern, M. Herrero, P. Desjeux, J. Cano, J. Jannin and M. den Boer (2012). "Leishmaniasis worldwide and global estimates of its incidence." PLoS One **7**(5): e35671.

Anthony, R. M., T. Kobayashi, F. Wermeling and J. V. Ravetch (2011). "Intravenous gammaglobulin suppresses inflammation through a novel T(H)2 pathway." Nature **475**(7354): 110-113.

Arumugham, R. G., T. C. Hsieh, M. L. Tanzer and R. A. Laine (1986). "Structures of the asparagine-linked sugar chains of laminin." Biochim Biophys Acta **883**(1): 112-126.

Ati, J., C. Colas, P. Lafite, R. P. Sweeney, R. B. Zheng, T. L. Lowary and R. Daniellou (2018). "The LPG1x family from Leishmania major is constituted of rare eukaryotic galactofuranosyltransferases with unprecedented catalytic properties." Scientific Reports **8**(1).

Atzeni, F. and P. Sarzi-Puttini (2013). Tumor Necrosis Factor. Brenner's Encyclopedia of Genetics (Second Edition). S. Maloy and K. Hughes. San Diego, Academic Press**:** 229-231.

Avila, J. L., M. Rojas and U. Galili (1989). "Immunogenic Gal alpha 1----3Gal carbohydrate epitopes are present on pathogenic American Trypanosoma and Leishmania." J Immunol **142**(8): 2828-2834.

Badiee, A., M. R. Jaafari, A. Khamesipour, A. Samiei, D. Soroush, M. T. Kheiri, F. Barkhordari, W. R. McMaster and F. Mahboudi (2009). "Enhancement of immune response and protection in BALB/c mice immunized with liposomal recombinant major surface glycoprotein of Leishmania (rgp63): the role of bilayer composition." Colloids Surf B Biointerfaces **74**(1): 37-44.

Balasegaram, M., K. Ritmeijer, M. A. Lima, S. Burza, G. Ortiz Genovese, B. Milani, S. Gaspani, J. Potet and F. Chappuis (2012). "Liposomal amphotericin B as a treatment for human leishmaniasis." Expert Opin Emerg Drugs **17**(4): 493-510.

Basu, R., S. Bhaumik, J. M. Basu, K. Naskar, T. De and S. Roy (2005). "Kinetoplastid membrane protein-11 DNA vaccination induces complete protection against both pentavalent antimonial-sensitive and -resistant strains of Leishmania donovani that correlates with inducible nitric oxide synthase activity and IL-4 generation: evidence for mixed Th1- and Th2-like responses in visceral leishmaniasis." J Immunol **174**(11): 7160-7171.

Bento, C. A., M. B. Melo, J. O. Previato, L. Mendonça-Previato and L. M. Peçanha (1996). "Glycoinositolphospholipids purified from Trypanosoma cruzi stimulate Ig production in vitro." The Journal of Immunology **157**(11): 4996.

Bern, C. (2015). "Chagas' Disease." N Engl J Med **373**(19): 1882.

Bern, C., D. L. Martin and R. H. Gilman (2011). "Acute and congenital Chagas disease." Adv Parasitol **75**: 19-47.

Bhaumik, S., R. Basu, S. Sen, K. Naskar and S. Roy (2009). "KMP-11 DNA immunization significantly protects against L. donovani infection but requires exogenous IL-12 as an adjuvant for comparable protection against L. major." Vaccine **27**(9): 1306-1316.

Buscaglia, C. A., V. A. Campo, A. C. Frasch and J. M. Di Noia (2006). "Trypanosoma cruzi surface mucins: host-dependent coat diversity." Nat Rev Microbiol **4**(3): 229-236.

Cabezas, Y., L. Legentil, F. Robert-Gangneux, F. Daligault, S. Belaz, C. Nugier-Chauvin, S. Tranchimand, C. Tellier, J. P. Gangneux and V. Ferrieres (2015). "Leishmania cell wall as a potent target for antiparasitic drugs. A focus on the glycoconjugates." Org Biomol Chem **13**(31): 8393-8404.

Cavaillon, J. M. (1994). "Cytokines and macrophages." Biomedicine & Pharmacotherapy **48**(10): 445-453.

Centers for Disease Control (2020). "Parasites - Leishmaniasis,."

Chagas, C. (1909). "Nova tripanozomiaze humana: estudos sobre a morfolojia e o ciclo evolutivo do Schizotrypanum cruzi n. gen., n. sp., ajente etiolojico de nova entidade morbida do homem." Memórias do Instituto Oswaldo Cruz **1**: 159-218.

Chlubnova, I., L. Legentil, R. Dureau, A. Pennec, M. Almendros, R. Daniellou, C. Nugier-Chauvin and V. Ferrières (2012). "Specific and non-specific enzymes for furanosyl-containing conjugates: biosynthesis, metabolism, and chemo-enzymatic synthesis." Carbohydrate Research **356**: 44-61.

Davies, C. R., R. Reithinger, D. Campbell-Lendrum, D. Feliciangeli, R. Borges and N. Rodriguez (2000). "The epidemiology and control of leishmaniasis in Andean countries." Cad Saude Publica **16**(4): 925-950.

de ARRUDA, M. V., W. COLLI and B. ZINGALES (1989). "Terminal β-d-galactofuranosyl epitopes recognized by antibodies that inhibit Trypanosoma cruzi internalization into mammalian cells." European Journal of Biochemistry **182**(2): 413-421.

de Lederkremer, R. M. and R. Agusti (2009). "Glycobiology of Trypanosoma cruzi." Adv Carbohydr Chem Biochem **62**: 311-366.

de Lederkremer, R. M. and W. Colli (1995). "Galactofuranose-containing glycoconjugates in trypanosomatids." Glycobiology **5**(6): 547-552.

de Lederkremer, R. M., C. Lima, M. I. Ramirez, M. A. Ferguson, S. W. Homans and J. Thomas-Oates (1991). "Complete structure of the glycan of lipopeptidophosphoglycan from Trypanosoma cruzi Epimastigotes." J Biol Chem **266**(35): 23670-23675.

De Pablos, L. M. and A. Osuna (2012). "Multigene families in Trypanosoma cruzi and their role in infectivity." Infect Immun **80**(7): 2258-2264.

Deshmane, S. L., S. Kremlev, S. Amini and B. E. Sawaya (2009). "Monocyte chemoattractant protein-1 (MCP-1): an overview." J Interferon Cytokine Res **29**(6): 313-326.

Desjeux, P. (2004). "Leishmaniasis: current situation and new perspectives." Comp Immunol Microbiol Infect Dis **27**(5): 305-318.

Dorlo, T. P., M. Balasegaram, J. H. Beijnen and P. J. de Vries (2012). "Miltefosine: a review of its pharmacology and therapeutic efficacy in the treatment of leishmaniasis." J Antimicrob Chemother **67**(11): 2576-2597.

Doudna, J. A. and E. Charpentier (2014). "Genome editing. The new frontier of genome engineering with CRISPR-Cas9." Science **346**(6213): 1258096.

Dufour, J. H., M. Dziejman, M. T. Liu, J. H. Leung, T. E. Lane and A. D. Luster (2002). "IFN-γ-Inducible Protein 10 (IP-10; CXCL10)-Deficient Mice Reveal a Role for IP-10 in Effector T Cell Generation and Trafficking1." The Journal of Immunology **168**(7): 3195-3204.

Dutra, W. O., C. A. Menezes, L. M. Magalhães and K. J. Gollob (2014). "Immunoregulatory networks in human Chagas disease." Parasite Immunol **36**(8): 377-387.

Emslie, D., K. D'Costa, J. Hasbold, D. Metcalf, K. Takatsu, P. O. Hodgkin and L. M. Corcoran (2008). "Oct2 enhances antibody-secreting cell differentiation through regulation of IL-5 receptor alpha chain expression on activated B cells." J Exp Med **205**(2): 409-421.

Ferrante, A., L. J. Beard and R. G. Feldman (1990). "IgG subclass distribution of antibodies to bacterial and viral antigens." Pediatr Infect Dis J **9**(8 Suppl): S16-24.

Fonseca, L. M. d., K. M. da Costa, V. d. S. Chaves, C. G. Freire-de-Lima, A. Morrot, L. Mendonça-Previato, J. O. Previato and L. Freire-de-Lima (2019). "Theft and Reception of Host Cell's Sialic Acid: Dynamics of Trypanosoma Cruzi Trans-sialidases and Mucin-Like Molecules on Chagas' Disease Immunomodulation." Frontiers in Immunology **10**.

Food and Drug Administration. (2014). "CDER Rare Disease And Orphan Drug Designated Approvals,." from https://www.fda.gov/media/116659/download.

Gaffen, S. L., R. Jain, A. V. Garg and D. J. Cua (2014). "The IL-23–IL-17 immune axis: from mechanisms to therapeutic testing." Nature Reviews Immunology **14**(9): 585-600.

Galili, U. (2016). "Natural anti-carbohydrate antibodies contributing to evolutionary survival of primates in viral epidemics?" Glycobiology **26**(11): 1140-1150.

Galili, U. (2018). The Natural Anti-Gal Antibody As Foe Turned Friend In Medicine. London, San Diego, Cambridge, Oxford, Academic Press, Elsevier.

Galili, U., M. R. Clark, S. B. Shohet, J. Buehler and B. A. Macher (1987). "Evolutionary relationship between the natural anti-Gal antibody and the Gal alpha 1----3Gal epitope in primates." Proceedings of the National Academy of Sciences **84**(5): 1369-1373.

Galili, U. and K. Swanson (1991). "Gene sequences suggest inactivation of alpha-1,3-galactosyltransferase in catarrhines after the divergence of apes from monkeys." Proceedings of the National Academy of Sciences of the United States of America **88**(16): 7401-7404.

Garg, N. and R. L. Tarleton (2002). "Genetic immunization elicits antigen-specific protective immune responses and decreases disease severity in Trypanosoma cruzi infection." Infection and immunity **70**(10): 5547-5555.

Gascon, J., C. Bern and M. J. Pinazo (2010). "Chagas disease in Spain, the United States and other non-endemic countries." Acta Trop **115**(1-2): 22-27.

Gazzinelli, R. T., M. M. Camargo, I. C. Almeida, Y. S. Morita, M. Giraldo, A. Acosta-Serrano, S. Hieny, P. T. Englund, M. A. Ferguson, L. R. Travassos and A. Sher (1997). "Identification and characterization of protozoan products that trigger the synthesis of IL-12 by inflammatory macrophages." Chem Immunol **68**: 136-152.

Gazzinelli, R. T., M. E. Pereira, A. Romanha, G. Gazzinelli and Z. Brener (1991). "Direct lysis of Trypanosoma cruzi: a novel effector mechanism of protection mediated by human anti-gal antibodies." Parasite Immunol **13**(4): 345-356.

Giorgi, M. E. and R. M. de Lederkremer (2011). "Trans-sialidase and mucins of Trypanosoma cruzi: an important interplay for the parasite." Carbohydrate research **346**(12): 1389-1393.

Giorgi, M. E. and R. M. Lederkremer (2020). "The Glycan Structure of T. cruzi mucins Depends on the Host. Insights on the Chameleonic Galactose." Molecules **25**(17).

Golgher, D. B., W. Colli, T. Souto-Padrón and B. Zingales (1993). "Galactofuranose-containing glycoconjugates of epimastigote and trypomastigote forms of Trypanosoma cruzi." Molecular and Biochemical Parasitology **60**(2): 249-264.

Guerin, P. J., P. Olliaro, S. Sundar, M. Boelaert, S. L. Croft, P. Desjeux, M. K. Wasunna and A. D. Bryceson (2002). "Visceral leishmaniasis: current status of control, diagnosis, and treatment, and a proposed research and development agenda." Lancet Infect Dis **2**(8): 494-501.

Handman, E., L. L. Button and R. W. McMaster (1990). "Leishmania major: production of recombinant gp63, its antigenicity and immunogenicity in mice." Exp Parasitol **70**(4): 427-435.

Haworth, W. N., H. Raistrick and M. Stacey (1937). "Polysaccharides synthesised by micro-organisms: The molecular structure of galactocarolose produced from glucose by Penicillium Charlesii G. Smith." Biochem J **31**(4): 640-644.

Hodi, F. S. and R. J. Soiffer (2002). Interleukins. Encyclopedia of Cancer (Second Edition). J. R. Bertino. New York, Academic Press**:** 523-535.

Hotez, P. J., D. H. Molyneux, A. Fenwick, J. Kumaresan, S. E. Sachs, J. D. Sachs and L. Savioli (2007). "Control of neglected tropical diseases." N Engl J Med **357**(10): 1018-1027.

Iniguez, E., N. S. Schocker, K. Subramaniam, S. Portillo, A. L. Montoya, W. S. Al-Salem, C. L. Torres, F. Rodriguez, O. C. Moreira, A. Acosta-Serrano, K. Michael, I. C. Almeida and R. A. Maldonado (2017). "An α-Gal-containing neoglycoprotein-based vaccine partially protects against murine cutaneous leishmaniasis caused by Leishmania major." PLoS Negl Trop Dis **11**(10): e0006039.

Iyer, S. S. and G. Cheng (2012). "Role of interleukin 10 transcriptional regulation in inflammation and autoimmune disease." Crit Rev Immunol **32**(1): 23-63.

Kaye, P. and P. Scott (2011). "Leishmaniasis: complexity at the host-pathogen interface." Nat Rev Microbiol **9**(8): 604-615.

Kopf, M., G. Le Gros, M. Bachmann, M. C. Lamers, H. Bluethmann and G. Köhler (1993). "Disruption of the murine IL-4 gene blocks Th2 cytokine responses." Nature **362**(6417): 245-248.

Landsteiner, K. and C. P. Miller (1925). "SEROLOGICAL STUDIES ON THE BLOOD OF THE PRIMATES : I. THE DIFFERENTIATION OF HUMAN AND ANTHROPOID BLOODS." J Exp Med **42**(6): 841-852.

Lewis, M. D., A. Fortes Francisco, M. C. Taylor, H. Burrell-Saward, A. P. McLatchie, M. A. Miles and J. M. Kelly (2014). "Bioluminescence imaging of chronic Trypanosoma cruzi infections reveals tissue-specific parasite dynamics and heart disease in the absence of locally persistent infection." Cell Microbiol **16**(9): 1285-1300.

Machado, F. S., W. O. Dutra, L. Esper, K. J. Gollob, M. M. Teixeira, S. M. Factor, L. M. Weiss, F. Nagajyothi, H. B. Tanowitz and N. J. Garg (2012). "Current understanding of immunity to Trypanosoma cruzi infection and pathogenesis of Chagas disease." Semin Immunopathol **34**(6): 753-770.

Macher, B. A. and U. Galili (2008). "The Galα1,3Galβ1,4GlcNAc-R (α-Gal) epitope: A carbohydrate of unique evolution and clinical relevance." Biochimica et Biophysica Acta (BBA) - General Subjects **1780**(2): 75-88.

Mamat, U., U. Seydel, O. Holst, D. Grimmecke and E. T. Rietschel (1999). Lipopolysaccharides. Carbohydrates and Their Derivatives Including Tannins, Cellulose, and Related Lignins. B. M. Pinto. Amsterdam, The Netherlands, Elsevier Science**:** 179-240.

Manne-Goehler, J., M. R. Reich and V. J. Wirtz (2015). "Access to care for Chagas disease in the United States: a health systems analysis." Am J Trop Med Hyg **93**(1): 108-113.

Manne-Goehler, J., C. A. Umeh, S. P. Montgomery and V. J. Wirtz (2016). "Estimating the Burden of Chagas Disease in the United States." PLoS Negl Trop Dis **10**(11): e0005033.

Marino, C., A. Rinflerch and R. M. de Lederkremer (2017). "Galactofuranose antigens, a target for diagnosis of fungal infections in humans." Future science OA **3**(3): FSO199-FSO199.

Marsden, P. D. (1986). "Mucosal leishmaniasis ("espundia" Escomel, 1911)." Trans R Soc Trop Med Hyg **80**(6): 859-876.

Mazumder, S., M. Maji, A. Das and N. Ali (2011). "Potency, efficacy and durability of DNA/DNA, DNA/protein and protein/protein based vaccination using gp63 against Leishmania donovani in BALB/c mice." PLoS One **6**(2): e14644.

McConville, M. J., T. A. Collidge, M. A. Ferguson and P. Schneider (1993). "The glycoinositol phospholipids of Leishmania mexicana promastigotes. Evidence for the presence of three distinct pathways of glycolipid biosynthesis." J Biol Chem **268**(21): 15595-15604.

McConville, M. J. and M. A. Ferguson (1993). "The structure, biosynthesis and function of glycosylated phosphatidylinositols in the parasitic protozoa and higher eukaryotes." Biochem J **294 (Pt 2)**(Pt 2): 305-324.

McGeachy, M. J., D. J. Cua and S. L. Gaffen (2019). "The IL-17 Family of Cytokines in Health and Disease." Immunity **50**(4): 892-906.

McNeil, M., S. J. Wallner, S. W. Hunter and P. J. Brennan (1987). "Demonstration that the galactosyl and arabinosyl residues in the cell-wall arabinogalactan of Mycobacterium leprae and Myobacterium tuberculosis are furanoid." Carbohydrate research **166**(2): 299-308.

Mendonça-Previato, L., L. Penha, T. C. Garcez, C. Jones and J. O. Previato (2013). "Addition of α-O-GlcNAc to threonine residues define the post-translational modification of mucin-like molecules in Trypanosoma cruzi." Glycoconjugate Journal **30**(7): 659-666.

Menon, A. P., B. Moreno, D. Meraviglia-Crivelli, F. Nonatelli, H. Villanueva, M. Barainka, A. Zheleva, H. M. van Santen and F. Pastor (2023). "Modulating T Cell Responses by Targeting CD3." Cancers (Basel) **15**(4).

Milani, S. R. and L. R. Travassos (1988). "Anti-alpha-galactosyl antibodies in chagasic patients. Possible biological significance." Braz J Med Biol Res **21**(6): 1275-1286.

Mohebali, M., A. Nadim and A. Khamesipour (2019). "An overview of leishmanization experience: A successful control measure and a tool to evaluate candidate vaccines." Acta Trop **200**: 105173.

Montoya, A. L., E. R. Gil, E. L. Heydemann, I. L. Estevao, B. E. Luna, C. C. Ellis, S. R. Jankuru, B. Alarcón de Noya, O. Noya, M. P. Zago, I. C. Almeida and K. Michael (2022). "Specific Recognition of β-Galactofuranose-Containing Glycans of Synthetic Neoglycoproteins by Sera of Chronic Chagas Disease Patients." Molecules **27**(2).

Moore, K. W., R. de Waal Malefyt, R. L. Coffman and A. O'Garra (2001). "Interleukin-10 and the interleukin-10 receptor." Annu Rev Immunol **19**: 683-765.

Mucci, J., A. B. Lantos, C. A. Buscaglia, M. S. Leguizamón and O. Campetella (2017). "The Trypanosoma cruzi Surface, a Nanoscale Patchwork Quilt." Trends Parasitol **33**(2): 102-112.

Ortega-Rodriguez, U., S. Portillo, R. A. Ashmus, J. A. Duran, N. S. Schocker, E. Iniguez, A. L. Montoya, B. G. Zepeda, J. J. Olivas, N. H. Karimi, J. Alonso-Padilla, L. Izquierdo, M. J. Pinazo, B. A. de Noya, O. Noya, R. A. Maldonado, F. Torrico, J. Gascon, K. Michael and I. C. Almeida (2019). "Purification of Glycosylphosphatidylinositol-Anchored Mucins from Trypanosoma cruzi Trypomastigotes and Synthesis of α-Gal-Containing Neoglycoproteins: Application as Biomarkers for Reliable Diagnosis and Early Assessment of Chemotherapeutic Outcomes of Chagas Disease." Methods Mol Biol **1955**: 287-308.

Pacheco-Fernandez, T., G. Volpedo, S. Gannavaram, P. Bhattacharya, R. Dey, A. Satoskar, G. Matlashewski and H. L. Nakhasi (2021). "Revival of Leishmanization and Leishmanin." Front Cell Infect Microbiol **11**: 639801.

Pereira-Chioccola, V. L., A. Acosta-Serrano, I. Correia de Almeida, M. A. Ferguson, T. Souto-Padron, M. M. Rodrigues, L. R. Travassos and S. Schenkman (2000). "Mucin-like molecules form a negatively charged coat that protects Trypanosoma cruzi trypomastigotes from killing by human anti-alpha-galactosyl antibodies." J Cell Sci **113 (Pt 7)**: 1299-1307.

Portillo, S., B. G. Zepeda, E. Iniguez, J. J. Olivas, N. H. Karimi, O. C. Moreira, A. F. Marques, K. Michael, R. A. Maldonado and I. C. Almeida (2019). "A prophylactic α-Gal-based glycovaccine effectively protects against murine acute Chagas disease." NPJ Vaccines **4**: 13.

Previato, J. O., P. A. Gorin, M. Mazurek, M. T. Xavier, B. Fournet, J. M. Wieruszesk and L. Mendonça-Previato (1990). "Primary structure of the oligosaccharide chain of lipopeptidophosphoglycan of epimastigote forms of Trypanosoma cruzi." J Biol Chem **265**(5): 2518-2526.

Previato, J. O., R. Wait, C. Jones, G. A. DosReis, A. R. Todeschini, N. Heise and L. M. Previato (2004). "Glycoinositolphospholipid from Trypanosoma cruzi: structure, biosynthesis and immunobiology." Adv Parasitol **56**: 1-41.

Rao, C. N., I. J. Goldstein and L. A. Liotta (1983). "Lectin-binding domains on laminin." Arch Biochem Biophys **227**(1): 118-124.

Rassi, A., Jr., A. Rassi and J. A. Marin-Neto (2010). "Chagas disease." Lancet **375**(9723): 1388-1402.

Reithinger, R., J. C. Dujardin, H. Louzir, C. Pirmez, B. Alexander and S. Brooker (2007). "Cutaneous leishmaniasis." Lancet Infect Dis **7**(9): 581-596.

Richards, M. R. and T. L. Lowary (2009). "Chemistry and Biology of Galactofuranose-Containing Polysaccharides." ChemBioChem **10**(12): 1920-1938.

Rios, L. E., J. C. Vázquez-Chagoyán, A. O. Pacheco, M. P. Zago and N. J. Garg (2019). "Immunity and vaccine development efforts against Trypanosoma cruzi." Acta tropica **200**: 105168-105168.

Rocha, M. O., M. M. Teixeira and A. L. Ribeiro (2007). "An update on the management of Chagas cardiomyopathy." Expert Rev Anti Infect Ther **5**(4): 727-743.

Rodríguez-Morales, O., V. Monteón-Padilla, S. C. Carrillo-Sánchez, M. Rios-Castro, M. Martínez-Cruz, A. Carabarin-Lima and M. Arce-Fonseca (2015). "Experimental Vaccines against Chagas Disease: A Journey through History." Journal of Immunology Research **2015**: 489758.

Roy, G., C. Dumas, D. Sereno, Y. Wu, A. K. Singh, M. J. Tremblay, M. Ouellette, M. Olivier and B. Papadopoulou (2000). "Episomal and stable expression of the luciferase reporter gene for quantifying Leishmania spp. infections in macrophages and in animal models." Mol Biochem Parasitol **110**(2): 195-206.

Sánchez-Valdéz, F. J., C. Pérez Brandán, A. Ferreira and M. Basombrío (2015). "Gene-deleted live-attenuated Trypanosoma cruzi parasites as vaccines to protect against Chagas disease." Expert Rev Vaccines **14**(5): 681-697.

Schenkman, S., M. S. Jiang, G. W. Hart and V. Nussenzweig (1991). "A novel cell surface trans-sialidase of Trypanosoma cruzi generates a stage-specific epitope required for invasion of mammalian cells." Cell **65**(7): 1117-1125.

Schnaidman, B. B., N. Yoshida, P. A. J. GORIN and L. R. TRAVASSOS (1986). "Cross-Reactive Polysaccharides from Trypanosoma cruzi and Fungi (Especially Dactylium dendroides)1." The Journal of Protozoology **33**(2): 186-191.

Schneider, P., J. P. Rosat, A. Ransijn, M. A. Ferguson and M. J. McConville (1993). "Characterization of glycoinositol phospholipids in the amastigote stage of the protozoan parasite Leishmania major." Biochem J **295 (Pt 2)**: 555-564.

Schroeder, J. and T. Aebischer (2011). "Vaccines for leishmaniasis: from proteome to vaccine candidates." Hum Vaccin **7 Suppl**: 10-15.

Scorza, B. M., E. M. Carvalho and M. E. Wilson (2017). "Cutaneous Manifestations of Human and Murine Leishmaniasis." Int J Mol Sci **18**(6).

Seničar, M., P. Lafite, S. V. Eliseeva, S. Petoud, L. Landemarre and R. Daniellou (2020). "Galactofuranose-Related Enzymes: Challenges and Hopes." International journal of molecular sciences **21**(10): 3465.

Serrano, A. A., S. Schenkman, N. Yoshida, A. Mehlert, J. M. Richardson and M. A. J. Ferguson (1995). "The Lipid Structure of the Glycosylphosphatidylinositol-anchored Mucin-like Sialic Acid Acceptors of Trypanosoma cruzi Changes during Parasite Differentiation from Epimastigotes to Infective Metacyclic Trypomastigote Forms (*)." Journal of Biological Chemistry **270**(45): 27244-27253.

Singh, S., D. Anshita and V. Ravichandiran (2021). "MCP-1: Function, regulation, and involvement in disease." Int Immunopharmacol **101**(Pt B): 107598.

Singh, S., J. A. Thompson, B. Yilmaz, H. Li, S. Weis, D. Sobral, M. Truglio, F. Aires da Silva, S. Aguiar, A. R. Carlos, S. Rebelo, S. Cardoso, E. Gjini, G. Nunez and M. P. Soares (2021). "Loss of alpha-gal during primate evolution enhanced antibody-effector function and resistance to bacterial sepsis." Cell Host Microbe **29**(3): 347-361 e312.

Souto-Padron, T., I. C. Almeida, W. de Souza and L. R. Travassos (1994). "Distribution of alpha-galactosyl-containing epitopes on Trypanosoma cruzi trypomastigote and amastigote forms from infected Vero cells detected by Chagasic antibodies." J Eukaryot Microbiol **41**(1): 47-54.

Späth, G. F. and S. M. Beverley (2001). "A lipophosphoglycan-independent method for isolation of infective Leishmania metacyclic promastigotes by density gradient centrifugation." Exp Parasitol **99**(2): 97-103.

Sundar, S. and J. Chakravarty (2010). "Antimony toxicity." Int J Environ Res Public Health **7**(12): 4267-4277.

Szarfman, A., V. P. Terranova, S. I. Rennard, J. M. Foidart, M. de Fatima Lima, J. I. Scheinman and G. R. Martin (1982). "Antibodies to laminin in Chagas' disease." J Exp Med **155**(4): 1161-1171.

Tarleton, R. L. (2001). "Parasite persistence in the aetiology of Chagas disease." Int J Parasitol **31**(5-6): 550-554.

Tau, G. and P. Rothman (1999). "Biologic functions of the IFN-gamma receptors." Allergy **54**(12): 1233-1251.

Tearle, R. G., M. J. Tange, Z. L. Zannettino, M. Katerelos, T. A. Shinkel, B. J. Van Denderen, A. J. Lonie, I. Lyons, M. B. Nottle, T. Cox, C. Becker, A. M. Peura, P. L. Wigley, R. J. Crawford, A. J. Robins, M. J. Pearse and A. J. d'Apice (1996). "The alpha-1,3-galactosyltransferase knockout mouse. Implications for xenotransplantation." Transplantation **61**(1): 13-19.

Thalhofer, C. J., J. W. Graff, L. Love-Homan, S. M. Hickerson, N. Craft, S. M. Beverley and M. E. Wilson (2010). "In vivo imaging of transgenic Leishmania parasites in a live host." J Vis Exp(41).

Thall, A. D., H. S. Murphy and J. B. Lowe (1996). "alpha 1,3-Galactosyltransferase-deficient mice produce naturally occurring cytotoxic anti-Gal antibodies." Transplant Proc **28**(2): 556-557.

Torres-Guerrero, E., M. R. Quintanilla-Cedillo, J. Ruiz-Esmenjaud and R. Arenas (2017). "Leishmaniasis: a review." F1000Res **6**: 750.

Towbin, H., G. Rosenfelder, J. Wieslander, J. L. Avila, M. Rojas, A. Szarfman, K. Esser, H. Nowack and R. Timpl (1987). "Circulating antibodies to mouse laminin in Chagas disease, American cutaneous leishmaniasis, and normal individuals recognize terminal galactosyl(alpha 1-3)-galactose epitopes." J Exp Med **166**(2): 419-432.

Travassos, L. R. and I. C. Almeida (1993). "Carbohydrate immunity in American trypanosomiasis." Springer Semin Immunopathol **15**(2-3): 183-204.

U.S Food and Drug Administration. (2018, March 27). "FDA approves first U.S. treatment for Chagas disease." from https://www.fda.gov/news-events/press-announcements/fda-approves-first-us-treatment-chagas-disease.

U.S Food and Drug Administration. (2021, January 08). "New Drug Therapy Approvals 2020." from https://www.fda.gov/drugs/new-drugs-fda-cders-new-molecular-entities-and-new-therapeutic-biological-products/new-drug-therapy-approvals-2020#additional-approvals.

Urbina, J. A. (2015). "Recent clinical trials for the etiological treatment of chronic chagas disease: advances, challenges and perspectives." J Eukaryot Microbiol **62**(1): 149-156.

Viana, S. M., A. L. Montoya, A. M. Carvalho, B. S. de Mendonca, S. Portillo, J. J. Olivas, N. H. Karimi, I. L. Estevao, U. Ortega-Rodriguez, E. M. Carvalho, W. O. Dutra, R. A. Maldonaldo, K. Michael, C. I. de Oliveira and I. C. Almeida (2022). "Serodiagnosis and therapeutic monitoring of New-World tegumentary leishmaniasis using synthetic type-2 glycoinositolphospholipid-based neoglycoproteins." Emerg Microbes Infect **11**(1): 2147-2159.

WHO (2011). "Working to overcome the global impact of neglected tropical diseases – Summary." Wkly Epidemiol Rec **86**(13): 113-120.

World Health Organization. (2020, March 02). "Leishmaniasis." from https://www.who.int/news-room/fact-sheets/detail/leishmaniasis.

Zhu, J. (2015). "T helper 2 (Th2) cell differentiation, type 2 innate lymphoid cell (ILC2) development and regulation of interleukin-4 (IL-4) and IL-13 production." Cytokine **75**(1): 14-24.

Zingales, B. (2018). "Trypanosoma cruzi genetic diversity: Something new for something known about Chagas disease manifestations, serodiagnosis and drug sensitivity." Acta Tropica **184**: 38-52.

Zingales, B., M. A. Miles, D. A. Campbell, M. Tibayrenc, A. M. Macedo, M. M. Teixeira, A. G. Schijman, M. S. Llewellyn, E. Lages-Silva, C. R. Machado, S. G. Andrade and N. R. Sturm (2012). "The revised Trypanosoma cruzi subspecific nomenclature: rationale, epidemiological relevance and research applications." Infect Genet Evol **12**(2): 240-253.

Zingales, B., M. E. Pereira, R. P. Oliveira, K. A. Almeida, E. S. Umezawa, R. P. Souto, N. Vargas, M. I. Cano, J. F. da Silveira, N. S. Nehme, C. M. Morel, Z. Brener and A. Macedo (1997). "Trypanosoma cruzi genome project: biological characteristics and molecular typing of clone CL Brener." Acta Trop **68**(2): 159-173.

APPENDIX

List of Abbreviations

Antibody	Ab
Antigen	Ag
BMK	Biomarker
BSA	Bovine serum albumin
CD	Chagas disease
CCD	Chronic Chagas disease
CD	Chagas disease
CD-#	Cluster of differentiation-[number]
Ch	Chagas disease-derived
ChMSP	Pool of Chagas disease mouse sera
CL	Cutaneous leishmaniasis
CRISPR	Clustered regularly interspaced short palindromic repeats
DL	Disseminated leishmaniasis
FBS	Fetal bovine serum
Gal	Galactose
α-Gal	α-Galactose
α-Gal*p*	α-Galactopyranose
Gal*f*	Galactofuranose
β-Gal*f*	β-Galactofuranose
αGalT	α1,3-Galactosyltransferase

βGal*f*T	β1,3-Galactofuranosyltransferase
GlcN	Glucosamine
GlcNAc	*N*-Acetyl-glucosamine
GIPL	Glycoinositolphospholipid
GM-CSF	Granulocyte-macrophage colony-stimulating factor
GPI	Glycosylphosphatidylinositol
GPI-AP	GPI-anchored protein
IL-1b	Interleukin-1b
IL-2	Interleukin-2
IL-4	Interleukin-4
IL-5	Interleukin-5
IL-6	Interleukin-6
IL-10	Interleukin-10
IL-17A	Interleukin-17A
INF-γ	Interferon-gamma
i.p.	Intraperitoneal
IP-10	Interferon gamma-induced protein 10
IVIS	*In vivo* imaging system
KC	Keratinocyte-derived cytokine (CXCL-1)
L. major	*Leishmania major*
L. major$_{luc}$	Transgenic *L. major* promastigotes expressing firefly luciferase
LPG	Lipophosphoglycan
LPPG	Lipopeptidophosphoglycan

MALDI-TOF-MS	Matrix-assisted laser desorption/ionization time-of-flight mass spectrometry
Man	Mannopyranose or mannose
MASP	Mucin-associated surface protein
MCP-1	Monocyte chemoattractant protein 1 (CCL-2)
MIP-1α	Macrophage inflammatory protein-1 alpha (CCL-3)
ML	Mucosal leishmaniasis
m.o.i.	Multiplicity of infection
MS	Mass spectrometry
myo-Ins	*myo*-Inositol
m/z	Mass to charge ratio
NGP	Neoglycoprotein
NMSP	Normal Mouse Sera Pool
NHS	Normal human serum
ON	Overnight
OWNHP	Old-World nonhuman primate
qPCR	real-time quantitative PCR
RANTES	Regulated upon activation, normal T-cell expressed and secreted (CCL5)
ROC	Receiver-operating characteristic
RT	Room temperature
T. cruzi	*Trypanosoma cruzi*
T. cruzi$_{luc}$	Red-shifted firefly luciferase-expressing *T. cruzi* CL Brener clone

TCT	Mammalian tissue culture-derived trypomastigotes
tGPI-MUC	Trypomastigote-derived glycosylphosphatidylinositol-anchored mucins
TL	Tegumentary leishmaniasis
TNF-α	Tumor Necrosis Factor-alpha
TS	*trans*-Sialidase
VL	Visceral leishmaniasis

Curriculum Vita

Colin Daniel Knight was born overlooking the Chesapeake Bay in Cape Charles, VA, and is receiving his PhD in Biological Sciences from the University of Texas at El Paso. Throughout his life, Colin has lived worldwide, including in Germany and Iraq, while serving in the United States Army as a Medic. Colin's military honors include the Meritorious Service Medal and Army Commendation Medal x4 and the Combat Action Badge to name a couple. After leaving the Army after 13 years of service, Colin began taking classes at the El Paso Community College (EPCC), where he focused on a pre-veterinary Biology degree path. During his first semester at EPCC, he had Dr. "Nic" Lanutti as his Biology professor. Nic recommended that Colin apply for his Bridges to the Baccalaureate summer research program. Colin was accepted into the Bridges to the Baccalaureate under the mentorship of Dr Charlotte Vines. Colin continued to conduct research focused on the role of the C-C chemokine 7 (CCR7) in Multiple Sclerosis and Breast Cancer in Dr. Vines' lab during both his time still at EPCC and after he transferred to UTEP to finish his BS in Cellular and Molecular Biochemistry which he obtained in May 2018. During his undergraduate time in Dr. Vines' lab, Colin was able to mentor not only fellow undergraduate students in the lab and as a TA but he also mentored nine high school sophomore students for a summer research program. After receiving his BS in cellular and molecular biochemistry, Colin was accepted directly into the Biological Sciences PhD program at UTEP where he received the Luis Stokes Alliance for Minority Participation (LSAMP) Bridges the Doctorate Fellowship that provided a total of approximately $80,000 in both tuition and financial support. During his rotations, he identified Dr. Igor Almeida as his dissertation advisor, Dr Almeida's research in vaccine development caught Colin's interest in further learning about the body's immune system, and

investigating a parasite that he had treated cases of infection while in Iraq was much more meaningful to him.

Colin plans to continue his government service as he has accepted a position as a Molecular Biologist at the National Institutes of Health in Bethesda, MD.